FINAL

ISC/23/ANNEX/08

ANNEX 08

23rd Meeting of the
International Scientific Committee for Tuna
and Tuna-Like Species in the North Pacific Ocean
Kanazawa, Japan
July 12-17, 2023

STOCK ASSESSMENT OF ALBACORE TUNA IN THE NORTH PACIFIC OCEAN IN 2023

July 2023

Left Blank for Printing

FINAL

STOCK ASSESSMENT OF ALBACORE TUNA IN THE NORTH PACIFIC OCEAN IN 2023

REPORT OF THE ALBACORE WORKING GROUP

International Scientific Committee for Tuna and Tuna-like Species in the North Pacific Ocean

12 - 17 July 2023

ISC Plenary Meeting in Kanazawa, Japan

Page Intentionally Blank for Printing

TABLE OF CONTENTS

LIST OF ACRONYMS

$14\%SSB_{current, F=0}$	14% of the current, dynamic SSB under zero fishing. Current limit reference point for North Pacific albacore tuna.
$30\%SSB_{current, F=0}$	30% of the current, dynamic SSB under zero fishing. Current threshold reference point for North Pacific albacore tuna.
ALBWG	Albacore Working Group of the ISC
ASPM	Age-structured production model, which is used for model diagnostics
CPUE	Catch-per-unit-effort
EPO	Eastern Pacific Ocean
IATTC	Inter-American Tropical Tuna Commission
ISC	International Scientific Committee for Tuna and Tuna-like Species in the North Pacific Ocean (https://isc.fra.go.jp/)
F-at-age	Instantaneous fishing mortality at age
$F_{\%SPR}$	Fishing intensity in %SPR
$F45_{\%SPR}$	Fishing intensity that results in the population reaching an SPR of 45% at equilibrium. Current target reference point for North Pacific albacore tuna.
JPLL	Japanese longline
JPPL	Japanese pole-and-Line
LRP	Limit reference point
MSY	Maximum Sustainable Yield
RFMO	Regional Fisheries Management Organization
SPR	Spawning Potential Ratio, which is the ratio of the equilibrium SSB per recruit that would result from an F-at-age relative to that of the unfished population.
SS	Stock Synthesis
SSB	Spawning Stock Biomass
ThRP	Threshold reference point
TRP	Target reference point
USA	United States of America
WCPFC	Western and Central Pacific Fisheries Commission
WCPFC NC	Northern Committee of the Western and Central Pacific Fisheries Commission
WCPO	Western and Central Pacific Ocean

ACKNOWLEDGEMENTS

The 2023 stock assessment of north Pacific albacore tuna is the result of a collaborative effort of the ALBWG. Members of the ALBWG who contributed to this assessment include Sarah Hawkshaw (Chair), Carolina Minte-Vera, Haikun Xu, Hirotaka Ijima, Jhen Hsu, Kevin Hill, Naoto Matsubara, Steve Teo, Yi-Jay Chang, Yoshinori Aoki, and Yuichi Tsuda. Steve Teo, with assistance from Hirotaka Ijima, was the lead modeller on this assessment.

EXECUTIVE SUMMARY

Stock Identification and Distribution: The north Pacific albacore tuna (*Thunnus alalunga*) stock area consists of all waters in the Pacific Ocean north of the equator to 55°N. All available fishery data from this area were used for the stock assessment with a fleets-as-areas approach, under the assumption that there is instantaneous mixing of albacore on a quarterly basis, i.e., a single well-mixed stock.

Major changes from the 2020 assessment: There were four main changes to the base case model compared to the previous assessment in 2020. **1**) Increased uncertainty was imposed on the size composition and abundance index data for 2020 and 2021because fishery operations and data collection protocols were likely affected by COVID-19 safety protocols. **2**) Two JPLL fleets were further subdivided nominally into juvenile and adult fleets to improve model fits and diagnostics. **3**) A new adult abundance index was developed from the JPLL fleet in Area 2, Quarter 2 and used as the abundance index. **4**) Selectivity patterns for the two main JPPL fleets were modified to have only a single time block (2016 – 2021) due to model convergence issues. Sensitivity of results to the model structure changes listed above are illustrated with a model using a similar structure to the base case model in the 2020 assessment, albeit with the same data as this assessment (Table ES1).

Catches: During the modeling period (1994-2021), the total reported catch of north Pacific albacore reached a peak of about 119,000 t in 1999 and then declined in the early 2000s, followed by a recovery in later years. However, catches have dropped to low levels during two out of the last three years of the time series, with catches of about 43,000 t in 2019 and 2021 (Fig. ES1). Surface gears (e.g., troll, pole-and-line), which primarily harvest juvenile albacore, have typically accounted for the majority of the albacore catch (Fig. ES2).

Data and Assessment: All north Pacific albacore catch and size composition data from ISC member (Canada, China~~,~~ Chinese Taipei, Japan, Korea, and the USA) and non-member countries were compiled for the assessment. The fleet structure was similar to the 2020 assessment but an attempt was made to improve model fits and diagnostics by further subdividing the JPLL fleets operating in Areas 1 and 3 during Quarter 1 nominally into juvenile and adult fleets. Four relative abundance indices (standardized CPUE) were provided by Japan and the USA. Based on a thorough review of all fishery data and preliminary model runs, the ALBWG fitted the base case model to one abundance index: the standardized CPUE of the JPLL fleet operating in Area 2 during Quarter 2 (F12 index; 1996 – 2021). This index was chosen because it represented the best information on trends for adult age-classes of female albacore, had good contrast, and ASPM analyses indicated the index was informative on both population trends and scale. Previous assessments used an index from the JPLL fleet in the same area but from Quarter 1, which is the primary albacore-targeting season. However, a re-examination of the data indicated that trends in the adult age-classes of female albacore were likely better represented by the Quarter 2 CPUE.

The north Pacific albacore tuna stock was assessed using a length-based, age-, and sex-structured Stock Synthesis (SS; Version 3.30.21) model over the 1994-2021 period. Biological parameters like growth and natural mortality (M), were the same as for the 2017 and 2020 assessments. Sex-specific growth curves were used because of sexually dimorphic growth, with adult males attaining a larger size-at-age than females after maturity. Sex-specific M-at-age vectors were developed from a meta-analysis, with a sex-combined M that scaled with size for ages 0-2, and sex-specific M fixed at 0.48 and 0.39 y^{-1} for age-3+ females and males, respectively. The steepness of the Beverton-Holt stock-recruitment relationship was assumed to be 0.9, based on two prior analyses. The base case model was fitted to the F12 index and all representative size composition data in a likelihood-based statistical framework. However, preliminary analyses indicated that fishery operations and data collection protocols in 2020 and 2021 were likely affected by COVID-19 safety protocols. Therefore, increased uncertainty was imposed on the size composition and abundance index data for those two years to reflect these effects. All but one fleet (USA longline) were assumed to have dome-shaped length selectivity patterns, and age-based selectivity for ages 1-5 were also estimated for surface fleets (primarily troll and pole-and-line) to address age-based changes in juvenile albacore availability and movement. Preliminary models with annually-varying age-selectivities for the two main JPPL fleets resulted in models without positive, definite Hessian matrices. However, models without any time varying age-selectivities matched the expected catch-at-age poorly and had poor ASPM diagnostics. Therefore, the ALBWG developed a model with a single age-selectivity time block for the two main JPPL fleets near the end of the historical period. This model adequately matched the catch-at-age and had good ASPM diagnostics. Selectivity patterns were also assumed to vary for fleets during periods consistent with important changes in fishing operations. Maximum likelihood estimates of model parameters, derived outputs, and their variances were used to characterize stock status. Several sensitivity analyses were conducted to evaluate changes in model performance or the range of uncertainty resulting from changes in model parameters, including growth, natural mortality, stock-recruitment steepness, selectivity patterns, and data weighting.

An ASPM diagnostic analysis showed that the estimated catch-at-age and fixed productivity parameters (growth, mortality and stock-recruitment relationships with and without annual recruitment deviates) were able to explain trends in the primary index. Based on these findings, the ALBWG concluded that the base case model was able to estimate the stock production function and the effect of fishing on the abundance of the north Pacific albacore stock. Similar to the 2017 and 2020 assessments, the link between catch-at-age and the primary index adds confidence to the data used and the results of the assessment. Due to the moderate exploitation levels relative to the productivity, the production function was weakly informative about north Pacific albacore stock size, resulting in asymmetric uncertainty in the absolute scale of the stock, with more uncertainty in the upper limit of the stock than the lower limit. It is important to note that the primary aim of estimating the female SSB in this assessment was to determine if the estimated SSB was lower than the adopted limit and threshold reference points. Since the lower bound is better defined, it adds confidence to the ALBWG's evaluation of stock condition relative to these reference points.

Conservation and Management: The WCPFC and IATTC are the tuna RFMOs that manage the north Pacific albacore stock in the WCPO and EPO, respectively, and have adopted similar harvest strategies and biological reference points for this stock (WCPFC HS 2022-01; IATTC Resolution C-22-04). These harvest strategies include target, threshold, and limit reference points. The target reference points are $F45_{\%SPR}$, which is the fishing intensity that results in the stock producing a SPR of approximately 45%. The threshold and limit reference points are $30\%SSB_{current,\ F=0}$ and $14\%SSB_{current,\ F=0}$, respectively, which are 30% and 14% of the current, dynamic SSB under zero fishing, and hence fluctuates with changes in recruitment. Importantly, three of the management objectives in the harvest strategies are to: 1) maintain SSB above the limit reference point, with a probability of at least 80% over the next 10 years; 2) maintain depletion of total biomass around historical (2006 – 2015) average depletion over the next 10 years; and 3) maintain fishing intensity at or below the target reference point with a probability of at least 50% over the next 10 years. In addition, both RFMOs have current management measures (WCPFC CMM 2019-03; IATTC Resolution C-05-02) that maintain albacore fishing effort at or below the average effort levels during 2002 – 2004.

Stock Status: Estimated summary biomass (males and females at age-1+) declined at the beginning of the time series until 2004 (Fig. ES3A). Subsequently, the summary biomass fluctuated without a trend until 2018, after which the biomass rapidly increased to historically high levels. It should be noted that the high summary biomass estimates during 2018 – 2021 were highly uncertain and should be treated with caution (Fig. ES3A). These high summary biomass estimates were due to historically high recruitment estimates in 2017 (~433 million fish; 95% CI: 194 – 671 million fish) (Fig. ES3C). However, it should be noted that the recruitment estimates in the last 5 years (2017-2021) were highly uncertain and should be treated with caution. Estimated female SSB exhibited a similar population trend to the summary biomass, albeit with a lag of several years, and showed an initial decline until 2007 followed by fluctuations without a clear trend through 2021 (Fig. ES3B).

The average fishing intensity during 2018 – 2020 was estimated to be $F59_{\%SPR}$ (95% CI: $F72_{\%SPR}$ – $F46_{\%SPR}$), which was relatively moderate and resulted in a population with an SPR of approximately 59%. Instantaneous fishing mortality at age (F-at-age) was similar in both sexes through age-5, peaking at age-4 and declining to a low at age-6, after which males experienced higher F-at-age than females up to age 12 (Fig. ES4). Juvenile albacore aged 2 to 4 years comprised approximately 64% of the annual catch-at-age in numbers between 1994 and 2021 (Fig. ES5) due to the larger fishery impact of surface fisheries (primarily troll, pole-and-line), which remove juvenile fish, relative to longline fisheries, which primarily remove adult fish (Fig. ES6).

Stock status is depicted in relation to the target ($F45_{\%SPR,}$), threshold ($30\%SSB_{current,\ F=0}$), and limit ($14\%SSB_{current,\ F=0}$) reference points (Fig. ES7A; Table ES1). The estimated female SSB has never fallen below the threshold and limit reference points since 1994, albeit with large uncertainty in the terminal year (2021) estimates. However, the estimated fishing intensity for five years (1999, 2002, 2003, 2004, and 2007) have exceeded the target reference point. Even when alternative hypotheses about key model uncertainties such as growth were evaluated, the point estimate of female SSB in 2021 (SSB_{2021}) did not fall below the threshold and limit reference points, although the risk increases with this more extreme assumption (Fig. ES7B). However, estimated average fishing intensity during 2018-2020 ($F_{2018\text{-}2020}$) did exceed the target reference point under one of these alternative hypotheses but did not exceed the average fishing intensity during 2002 – 2004 (Fig. ES7B; Table ES1).

The SSB_{2021} was estimated to be approximately 54% (95% CI: 40 – 68%) of $SSB_{current,\ F=0}$ and 1.8 (95% CI: 1.3 – 2.3) times greater than the estimated threshold reference point (Fig. ES8A and Table ES1). The estimated current fishing intensity ($F_{2018\text{-}2020}$) was estimated to be $F59_{\%SPR}$ (95% CI: $F72_{\%SPR}$ – $F46_{\%SPR}$) and was lower than both the $F45_{\%SPR}$ target reference point and the average fishing intensity during 2002 – 2004 (Fig. ES8B and Table ES1).

Based on these findings, the following information on the status of the north Pacific albacore stock is provided:

1. The stock is likely not overfished relative to the threshold ($30\%SSB_{current,\ F=0}$) and limit ($14\%SSB_{current,\ F=0}$) reference points adopted by the WCPFC and IATTC, and
2. The stock is likely not experiencing overfishing relative to the adopted target reference point ($F45_{\%SPR}$).
3. Current fishing intensity ($F_{2018\text{-}2020}$) is lower than the fishing intensity from the 2002-2004 period (the reference level for IATTC Resolution C-05-02 and WCPFC CMM-2019-03).

Future Projections: A new version of the SSfuture C++software package (ssfcpp_simple_2023.cpp) was developed to perform future projections for this assessment. Two 10-yr projection scenarios, constant $F_{2018\text{-}2020}$ and randomly resampled F (2005 – 2019) scenarios, were used to evaluate the impacts of fishing on the management objectives of IATTC and WCPFC. Each projection scenario consisted of 160,000 (400 x 400) runs, starting in 2022 and continuing for 10 years through 2031.

For each scenario, 400 initial populations, together with their stock-recruitment relationships, were simulated by sampling from the estimated N-at-age distributions in 2021. Each initial population was in turn projected using 400 runs with an F-at-age and random recruitment. Most of the uncertainties from the base case model, except for estimation uncertainties of the selectivities and recruitment deviates, were incorporated into the projections. The ALBWG considered these projections to be an improvement over projections from previous assessments but more improvements will still be needed in the future. Depending on scenario, the F-at-age used was either based on the average F-at-age during 2018 – 2020, or randomly resampled from 2005 – 2019.

Both projection scenarios showed similar trends. The constant fishing intensity scenario showed that the current fishing intensity ($F_{2018\text{-}2020}$) is expected to result in female SSB increasing to 90,098 t (95% CI: 23,218 – 156,978 t) by 2031. Over the next 10 years, there was: 1) a 97.7% probability of the female SSB remaining above the 14%$SSB_{current,\ F=0}$ LRP for all 10 years; 2) a 72.0% probability of the total biomass (age-1+) being above the average of 2006 – 2015 for any year; and 3) a 95.5% probability of the fishing intensity remaining at or below the $F45_{\%SPR}$ TRP for any year (Fig. ES9). Similarly, The randomly resampled fishing intensity scenario showed that if future fishing intensity is similar to the 2005 – 2019 period, it is expected to result in female SSB increasing to 87,669 t (95% CI: 22,219 – 153,119 t) by 2031. Over the next 10 years, there was: 1) a 98.1 % probability of the female SSB remaining above the 14%$SSB_{current,\ F=0}$ LRP for all 10 years; 2) a 69.5 % probability of the total biomass (age-1+) being above the average of 2006 – 2015 for any year; and 3) a 79.6 % probability of the fishing intensity remaining at or below the $F45_{\%SPR}$ TRP for any year (Fig. ES10).

Conservation Information: Two harvest scenarios were projected to evaluate impacts on the management objectives of IATTC and WCPFC for this stock: 1) maintain SSB above the limit reference point, with a probability of at least 80% over the next 10 years; 2) maintain depletion of total biomass around historical (2006 – 2015) average depletion over the next 10 years; and 3) maintain fishing intensity at or below the target reference point with a probability of at least 50% over the next 10 years (WCPFC HS 2022-01; IATTC Resolution C-22-04).

The constant fishing intensity scenario showed that the current fishing intensity ($F_{2018\text{-}2020}$) is expected to result in female SSB increasing to 90,098 t (95% CI: 23,218 – 156,978 t) and a $SSB/SSB_{current,\ F=0}$ ratio of 0.54 by 2031. Over the next 10 years, there was: 1) a 97.7% probability of the female SSB remaining above the 14%$SSB_{current,\ F=0}$ LRP for all 10 years; 2) a 72.0% probability of the total biomass (age-1+) being above the average of 2006 – 2015 for any year; and 3) a 95.5% probability of the fishing intensity remaining at or below the $F45_{\%SPR}$ TRP for any year.

The randomly resampled fishing intensity scenario showed that if future fishing intensity is similar to the 2005 – 2019 period, it is expected to result in female SSB increasing to 87,669 t (95% CI: 22,219 – 153,119 t) and a $SSB/SSB_{current,\ F=0}$ ratio of 0.52 by 2031. Over the next 10 years, there was: 1) a 98.1 % probability of the female SSB remaining above the 14%$SSB_{current,\ F=0}$ LRP for all 10 years; 2) a 69.5 % probability of the total biomass (age-1+) being above the average of 2006 – 2015 for any year; and 3) a 79.6 % probability of the fishing intensity remaining at or below the $F45_{\%SPR}$ TRP for any year.

Based on these findings, the following conservation information is provided:

1. If fishing intensity over the next ten years is maintained at the current fishing intensity ($F_{2018\text{-}2020}$), then female SSB is expected to remain around 54%$SSB_{current,\ F=0}$ (90,098 t), with a 97.7% probability of the female SSB remaining above the 14% $SSB_{current,\ F=0}$ LRP for all ten years, and the management objectives of IATTC and WCPFC will likely be met.

2. If fishing intensity over the next ten years is similar to the 2005 – 2019 period, then female SSB is expected to decrease to 52%$SSB_{current, F=0}$ (87,669 t), with a 98.1% probability of the female SSB remaining above the 14% $SSB_{current, F=0}$ LRP for all ten years, and the management objectives of IATTC and WCPFC will likely be met.

Key Uncertainties: The ALBWG notes that the lack of sex-specific size data, uncertainty in growth and natural mortality, uncertainty in the impacts of COVID safety protocols on fishery operations and data collection, and the simplified treatment of the spatial structure of north Pacific albacore population dynamics are important sources of uncertainty in the assessment.

Exceptional Circumstances: The adopted harvest strategies of WCPFC and IATTC for north Pacific albacore tuna included the identification of exceptional circumstances during the stock assessment. The ALBWG developed and considered the preliminary criteria for identifying exceptional circumstances for north Pacific albacore tuna, and did not find any strong evidence of exceptional circumstances with respect to the conservation and management of this stock. At this time, the ALBWG stresses that the preliminary criteria are still incomplete and without implementation indicators based on adopted HCRs, the application of these incomplete criteria may bias results and introduce uncertainty.

Table ES1. Estimates of maximum sustainable yield (MSY), female spawning stock biomass (SSB), fishing intensity (F), and reference point ratios for north Pacific albacore tuna for: 1) the base case model; 2) two important sensitivity models due to uncertainty in growth parameters; and 3) a model representing an update of the 2020 base case model to 2023 data. SSB_0, $SSB_{current, F=0}$ and SSB_{MSY} are the expected female SSB of a population in the equilibrium, unfished state; in the current, dynamic, unfished state; and at MSY, respectively. The Fs in this table are indicators of fishing intensity based on spawning potential ratio (SPR) and calculated as %SPR. SPR is the ratio of the equilibrium SSB per recruit that would result from the estimated F-at-age relative to that of an unfished population. Depletion is calculated as the proportion of the age-1+ biomass during the specified period relative to an unfished age-1+ equilibrium biomass. The model representing an update of the 2020 base case model is similar to but not identical to the 2020 base case model due to changes in data preparation and model structure. *Model may not have converged and uncertainty estimates were unreliable because of the lack of a positive, definite Hessian matrix. †A value of >1 for the depletion ratio indicates higher age-1+ biomass in 2021 relative to the 2006 – 2015 period. §Higher %SPR values indicate lower fishing intensity levels. ¶Values of >1 for ratios of $F_{\%SPR}$ to $F_{\%SPR}$-based reference points indicate fishing intensity levels lower than the reference points.

Quantity	Base Case	Growth CV = 0.06 for L_{inf}	Growth All parameters estimated	Update of 2020 base case model to 2023 data*
MSY (t)	121,880	93,167	144,792	97,777
SSB_{MSY} (t)	23,154	18,133	30,435	18,756
SSB_0 (t)	165,567	128,155	198,913	132,570
SSB_{2021} (t)	70,229	35,418	101,161	36,909
$SSB_{current, F=0}$ (2021 estimate)	129,581	97,368	155,542	93,808
$SSB_{2021}/SSB_{current, F=0}$	0.54	0.36	0.65	0.39
$SSB_{2021}/30\%SSB_{current, F=0}$	1.81	1.21	2.17	1.31
$SSB_{2021}/14\%SSB_{current, F=0}$	3.87	2.60	4.65	2.81
†$Depletion_{2021}/Depletion_{2006\text{-}2015}$	1.34	1.33	1.37	1.30
§ $F_{\%SPR,\ 2018\text{-}2020}$ (%SPR)	59.0	41.4	70.4	43.2
§ $F_{\%SPR,\ 2011\text{-}2020}$ (%SPR)	55.0	36.6	63.8	37.9
¶ $F_{\%SPR,\ 2018\text{-}2020}/F_{\%SPR,\ MSY}$	2.04	1.42	2.78	1.47
¶ $F_{\%SPR,\ 2011\text{-}2020}/F45_{\%SPR}$	1.22	0.81	1.42	0.84
¶ $F_{\%SPR,\ 2018\text{-}2020}/F45_{\%SPR}$	1.31	0.92	1.56	0.96
¶ $F_{\%SPR,\ 2018\text{-}2020}/F_{\%SPR,\ 2002\text{-}2004}$	1.48	1.63	1.40	1.25

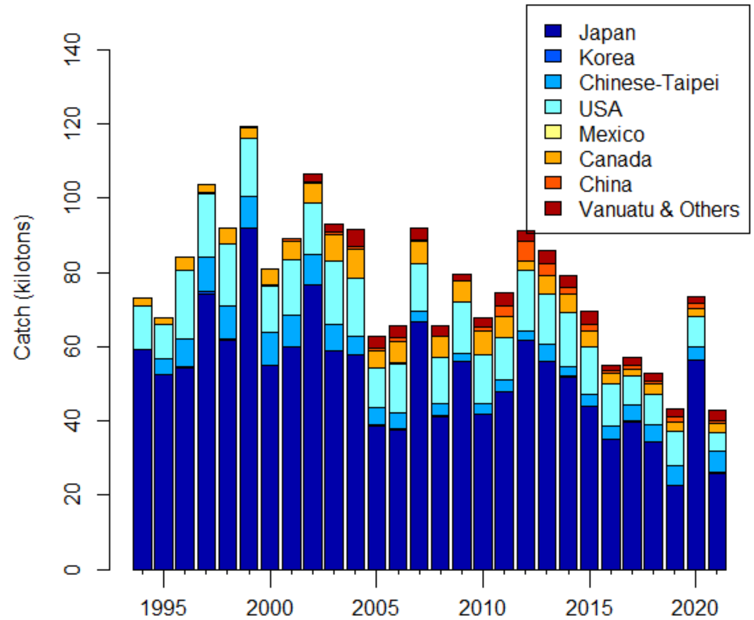

Figure ES1. Estimated total annual catch of north Pacific albacore (*Thunnus alalunga*) by all countries harvesting the stock, 1994-2021. Catches by Vanuatu and other countries includes small amount of catch by other countries such as Tonga, Belize, Cook Islands, and Marshall Islands.

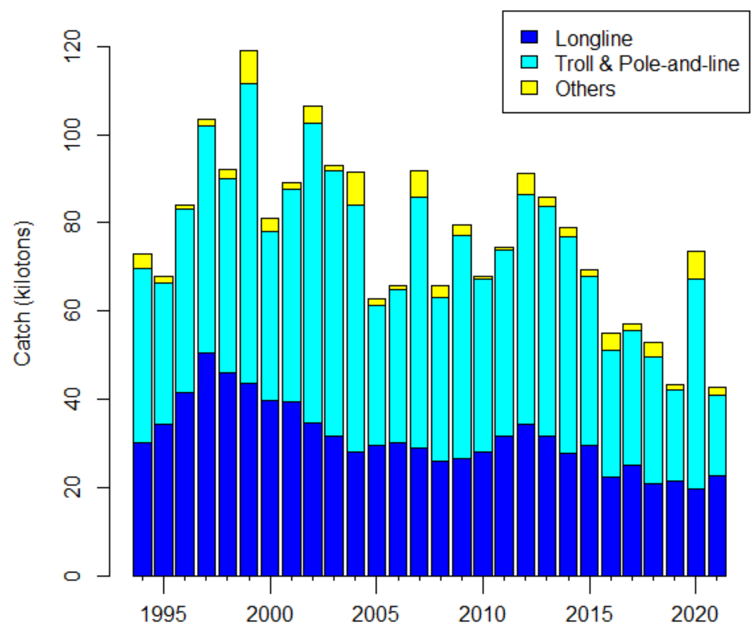

Figure ES2. Estimated catches of north Pacific albacore (*Thunnus alalunga*) by major gear types, 1994-2021. The Other gear category includes catches with purse seine, gillnet, hand lines, and harpoons.

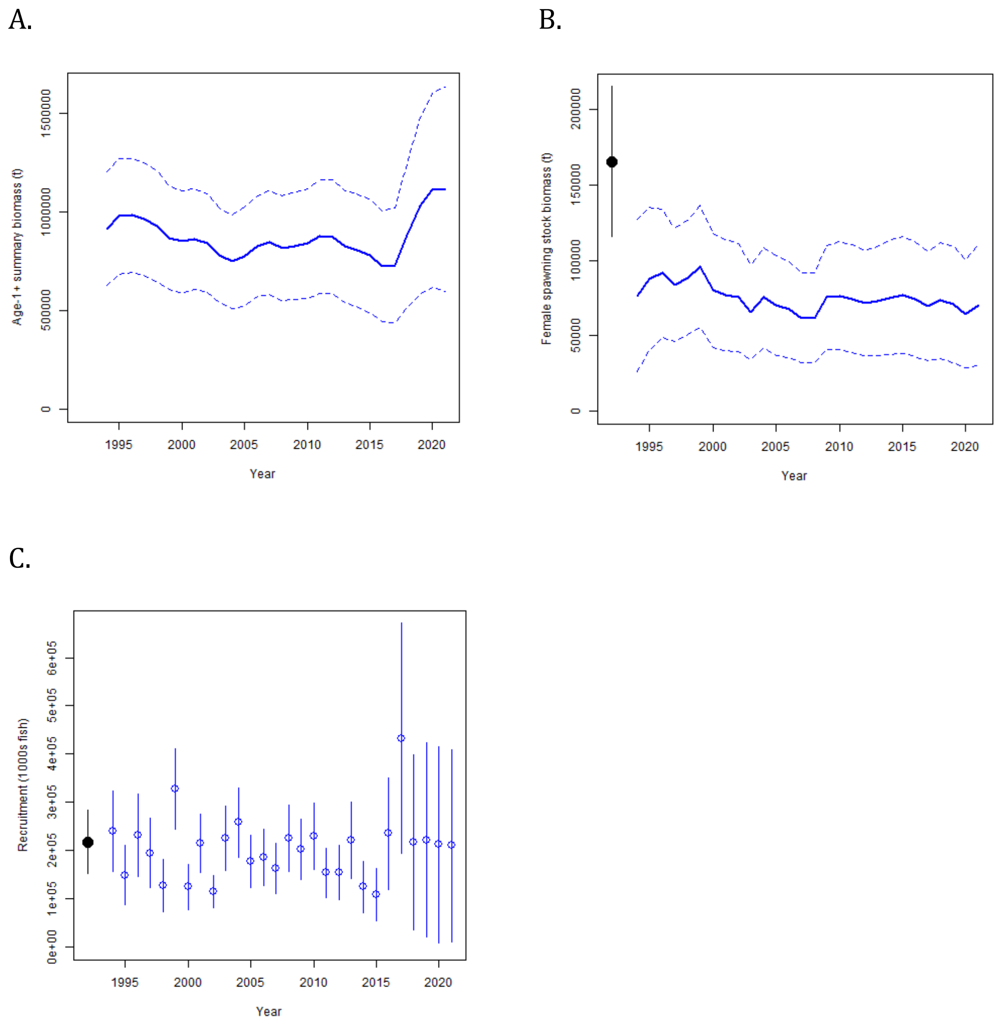

Figure ES3. Maximum likelihood estimates of (A) age-1+ biomass (B), female spawning biomass (SSB), and (C) age-0 recruitment of north Pacific albacore tuna (*Thunnus alalunga*). Dashed lines (A and B) and vertical bars (C) indicate 95% confidence intervals. Closed black circle and error bars in (B) and (C) are the maximum likelihood estimate and 95% confidence intervals of unfished female spawning biomass, SSB_0, and unfished recruitment, respectively, at equilibrium.

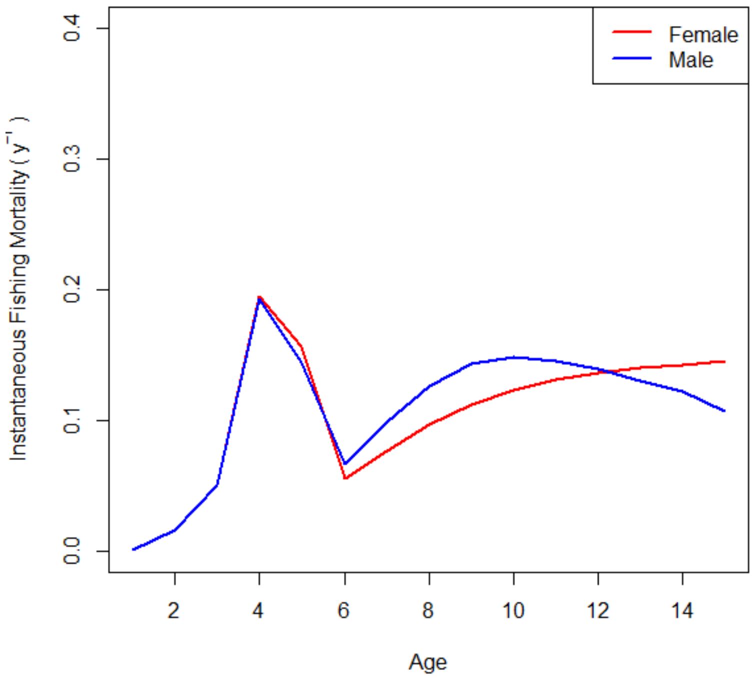

Figure ES4. Estimated sex-specific instantaneous fishing mortality-at-age (F-at-age) for the 2023 base case model, averaged across 2018-2020.

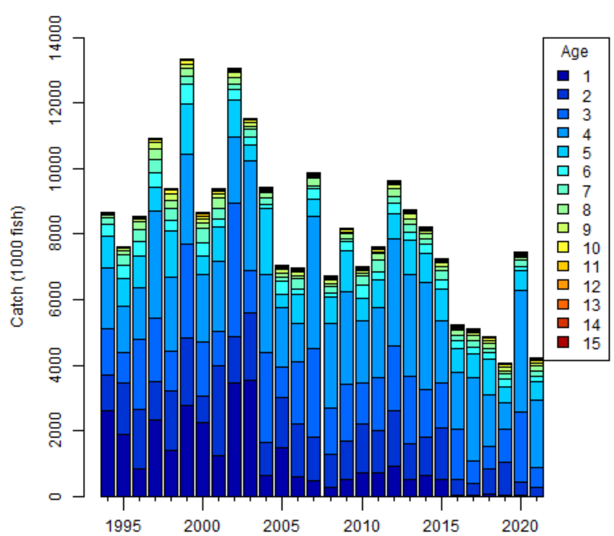

Figure ES5. Historical catch-at-age of north Pacific albacore (*Thunnus alalunga*) estimated by the 2023 base case model.

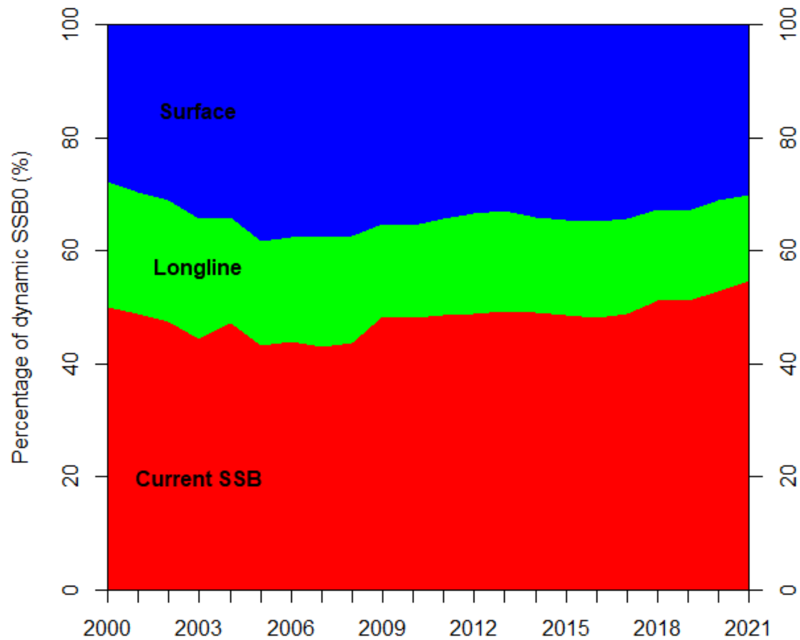

Figure ES6. Fishery impact analysis on north Pacific albacore (*Thunnus alalunga*) showing female spawning biomass (SSB) (red) estimated by the 2023 base case model as a percentage of dynamic, unfished female SSB ($SSB_{current,\ F=0}$). Colored areas show the relative proportion of fishing impact attributed to longline (green) and surface (blue) fisheries (primarily troll and pole-and-line gear, but including all other gears except longline).

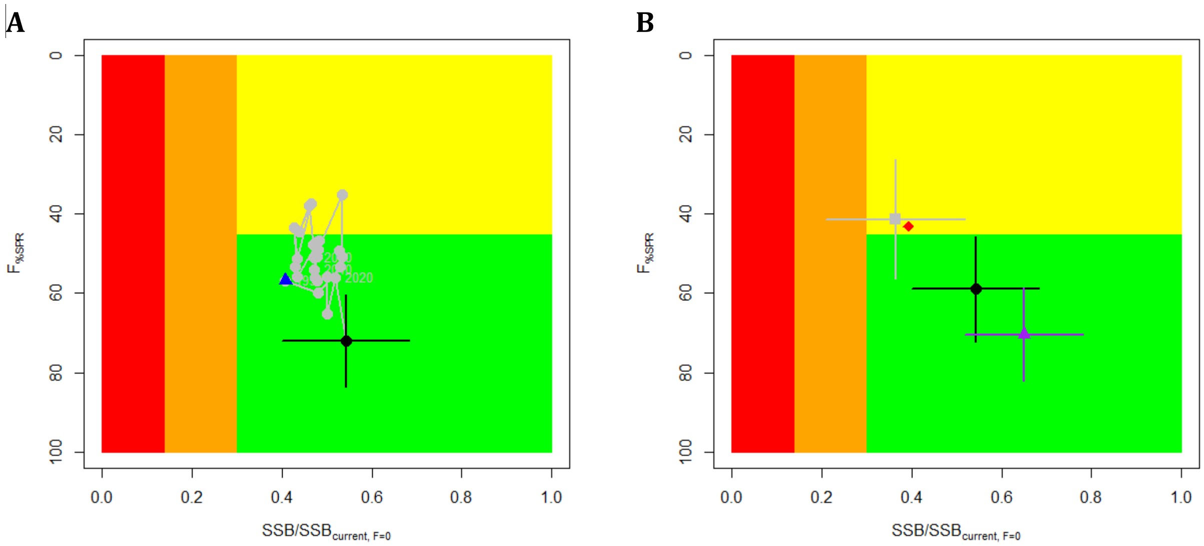

Figure ES7. (**A**) Stock status phase plot showing the status of the north Pacific albacore (*Thunnus alalunga*) stock relative to the biomass-based threshold ($30\%SSB_{current,\ F=0}$) and limit ($14\%SSB_{current,\ F=0}$) reference points, and fishing intensity-based target reference point ($F45_{\%SPR}$) over the modeling period (1994 – 2021). Blue triangle indicates the start year (1994) and black circle with 95% confidence intervals indicates the terminal year (2021). (**B**) Stock status plot showing current stock status and 95% confidence intervals of the base case model (black circle), an important sensitivity run of CV = 0.06 for L_{inf} in the growth model (gray square), an important sensitivity run with an estimated growth model (purple triangle), and a model representing an update of the 2020 base case model to 2023 data (red diamond). 95% confidence intervals are not shown for the update of the 2020 base case model (red diamond) because the model did not have a positive definite Hessian matrix and uncertainty estimates were unreliable. Red zones in both panels indicate female SSBs falling below the limit reference point while the orange zones indicate female SSBs between the threshold and limit reference points. Green zones indicate female SSBs above the threshold reference point and fishing intensity levels below the target reference point. Yellow areas indicate female SSBs above the threshold reference point and fishing intensity levels above the target reference point. The Fs in this figure are indicators of fishing intensity based on spawning potential ratio (SPR) and calculated as %SPR. SPR is the ratio of the equilibrium SSB per recruit that would result from the estimated F-at-age relative to that of an unfished population. A higher %SPR indicates lower fishing intensity. Current fishing intensity values and $SSB/SSB_{current,F=0}$ ratios in (B) were calculated as the average during 2018-2020 ($F_{\%SPR,\ 2018\text{-}2020}$) and 2021 ($SSB_{2021}/SSB_{current,\ F=0}$), respectively. The model representing an update of the 2020 base case model is similar to but not identical to the 2020 base case model due to changes in data preparation and model structure.

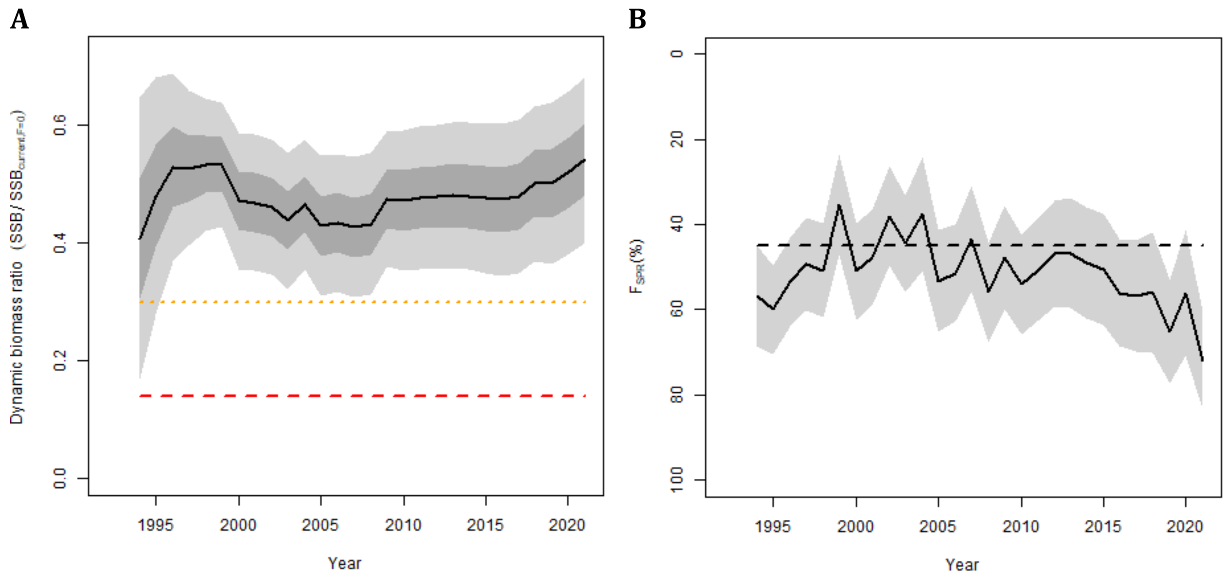

Figure ES8. (**A**) Estimated dynamic biomass ratio ($SSB/SSB_{current, F=0}$) of north Pacific albacore relative to biomass-based threshold ($30\%SSB_{current, F=0}$) (orange dotted line) and limit ($14\%SSB_{current, F=0}$) reference points (red dashed line) over the modeling period (1994 – 2021); and **(B)** estimated fishing intensity relative to the fishing intensity-based target reference point ($F45_{\%SPR}$) over the modeling period (1994 – 2021). Light and dark gray areas indicate 95% and 60% confidence intervals respectively. The limit reference point is considered to be breached if the lower bound of the 60% confidence intervals overlaps the limit reference point,

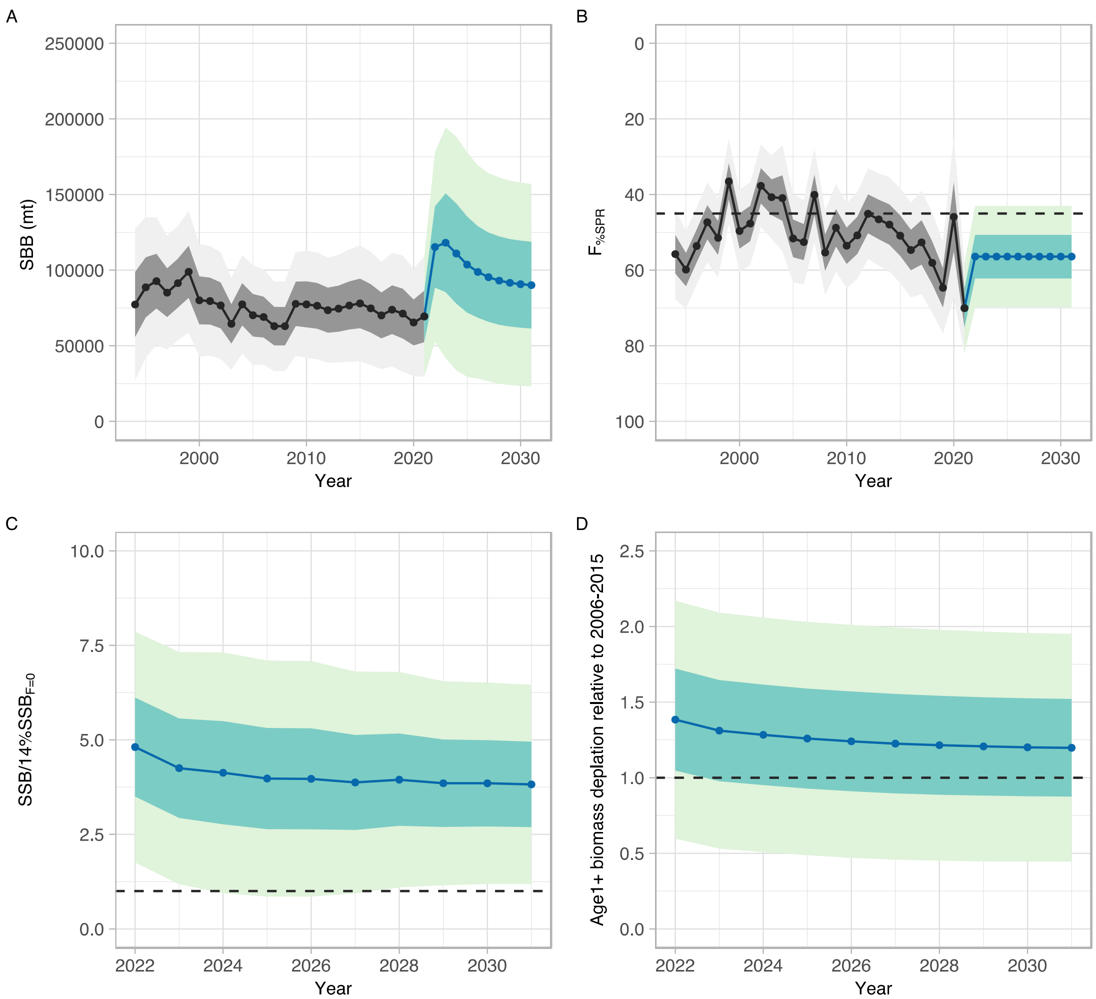

Figure ES9. Future projection results under a constant fishing intensity ($F_{2018\text{-}2020}$) harvest scenario. Solid lines indicate mean values, uncertainty ranges indicate 60% and 95% confidence intervals, and the dashed line is the reference point, respectively. (A) Annual changes in spawning biomass; (B) Interannual changes in fishing mortality ($F_{\%SPR}$); (C) Projected ratios to the limit reference point thresholds; and (D) Projected ratios to management targets for the total biomass.

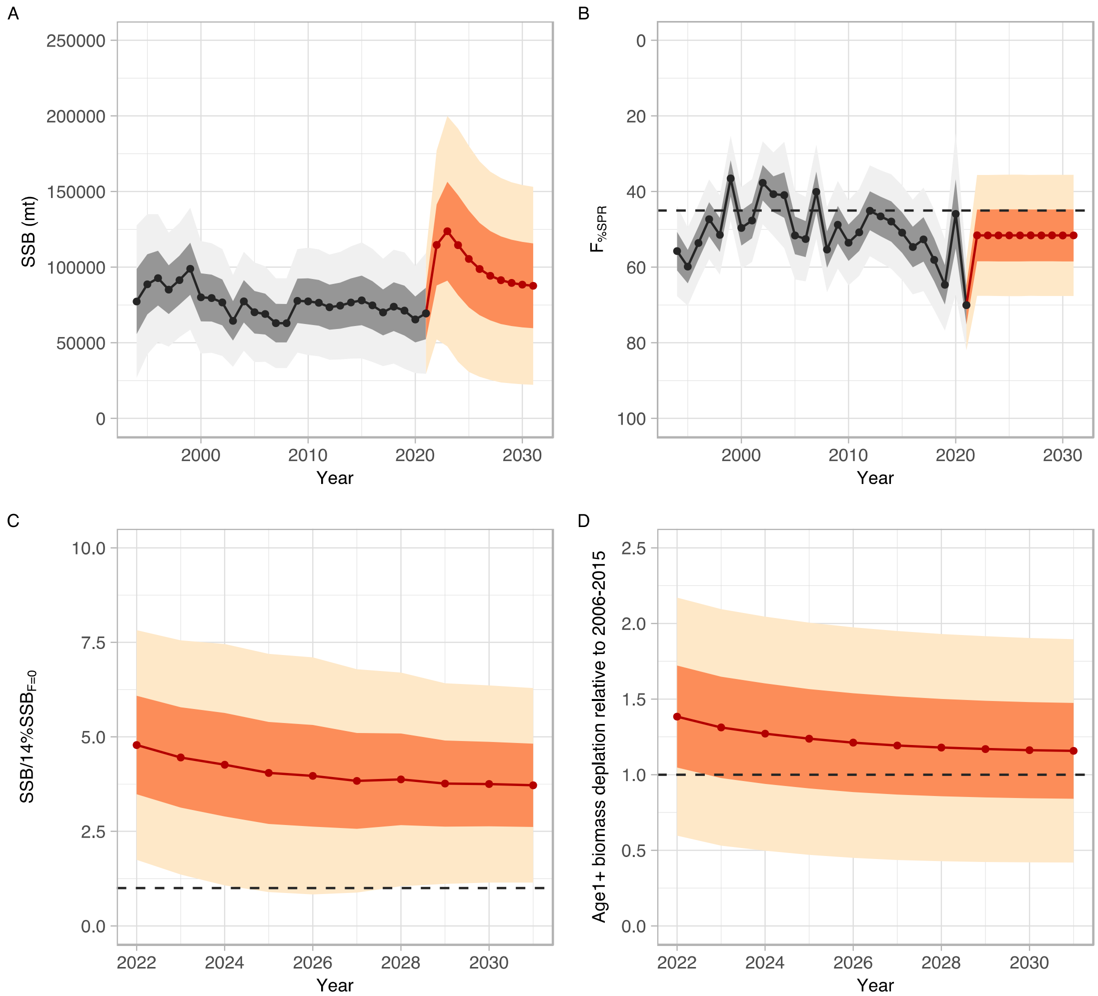

Figure ES10. Future projection results under a randomly F (2005-2019) scenario. Solid lines indicate mean values, and uncertainty ranges indicate 60% and 95% confidence intervals, and the dashed line is the reference point, respectively. (A) Annual changes in spawning biomass; (B) Interannual changes in fishing mortality ($F_{\%SPR}$); (C) Projected ratios to the limit reference point thresholds; and (D) Projected ratios to management targets for the total biomass.

1.0 INTRODUCTION

The ALBWG of the ISC is tasked with conducting regular stock assessments of north Pacific albacore tuna (*Thunnus alalunga*) to estimate population parameters, summarize stock status, and develop scientific advice on conservation and management needs for fisheries managers. The origins of the ALBWG date to 2005 when the *North Pacific Albacore Workshop*, which was established in 1974 to promote cooperative research and stock assessment analyses on north Pacific albacore, was integrated into the ISC. The ALBWG includes members from coastal states and fishing entities of the region (Canada, China, Chinese-Taipei, Japan, Korea, Mexico, USA) and members from relevant regional fishery and marine science organizations (e.g., IATTC, SPC).

The WCPFC and IATTC are the tuna RFMOs that manage the north Pacific albacore stock in the WCPO and EPO, respectively. Both RFMOs have adopted similar harvest strategies and biological reference points for this stock (WCPFC HS 2022-01; IATTC Resolution C-22-04). These harvest strategies include target, threshold, and limit reference points. The target reference points are $F45_{\%SPR}$, which is the fishing intensity that results in the stock producing a SPR of approximately 45%. The threshold and limit reference points are $30\%SSB_{current,\ F=0}$ and $14\%SSB_{current,\ F=0}$, respectively, which are 30% and 14% of the current, dynamic SSB under zero fishing, and hence fluctuates with changes in recruitment. Prior to the adoption of the harvest strategies in 2022, the WCPFC used a limit reference point of $20\%SSB_{current,\ F=0}$ for this stock. Importantly, the management objectives in the harvest strategies are to: 1) maintain SSB above the limit reference point, with a probability of at least 80% over the next 10 years; 2) maintain depletion of total biomass around historical (2006 – 2015) average depletion over the next 10 years; and 3) maintain fishing intensity at or below the target reference point with a probability of at least 50% over the next 10 years. In addition, both RFMOs have current management measures (WCPFC CMM 2019-03; IATTC Resolution C-05-02) that maintain albacore fishing effort at or below the average effort levels during 2002 – 2004.

The previous stock assessment in 2020 (ALBWG 2020a) used an integrated, length-based, and age- and sex-structured forward-simulating statistical stock assessment model in the Stock Synthesis (SS) modeling framework (Methot and Wetzel 2013) to assess stock status. Model diagnostics indicated that the model was able to estimate the stock production function and the effect of fishing on the abundance of the north Pacific albacore stock. The link between catch-at-age and the abundance index added confidence to the data used, the results of the assessments, and the estimated population scale. Although biomass scale was uncertain, female SSB in the terminal year of the assessment (i.e., 2018) was estimated to be 43.0 % of unfished SSB and fishing intensity on the stock was relatively low (i.e., $F_{2015\text{-}2017} = F50_{\%SPR}$). In 2020, the ALBWG concluded that the north Pacific albacore stock was not likely in an overfished condition relative to the $20\%SSB_{current,\ F=0}$ limit reference point used by the WCPFC in 2020. Although there were no adopted reference points based on fishing intensity or mortality in 2020, the ALBWG evaluated the average fishing intensity during 2015 – 2017 against seven potential reference points during the 2020 assessment, and concluded that the stock was not likely experiencing overfishing.

The adoption of the abovementioned biological reference points in 2022 re-emphasized the importance of estimating population scale from the assessment models. Therefore, during the 2023 assessment, the ALBWG focused on maintaining the ability of the assessment model to estimate the stock production function and the effect of fishing on the abundance of the north Pacific albacore stock. Based on analyses of the data and preliminary models, the ALBWG made four important changes to the base case model in this assessment compared to the previous assessment in 2020 (Section 2.4). However, these changes were relatively minor compared to the changes between the

2014 and 2017 assessments (ALBWG 2014, 2017). First, increased uncertainty was imposed on the size composition and abundance index data for 2020 and 2021 because fishery operations and data collection protocols were likely affected by COVID-19 safety protocols and/or behavioral changes during the pandemic. Second, two JPLL fleets were further subdivided into nominally juvenile and adult fleets to improve model fits and diagnostics. Third, a new adult abundance index was developed from the JPLL fleet in Area 2, Quarter 2 to better represent adult SSB trends. Fourth, selectivity patterns for the two main JPPL fleets were modified to no longer have annually changing selectivities due to model convergence issues.

This report presents the results of the 2023 assessment of north Pacific albacore tuna, and provides scientific advice on stock status and conservation information to fisheries managers. The assessment uses updated fishery data through 2021 in a length-based, age- and sex-structured integrated statistical stock assessment model fitted to an abundance index derived from JPLL data that was considered to be representative of adult albacore abundance in the north Pacific Ocean. The biological parameters used in the base case model were identical to the 2020 assessment. This assessment was conducted through a series of in-person and online meetings during 2022 – 2023, and supersedes the 2020 assessment (ALBWG 2020a). The objectives of this assessment are to: 1) understand the population dynamics of the north Pacific albacore tuna stock by estimating population parameters such as time series of recruitment, biomass and fishing intensity; 2) determine stock status by summarizing results relative to the suite of adopted biological reference points; and 3) to provide conservation information for fisheries managers on whether management objectives in the harvest strategies are likely to be met, based on projections using two historical harvest scenarios.

2.0 BACKGROUND

2.1 Biology

2.1.1 Stock structure

Albacore tuna in the Pacific Ocean consist of the north Pacific stock (focus of this assessment) and the south Pacific stock. The discreteness of these stocks is supported by fishery data [lower catch rates in equatorial regions; Suzuki et al. (1977)], tagging data [there are no south Pacific Ocean recoveries of fish tagged in the north Pacific Ocean; Ramon and Bailey (1996)], ecological data [albacore larvae are rare in samples from equatorial waters; Ueyanagi (1969)], and genetic data [genetic differentiation between north and south Pacific albacore; Takagi et al. (2001)]. In addition, a recent study of single nucleotide polymorphisms of north Pacific albacore from a wide range of locations suggested that the north Pacific albacore stock is best thought of as a single, well-mixed stock with limited amounts of mixture from the south Pacific albacore stock (Vaux et al. 2021). Thus, north Pacific albacore is assumed to be a discrete, reproductively isolated stock, with no internal sub-group structure within the stock.

2.1.2 Reproduction

Albacore are batch spawners, shedding hydrated oocytes, in separate spawning events, directly into the sea where fertilization occurs. Spawning frequency is estimated to be 1.7 d in the western Pacific Ocean (Chen et al. 2010), and batch fecundity ranges between 0.17 and 2.6 million eggs (Ueyanagi 1957; Otsu and Uchida 1959; Chen et al. 2010). Female albacore mature at lengths ranging from 83 cm fork length (FL) in the western Pacific Ocean (Chen et al. 2010) to 90 cm FL in the central Pacific Ocean (Ueyanagi 1957), and 93 cm FL in waters north of Hawaii (Otsu and Uchida 1959).

Spawning occurs primarily in tropical and sub-tropical waters between Hawaii (155°W) and the east coast of Taiwan and the Philippines (120°E) and between 10 and 25°N latitudes at depths exceeding 90 m (Ueyanagi 1957, 1969; Otsu and Uchida 1959; Yoshida 1966; Chen et al. 2010). Although spawning probably occurs over an extended period from March through September in the western and central Pacific Oceans, recent evidence based on a histological assessments of gonadal status and maturity (Chen et al. 2010) shows that spawning peaks in the March-April period in the western Pacific Ocean, which is consistent with evidence from larval sampling surveys in the same region (Nishikawa et al. 1985). In contrast, studies of albacore reproductive biology in the central Pacific Ocean have concluded that there was a probable peak spawning period between June and August (Ueyanagi 1957; Otsu and Uchida 1959) but these studies were based on indirect observation methods, were more than 50 years old, and have not been updated using modern histological techniques (e.g., see Chen et al. 2010).

2.1.3 Growth

Growth of albacore tuna is commonly modeled by a von Bertalanffy growth function, with rapid growth in immature fish followed by a slowing of growth rates at maturity and through the adult period. Growth in the first year of life is uncertain since these young fish are rarely captured in any of the active fisheries in the north Pacific Ocean. However, juvenile albacore recruit into intensive surface fisheries in both the eastern and western Pacific Oceans at age-2 and as a result, much better size-at-age and growth information is available. Early growth models combined both sexes because sex-specific fishery data were not collected, although it was known that adult males attained a larger size than females (Otsu and Uchida 1959; Yoshida 1966; Otsu and Sumida 1968). Chen et al. (2012) provided clear evidence of sexually dimorphic growth functions for males and females after they reach sexual maturity and reported that males attained a larger size and older age than females (114 cm FL and 14 years vs. 103.5 cm FL and 10 years, respectively).

A re-examination of the age and growth data compiled by Wells et al. (2013), some of which were used as conditional age-at-length data in the 2011 assessment, showed that for those individuals in which sex was recorded, there was clear evidence of sexually dimorphic growth between males and females (Xu et al. 2014). Given the clear evidence of sexual dimorphism in the growth and longevity of north Pacific albacore, the ALBWG used the same sex-specific male and female von Bertalanffy growth functions in this assessment as used in the assessments from 2014 through 2020. These growth parameters were estimated externally to the stock assessment model by Xu et al. (2014), who combined the sex-specific datasets compiled by Chen et al. (2012) and Wells et al. (2013). James et al. (2020a) concurred that the current sex-specific growth parameters are the best available scientific information but also suggested that the ALBWG collect sex-specific age-length samples using a coordinated biological sampling plan (James et al. 2020b) to improve current growth curves, and examine regional and temporal differences in length-at-age.

2.1.4 Movements

North Pacific albacore are highly migratory and these movements are influenced by oceanic conditions (e.g., Polovina et al. 2001; Zainuddin et al. 2006, 2008). The majority of the migrating population is believed to be composed of juvenile fish (i.e., immature animals that are less than 5 years old and 85 cm FL), which generally inhabit surface waters (0-50 m) in the Pacific Ocean. Some juvenile albacore undertake trans-Pacific movements and display seasonal movements between the eastern or western and central Pacific Ocean (Ichinokawa et al. 2008; Childers et al. 2011). The trans-Pacific movements track the position of the transition zone chlorophyll front (Polovina et al. 2001; Zainuddin et al. 2006, 2008) and increase when large meanders in the Kuroshio current occur, increasing albacore prey availability in the transition zone (Kimura et al. 1997; Watanabe et al. 2004). Westward movements of juveniles tend to be more frequent than eastward movements (Ichinokawa et al. 2008), corresponding to the recruitment of juvenile fish into fisheries in the western and eastern Pacific Ocean and are followed by a gradual movement of older juveniles and mature fish to low latitude spawning grounds in the western and central Pacific Ocean. These general patterns may be complicated by seasonal movements of juvenile and adult fish, as well as sex-specific movements of large adult fish, which may be predominately male, to areas south of 20°N. The significance of sex-specific movements on the population dynamics of this stock is uncertain at present.

2.2 Fisheries

Albacore tuna is a valuable species with a long history of exploitation in the north Pacific Ocean by numerous nations and with a variety of gears (e.g., Clemens 1961). Over the assessment period (1994 – 2021), the total reported catch of north Pacific albacore for all nations combined (Fig. 2.1) peaked at a 119,210 t in 1999 and reached lows of 42,828 and 43,264 t in 2021 and 2019, respectively. Average catch over the model time frame (1994-2021) was 77,101 t. Over the last five years (2017-2021), Japanese fisheries accounted for 66.2 % of the annual total harvest on average, followed by fisheries from the United States (14.1 %), Chinese-Taipei (8.9 %), Canada (4.3 %), China (2.0 %), Korea (0.3 %), and Mexico (0.0 %). During the same five-year period, non-ISC countries, primarily Vanuatu, harvested an average of 4.1 % of the total annual catch.

The main gears deployed to harvest albacore in the north Pacific Ocean are longline, and surface gears like troll and pole-and-line (Fig. 2.2). Surface fisheries capture smaller, juvenile fish, and include the Canada and USA troll and pole-and-line fisheries and JPPL fisheries. Over the assessment time frame (1994 – 2021), surface fisheries have harvested approximately 55.9 % of the north Pacific albacore catch. Longline fisheries, which fish deeper in the water column and tend to capture a larger mix of age classes, were responsible for harvesting about 40.5 % of the albacore during the same period, with major fleets from Japan, Chinese-Taipei, the USA, and more recently China and Vanuatu. Pole-and-line catches in the 2000s exhibited greater year-to-year variability than other gear types due to target switching between skipjack (*Katsuwonus pelamis*) and albacore by some vessels on the fishing grounds off the east coast of Japan (Kiyofuji and Uosaki 2010).

An important fishery in previous assessments was the high seas drift gillnet fishery that began in 1978 and ceased operations in 1993 as a result of United Nations General Assembly Resolution 44/225, which put in place a moratorium on the use of high seas driftnets (Uosaki et al. 2011). The high seas drift gillnet fisheries consisted of two main gear types using: 1) large-mesh nets primarily targeting tunas, billfishes, sharks (i.e., tuna gillnet); and 2) small-mesh nets targeting flying squid (i.e. squid gillnet) (Ito et al. 1993). Previous assessments developed base case or sensitivity models with a start year of 1966. However, the ALBWG decided not to do so for this assessment because of recently identified problems with the data from this fishery (ALBWG 2022). Most importantly, the ALBWG found that the records of Japanese drift gillnet catches of north Pacific albacore consisted primarily of landings by large-mesh gillnets but did not include large amounts of removals by the squid gillnets. Estimates of these unaccounted albacore removals by the Japanese squid gillnet fishery approximated 1.4 and 0.9 million fish for 1989 and 1990, respectively (Yatsu et al. 1993). The squid gillnet fisheries of Korea and Chinese-Taipei were also substantial and on a similar scale to the Japanese squid gillnet fishery but there have been no estimates of albacore bycatch for these fisheries (Gong et al. 1993; Yeh and Tung 1993). The ALBWG therefore recommended that research be performed to develop timeseries of catch and size compositions from these fisheries in part from available observer data (Fitzgerald et al. 1993; ALBWG 2022). Given the start year of 1994 and the initial conditions used for this assessment, the problems with the data from the high seas drift gillnet fisheries are not important for this assessment.

2.3 Conceptual Model

Based on numerous discussions on the biology and fisheries of north Pacific albacore tuna, the ALBWG developed a conceptual model for the 2017 assessment (Fig. 2.3), and subsequently developed a population dynamics model from the conceptual model (ALBWG 2017). The use of a conceptual model improved the population dynamics model, resulting in substantially improved model diagnostics. Most importantly, an ASPM diagnostic analysis showed that the estimated catch-at-age and fixed productivity parameters (growth, mortality and stock-recruitment relationships with and without annual recruitment deviates) were able to explain trends in the adult abundance index. Based on these findings, the ALBWG concluded that the 2017 base case model was able to estimate the stock production function and the effect of fishing on the abundance of the north Pacific albacore stock.

The basic components of the conceptual model were that: 1) movements of juvenile albacore were highly variable and varied by season, year, and cohort but tended to stay in temperate waters (north of 25 – 30°N); 2) this variable movement and hence availability of juvenile albacore to fisheries targeting them resulted in highly variable size composition data for these fisheries; 3) after maturity, adult albacore exhibited movements into subtropical waters (south of 25 – 30°N); 4) adult albacore tended to stay in subtropical waters but also exhibited relatively consistent seasonal movements; 5) albacore exhibited sex- and age-specific differences in mortality, growth, and distribution; and 6) sex ratios of adult albacore in subtropical waters appeared to be biased towards adult males but the degree of bias varied by longitude, with the highest proportion of adult females in the area west of 160°E.

2.4 Important Changes from 2020 Assessment

There were four main changes to the base case model compared to the previous assessment in 2020.

2.4.1 Increased uncertainty in 2020 and 2021

The World Health Organization declared COVID-19 to be a global pandemic on 11 March, 2020 (Liu et al. 2020). The safety protocols, social restrictions, and behavioral changes associated with the pandemic strongly impacted human activities on a global scale, and was undoubtedly a large shock to fisheries, seafood markets, and data collection systems (White et al. 2021; Link et al. 2021; Smith et al. 2022; Kobayashi 2022). The peak of these impacts, which was likely in 2020 and may have extended to 2021, overlapped with the terminal years of this assessment.

The ALBWG examined the data for 2020 – 2021 and found that fisheries operations and data collection of albacore fisheries were likely impacted during this period. For example, the abundance index of adult albacore used in this assessment showed a large drop to a historical low in 2020 but subsequently rebounded by almost 3-fold in 2021 to above average levels. Such large fluctuations in an adult index for albacore tuna were considered biologically implausible for the stock and suggested that the catchability of the index likely fluctuated greatly during the period despite the standardization process. Members of the ALBWG also reported that data collection for some fisheries were impacted by COVID-19 safety protocols. Preliminary models indicated that the 2020

– 2021 data resulted in a very large spike in the 2017 estimated recruitment, which was the historically highest estimate and 2 times higher than the next highest. The ALBWG considered the very high recruitment estimate for 2017 to be implausible.

Given the impacts of the pandemic on fisheries, seafood markets, and data collection systems, it is important to better understand these impacts on the data from this period. However, more work and observations from the pandemic and post-pandemic periods would be required. Therefore, for the time being, the ALBWG considered that the data from 2020 – 2021 to be more uncertain than other years. Over time and with more research, there may be a better understanding of the data from this period and this uncertainty may be reduced. The ALBWG represented this increased uncertainty in the 2020 and 2021 data by adding 0.1 to the CVs of the abundance index, which had an average CV of 0.2 for the other years, and multiplied the input sample sizes of the size composition data by 0.1, for these two years.

2.4.2 Japan longline fleet structure

In the 2020 assessment, the ALBWG recommended further investigations into the fleet structure of the two JPLL fleets in Quarter 1 of Area 1 and 3 (ALBWG 2020b). These fleets had relatively large amounts of catch and it was important to model the observed removals (i.e., catch-at-age) well. The two fleets had different catch units but shared the same size composition data and estimated selectivity. The size composition data in the 2020 assessment from these two fleets suggested a mixture of two fisheries, with one fishery catching predominantly juveniles and another catching predominantly adult fish.

Prior to the 2023 assessment, the WG analyzed the size composition and average-weight data from these fleets, and separated each of these fleets into nominally juvenile and adult fisheries (Ijima and Tsuda 2022). Therefore, there were four JPLL fleets in Quarter 1 of Area 1 and 3 for this assessment, with two nominally juvenile JPLL fleets with catch units in tons and number of fish respectively, and two nominally adult JPLL fleets with catch units in tons and number of fish respectively.

2.4.3 Abundance index

In the 2020 assessment, the base case model was fit to one abundance index, which was based on the CPUE of the JPLL fleet in Quarter 1 of Area 2 and considered to be representative of the adult female albacore population trends (Fujioka et al. 2019, 2020; ALBWG 2020b). The size composition data in Area 2 suggested that the CPUE in this area would be more representative of the adult female albacore population than other areas, and the JPLL fleet targeted adult albacore in Quarter 1. However, the ALBWG noted that the primary spawning area and season was Area 2 in Quarter 2, and therefore recommended research on whether an index from Quarter 1 or 2 was more representative of adult female population trends.

An analysis of the size composition and average-weight data from the JPLL fleets in Area 2 suggested that the Quarter 1 catch was a mix of juvenile and adult albacore (Matsubayashi et al. 2023). By contrast, the Quarter 2 catch consisted predominantly of adult albacore, and was therefore considered to be more representative of adult albacore population trends. Therefore, for the 2023 assessment, a new index was developed from the CPUE of the JPLL fleet in Quarter 2 of Area 2, using a spatiotemporal model (Ijima and Tsuda 2023; Matsubayashi et al. 2023).

2.4.4 Selectivity

An important feature of the 2020 assessment was highly time-varying selectivity patterns for the two most important JPPL fleets. These two fleets caught the largest amounts of albacore and had highly variable and multimodal size compositions. The WG considered it important to fit the observed removals (i.e., catch-at-age) well and found that doing so improved model diagnostics (ALBWG 2020b). However, during the model development of the 2023 base case model, the WG found that preliminary models with highly time-varying age-selectivities for the two main JPPL fleets resulted in models without positive, definite Hessian matrices, which indicated potentially poor model convergence and unreliable uncertainty estimates. However, models without any time varying age-selectivities matched the expected catch-at-age poorly and had poor ASPM diagnostics. Therefore, the WG developed a model with a single age-selectivity time block for the two main JPPL fleets near the end of the historical period. This model adequately matched the catch-at-age and had good ASPM diagnostics.

3.0 DATA

Three types of data were used in this assessment: fishery-specific catches, size compositions, and abundance indices. Although data prior to 1994 were available, data for this assessment were compiled from 1994 through 2021 because the ALBWG agreed to follow the decision made for the 2017 and 2020 assessments (ALBWG 2017, 2020b) and start the base case model in 1994 (Section 3.2). Therefore, only data from 1994 – 2021 are shown in this section. Data sources and temporal coverage of the available datasets are summarized in Figure 3.1.

3.1 Spatial Stratification

The geographic area of this assessment is the Pacific Ocean north of the equator (0°) to 55°N and from 120°E to 100°W (Fig. 3.2). This area includes all of the known catches of north Pacific albacore from 1994 through 2021. The base case model is not spatially explicit but instead used a fleets-as-areas approach (Hurtado-Ferro et al. 2014a). Fisheries were defined using multiple criteria, including fishing area, and therefore implicitly included spatial inferences (Table 3.1). Analyses of fishing operations and size composition data from JPLL and USLL vessels in the north Pacific showed that there were five areas with relatively consistent size distributions of albacore (ALBWG 2016; Ochi et al. 2016; Teo 2016) (Fig 3.2). These five fishing areas were used to define fisheries in the base case model (Section 3.3).

3.2 Temporal Stratification

The time frame of the 2023 assessment was 1994−2021. Catch and size composition data were compiled into quarters (Jan−Mar, Apr−Jun, Jul−Sep, Oct−Dec) and a quarterly time step was used in the base case model.

The 1994–2021 time frame for this assessment is an extension of the 2017 and 2020 assessments (1993–2015; 1994-2018) (ALBWG 2017, 2020b) but is substantially shorter than the time frames used for earlier assessments, which had start years of 1966 (e.g., ALBWG 2014). Although the catch time series extended back to at least 1952 for some fisheries, a start year of 1994 was used because previous assessments had identified issues with the data and model parameters prior to 1994, especially during the 1980s and early 1990s (ALBWG 2014, 2017). These issues, still unresolved, included: 1) unaccounted catch and bycatch of high seas driftnet vessels during the 1980s and early 1990s; 2) a large proportion of size samples from Japanese longline vessels during the 1980s and early 1990s consisted of large albacore (≥100 cm FL) that were poorly fit with reasonable selectivity processes; 3) these observations of large albacore may be due to differences in growth, especially the L_{inf} parameter, during the 1980s and early 1990s; and 4) conflicts between poorly fit size composition data and the primary longline indices during the 1980s and early 1990s. Most importantly, starting the base case model in 1994 allowed the ALBWG to estimate population scale from the adult albacore index, which was informative on population scale. In addition, starting the model in 1994 allowed the ALBWG to avoid modelling potentially unrepresentative size composition data from the 1980s and early 1990s that may be misinformative on population scale.

3.3 Fleet Definitions

Thirty-five fishing fleets were defined for the assessment on the basis of gear, fishing area, season, and unit of catch (numbers or weight), and all catch and effort data were allocated to these fleets (Table 3.1). The aim was to define relatively homogeneous fisheries with greater differences in selectivity and catchability between fisheries than temporal changes in these parameters within fleets. This approach allowed the ALBWG to use differences in selectivity between fleets as proxies for movement between fishing areas (Hurtado-Ferro et al. 2014a; Waterhouse et al. 2014) since movement information is not available. These fleets consisted primarily of 28 longline fleets from Japan (F01 – F20), USA (F26 & F27), Chinese-Taipei (F28 & F29), Korea (F30), China (F31 & F32), and Vanuatu and others (F33) (Table 3.1). There were also five pole-and-line fleets from Japan (F21 – F25), and the surface gears (primarily troll and pole-and-line) from Canada, Mexico, and the USA, which were combined into a single EPO surface fleet (F34). In addition, high seas drift net catches from Japan, Korea, and Chinese-Taipei, which were important in the past but had zero catch during the modeling period, and catch from all other miscellaneous gears (e.g., purse-seine) from Japan and Chinese-Taipei were combined into a single miscellaneous fleet (F35). The approximate fishing area of each fleet can be deduced from Table 3.1 and Figure 3.2.

3.4 Catch

Estimates of total catch in each fleet were compiled by calendar year and quarter for 1994 – 2021 (Fig. 3.3). Catch was reported and compiled in original units consisting of weight in metric tons (t) or 1000s of fish (Table 3.1).

3.5 Relative Abundance Indices

The ALBWG reviewed nine abundance indices from JPLL (Matsubayashi et al. 2022, 2023, 2023), JPLL (Matsubara et al. 2022a, 2022b), TWLL (Hsu et al. 2022), and EPO surface (Teo 2022a) fisheries (ALBWG 2022, 2023). Based on this review and experience from previous assessments, the ALBWG decided to use the spatiotemporal abundance index from the JPLL fleet in Area 2 and Quarter 2 (F12; 1996-2021) as the index of adult abundance (Matsubayashi et al. 2023) for the base case model. This index has some similarity to the adult index used in the 2020 assessment, same JPLL fishery and area (Area 2) but with three additional terminal years of data, different quarter (Quarter 2 instead Quarter 1), and different standardization model (AR1 spatiotemporal model using INLA instead of a Generalized Additive Mixed Model using STAN). The F12 index used in this assessment is an appropriate index for adult albacore in the north Pacific because the majority of the adult female albacore population in the north Pacific Ocean is thought be in the western Pacific, especially Area 2 during Quarter 2 (main spawning area and season). In addition, the F12 index had good contrast and preliminary ASPM analysis results showed that an ASPM was able to fit well to the index, which the ALBWG interpreted as an indication that the F12 index was informative on both population trend and scale.

Three of the candidate indices were used in sensitivity runs: 1) JPLL fleet in Area 2 and Quarter 1 (F11; 1996 – 2021); 2) JPPL fleet in Areas 3 and 5 and Quarter 2 (F22; 1994 – 2021); and 3) EPO surface fleet in Areas 3 and 5 and Quarter 3 (F34; 1999 – 2021). The other candidate abundance indices were considered inappropriate or insufficiently developed for use in this assessment, and will be re-evaluated for the upcoming 2026 assessment.

Standardized annual values and input coefficients of variation (CVs) for the F12 index used in the base case model and indices used in sensitivity runs are shown in Tables 3.2 and 3.3, and Figures 3.4 and 3.5. The relative weighting of the indices was controlled by adjusting the input CVs (Section 4.4).

3.5.1 F12 – Japanese longline index, Area 2 and Quarter 2 (1996 – 2021)

The only index that was fitted in the base case model was developed using set-by-set catch (number of albacore) and effort (1000s of hooks) data from logbooks of JPLL vessels operating in Area 2 during 1996–2021 (Ijima and Tsuda 2023; Matsubayashi et al. 2023). A Bayesian spatiotemporal zero-inflated negative binomial generalized linear mixed effects model, with first-order autoregression (AR1), was developed using the R-INLA software package (Rue et al. 2009; Lindgren et al. 2011; Martins et al. 2013) and used to standardize the catch and effort data.

The model was described by:

$$
\begin{aligned}
Catch_{alb} \sim intercept + year{:}\,qtr + f(fleet, model = iid) + f(hpb, model = iid) \\
+ f(vessel\,ID, model = iid) + f(w, model = AR1) + offset\left(\frac{hooks}{1000}\right)
\end{aligned}
$$

where *year:qtr* were quarterly fixed explanatory factors, *w* were the spatial random effects calculated with a stochastic partial differential equation approach and had a first-order temporal autoregression, and *hpb*, *fleet*, and *vessel ID* were random effects for hooks pre basket, fleet, and vessel respectively. The model was fit to data from all four quarters in 1996 – 2021 but the abundance index was calculated for Quarter 2 of all years. Quarter 2 was chosen for this index because Quarter 2 is the primary spawning season and likely had a higher proportion of adult females compared to other area and quarter combinations (Section 2.4.3). Quarter 2 size composition data also appeared to have more consistent size compositions compared to the other quarters. The ALBWG observed that the proportion of sets with zero albacore catch, species composition, and Pearson residuals were biased in 1994 and 1995 (ALBWG 2019; Fujioka et al. 2020). Therefore, similar to the 2017 and 2020 assessments, the ALBWG decided to start the index in 1996 instead of 1994 (ALBWG 2019). In addition, the CV of the F12 index could not be estimated due to software issues with the resampling of the posteriors (Ijima and Tsuda 2023). The ALBWG therefore assumed a CV of 0.2 for 1996 – 2019, and 0.3 for 2020 – 2021 (Section 2.4.1). Further details on the data and standardization model can be found in Matsubayashi et al. (2023), and Ijima and Tsuda (2023).

3.5.2 F11 – Japanese longline index, Area 2 and Quarter 1 (1996 – 2021; sensitivity run)

In the 2020 assessment, the only index that was fit in the base case model was the index from the JPLL fleet in Area 2 and Quarter 1 (i.e., F09 index in the 2020 assessment). Therefore, for this assessment, the ALBWG developed an abundance index from the JPLL fleet in Area 2 and Quarter 1 (F11) and used it in a sensitivity run and bridging analysis.

Similar to the F12 index, a Bayesian spatiotemporal zero-inflated negative binomial generalized linear mixed effects model, with first-order autoregression (AR1), was used to standardize the catch and effort data from the F11 fleet. The only difference was that only data from Quarter 1 was fit to the model and *year* instead of *year:qtr* were the fixed explanatory factors. This difference allowed the F11 index to be more similar to the F09 index used in the 2020 assessment.

3.5.3 F22 – Japanese pole-and-line index, Areas 3 and 5 in Quarter 2 (1994 – 2021; sensitivity run)

The ALBWG considered using the standardized CPUE of the JPPL fishery operating in Areas 3 and 5 to represent the population trends of juvenile albacore (ALBWG 2022). After filtering the data with a suite of criteria, the CPUE of the JPPL fishery from quarters 2 and 3 were standardized with a delta-lognormal generalized linear model that had year, location (5x5°), and vessel ID as fixed effects (Matsubara et al. 2022a). However, the ALBWG found that the index from this fishery to be inappropriate for use in the base case model of the assessment. First, the fishery exhibits highly variable size compositions that vary by year and season, which suggests that the catchability of the fishery is also likely highly variable. Second, the fishery switches between targeting albacore and skipjack, and large increases in the index are observed when the fishery switches to targeting albacore, suggesting that the model is unable to correct for the target switching. Thirdly, although this fishery is the largest albacore fishery, it only covers portion of the distribution of juvenile albacore. Fourth, it was assumed that the abundance index for quarter 2 and 3 would be the same but there was no evidence to support this assumption. Therefore, the ALBWG only considered that this index was suitable for a sensitivity.

3.5.4 F34 – EPO surface index, Areas 3 and 5 in Quarter 3 (1999 – 2021)

The ALBWG also considered using the standardized CPUE of the US troll and pole-and-line fishery operating in Areas 3 and 5 to represent the population trends of juvenile albacore (ALBWG 2022). The EPO surface fishery (F34) consists largely of US and Canadian vessels using troll and pole-and-line, and standardized CPUE of US and Canadian vessels were highly similar (Teo et al. 2010). After filtering the data with a suite of criteria, the CPUE of the US surface fishery from quarters 2, 3 and 4 were standardized with a lognormal generalized linear model that had year, location, and quarter as fixed effects (Teo 2022a). However, the ALBWG found the index from this fishery to be inappropriate for use in the base case model of the assessment. Most importantly, the EPO surface fishery is dependant on the seasonal migration of juvenile albacore into the EPO and being available to the fishery. Given that this migration is variable between years, the CPUE of this fishery also varies in part due to changes in availability. The standardization model was not able to standardize for the changes in availability. Therefore, the ALBWG only considered that this index was only suitable for a sensitivity analysis. It should be noted that a pause in fishing operations under the US-Canada albacore treaty in 2012 resulted in changes to the fishery operations of the EPO surface fishery during that year, and 2012 is therefore excluded from this index.

3.6 Size Composition

Quarterly length composition data from 1994 through 2021 were used in this assessment. Length data were available for 23 of the 35 fleets in the base case model (Table 3.1 and Fig. 3.6) and were compiled into 2-cm size bins, ranging from 26 to 142 cm FL, where the labels are the lower boundary of each bin. Most of these fleets exhibited clear modes when lengths were aggregated across quarters and years (Fig. 3.6). The length data for the JPPL fleets (F21 – F25) exhibited exceptionally high variability in the number of modes and mean sizes between quarters and years.

The length frequency observations were the estimated catch-at-size (i.e., size compositions were raised to the catch) for 20 of the fleets with size composition data and these size composition data were fitted in the base case model (Table 3.1). However, the size composition data from three of the fleets (F31 – F33) were not raised to the catch and the base case model was not fitted to these data Fig. 3.7). Instead, it was assumed that the selectivity of these fleets were the same as other longline fleets with similar fishing operations and fishing area (Section 4.3.1).

The majority of albacore length composition data were collected through port sampling or on-board sampling by vessel crews or observers. Length data for the JPLL (F01 – F05; F11 – F14; F19 – 20) and JPPL fleets (F21 – F25) were measured to the nearest cm at the landing ports or onboard fishing vessels from which catch-at-size data were derived (Ijima et al. 2017). Fork lengths of albacore in the EPO surface fleet (F34) were compiled from port samples of the US troll and pole-and-line fisheries (Teo 2022b). Although length composition data were available for the Canadian component of this fleet (2008-present), these data were not used because the USA and Canada components of the fleet overlap greatly in their fishing areas and size composition plots of both fisheries are very similar. The data from the USA component were thus considered representative of the entire fleet. Length compositions for the USLL fleet were collected by observers (Teo 2022c). Albacore lengths for the TWLL fleet (F28) were measured onboard fishing vessels and compiled for 1995-2021 by the Overseas Fisheries Development Council of Chinese-Taipei (Hsu et al. 2022). Length composition data prior to 2003 were not considered representative of catches by this fleet because they were sampled from a restricted geographic area and shorter annual time period than the spatial and temporal scope at which the fleet was operating (ALBWG 2014). Thus, only the 2003-2021 size composition data were fitted in the base case model.

3.7 Sex Composition

Size composition data from Japanese longline training and research vessels are currently the primary source of sex ratio information for north Pacific albacore because sex composition data are not commonly collected by commercial fisheries. Although sample sizes of sexed individuals only ranged from about 10 to 300 fish per year, the sex composition data show that males reach larger sizes than females (Figure 3.8), and that the sex ratio of males to females becomes heavily biased towards males at large sizes (>100 cm FL) (Ashida et al. 2016; Aoki et al. 2023). This bias towards males at large sizes has also been observed in south Pacific albacore (Farley et al. 2013), and is likely due to the sex-specific differences in growth (Williams et al. 2012; Chen et al. 2012) and/or natural mortality (Kinney and Teo 2016). Although sex composition data from Japanese training and research vessels were collected, the data were undocumented and not considered for the assessment. The sex composition data were instead compiled into two survey fleets (i.e., without catch) for Areas 2 (S36) and 4 (S37), and used as a visual reference to the expected sex ratio from the base case model.

Japanese and US scientists have made substantial progress towards a polymerase chain reaction based sex identification method for albacore tuna (Craig and Hyde 2020). Once the precision of this sex identification method has been established, the ALBWG would endeavour to collect sex ratio data from commercial fisheries for future assessments.

4.0 MODEL DESCRIPTION

The 2023 stock assessment of north Pacific albacore tuna was conducted using the SS modeling platform (Methot 2000; Methot and Wetzel 2013). A sex-specific, length-based, age-structured, forward-simulating, fully-integrated, statistical model was developed for the stock assessment. The specification of the base case model for north Pacific albacore followed several steps. First, the spatial and temporal extent of fleets in the assessment were defined based on analyses of the biology and historical fishing operations of albacore fisheries (ALBWG 2016, 2019). Second, the data sources and inputs for these fleets in the model, including total catch, indices of relative abundance, and size compositions were identified, collated and reviewed for completeness, trends, and outliers or unusual behaviour. Third, important biological parameters (e.g., growth, stock-recruitment relationship) were obtained from previous studies after review by the ALBWG and included in the model as fixed parameters, or estimated within the assessment model (Table 4.1). Based on these inputs, preliminary models were developed and iteratively refined through an analysis of model fits (e.g., total and component negative log-likelihoods) and diagnostic outputs (e.g., ASPM, R_0 profiles, Pearson residuals) (ALBWG 2023), resulting in a base case model with several differences from the base case model in the 2020 stock assessment (ALBWG 2020b). These differences included: 1) imposing increased uncertainty onto the size composition and abundance index data for 2020 and 2021 because fishery operations and data collection protocols were likely affected by COVID-19 safety protocols; 2) subdividing two JPLL fleets into nominally juvenile and adult fleets to improve model fits and diagnostics; 3) developing and fitting to a new adult abundance index from the JPLL fleet in Area 2, Quarter 2; and 4) modifying selectivity patterns for the two main JPPL fleets to have only a single time block (2016 – 2021) due to model convergence issues (Section 2.4).

4.1 Stock Synthesis

Stock Synthesis is a highly flexible, statistical age-structured population modeling platform that can incorporate multiple data types and account for a variety of biological, fishery, and environmental processes (Methot and Wetzel 2013). Importantly for this assessment, SS can model sex-specific growth but fit to non-sex-specific observations. Although SS was initially developed for and used in US domestic stock assessments, particularly groundfish assessments on the US west coast, its use has spread to stock assessments of large pelagic fish like tunas and sharks because of the flexibility it provides for modelling multiple data types and processes.

The SS platform consists of three subcomponents: 1) a population dynamics subcomponent that simulates the assessed population (i.e., population numbers and biomass at age) using processes such as natural and fishing mortality, and the stock-recruitment relationship; 2) an observational subcomponent that relates the modeled population dynamics to observed quantities including abundance indices and size composition data; and 3) a statistical subcomponent that quantifies the fit of the observations to the simulated population using maximum likelihood methods. The 2023 north Pacific albacore assessment model was implemented using SS version 3.30.21, which is publicly available (https://github.com/nmfs-stock-synthesis/stock-synthesis) (Methot 2000; Methot and Wetzel 2013).

4.2 Biological and Demographic Assumptions

4.2.1 Maximum age

The maximum age bin in the model was 15 years based on the maximum observed age (Wells et al. 2013). This bin served as the accumulator for all older ages. To avoid potential biases associated with the approximation of dynamics in the accumulator age, the maximum longevity was set at an age sufficient to result in near zero fish in this age bin (≈ 1 percent of an unfished cohort).

4.2.2 Growth

The 2023 assessment used the same sex-specific growth curves as the base case model for the previous assessments since 2014, which were based on the study by Xu et al (2014). Sex-specific growth curves were used because studies have found that north Pacific albacore tuna exhibit sex-specific growth, with male albacore exhibiting larger size at age after maturing and growing to larger size (Chen et al. 2012; Xu et al. 2014). Xu et al. (2014) combined age-at-length data from Chen et al. (2012), who primarily aged otolith samples from the northwestern Pacific, and Wells et al. (2013), who primarily obtained samples from the central and eastern North Pacific, to develop sex-specific growth curves covering the entire north Pacific Ocean.

A von Bertalanffy growth function, as parameterized by Schnute (1981), was used to model the relationship between fork length (cm) and age for north Pacific albacore:

$$L_2 = L_{inf} + \left(L_1 - L_{inf}\right)e^{-K(A_2 - A_1)}$$

where L_1 and L_2 are the sizes associated with ages, A_1 and A_2, respectively, L_{inf} is the asymptotic length, and K is the growth coefficient.

In this assessment, L_1 was fixed at 43.504 and 47.563 cm for females and males at age 1, respectively (Table 4.1). The L_{inf} and K parameters were also fixed at sex-specific values from Xu et al. (2014) (L_{inf} - female: 106.570 cm, male: 119.150 cm; K - female: 0.2976 y^{-1}, male: 0.2077 y^{-1}) (Fig. 4.1). The coefficients of variation (CVs) of size-at-age at L_1 (CV_1) and L_{inf} (CV_2) were fixed at 0.06 and 0.04 for both female and male albacore in the base case model, based on estimates of these CVs during preliminary runs of the 2017 assessment. The CV_1 parameter was well estimated in the preliminary runs because of the clear modal structure in juvenile size composition data and the model results were not highly sensitive to this parameter. However, the CV_2 parameter was highly influential in the preliminary model results because of an interaction with the L_{inf} parameter. An analysis of conditional age-at-length data found that the variability of size-at-age for older albacore was similar to juvenile albacore and that the CV was approximately 0.04 (Xu et al. 2014). Sensitivity analyses on the CV_2 parameter and alternative growth models were performed (Section 5.6.3).

4.2.3 Weight-at-length

Non sex-specific weight-length relationships are used to convert catch-at-length to weight-at-length data (Fig. 4.2). A previous study (Watanabe et al. 2006) reported that there were seasonal differences in the relationship between weight (kg) and fork length (cm) of north Pacific albacore. These non sex-specific seasonal weight-at-length relationships were used in this assessment (Table 4.1) and previous assessments since 2014 (ALBWG 2014) because there were no previous studies documenting sex-specific differences in the weight-length relationships of north Pacific albacore.

4.2.4 Natural mortality

The 2023 assessment used the same age and sex-specific parameters for *M* as the base model for the previous assessment in 2017 and 2020, which were based on study by Teo (2017) (Table 4.1). In assessments prior to 2017, *M* was assumed to be 0.3 y^{-1} for both sexes at all ages but this assumption was not well supported (Kinney and Teo 2016). First, the ALBWG incorporated results from studies that used meta-analytical methods on a range of empirical relationships between M and life history parameters (Hamel 2015; Then et al. 2015; Kinney and Teo 2016; Teo 2017), which identified an *M* of 0.38 and 0.49 y^{-1} for adult male and female albacore tuna, respectively. These results corresponded well to an independent study of tagging data, which estimated a non sex-specific *M* of 0.45 – 0.5 y^{-1} for north Pacific albacore (Ichinokawa et al. 2008). Based on these results, the ALBWG assumed that the M of juvenile north Pacific albacore tuna followed a Lorenzen (1996) relationship between size and M for age-0 to age-2, with no difference between the sexes until age-3. Upon reaching age-3, the M for male albacore is assumed to be 0.38 y^{-1} and the M for female albacore is assumed to be higher, reaching 0.49 y^{-1}, which may reflect the cost of reproduction. Sensitivity analyses on the M parameters were performed (Section 5.6).

4.2.5 Sex specificity

A sex-specific (two sex) model was used for this assessment because of sex-specific differences in growth (Chen et al. 2012; Xu et al. 2014) and natural mortality (Kinney and Teo 2016; Teo 2017) of north Pacific albacore. In addition, males predominate in longline catches of large, mature albacore from Japanese research and training vessels, while juveniles <85 cm generally have a sex ratio of 1:1 (Ashida et al. 2016). However, there are currently no data on the sex of individual fish caught by commercial fisheries. As described above, sex-specific growth curves and natural mortality were used in the base case model. However, the base case model did not include sex-specific selectivity, and sex ratio at birth was assumed to be 1:1.

4.2.6 Movement

This stock assessment did not have explicit spatial structure and did not explicitly model the movements of north Pacific albacore. North Pacific albacore are known to exhibit seasonal and ontogenetic movements (e.g., Ichinokawa et al. 2008; Childers et al. 2011), but it is not currently feasible to develop a spatially explicit assessment model due to the lack of well designed, and consistent tagging data. Instead, selectivity patterns for fisheries were used as a proxy for spatial structure, which helps to compensate for potential biases caused by the lack of explicit spatial structure in the assessment model (Hurtado-Ferro et al. 2014a). This fleets-as-areas approach entailed the collection and pre-processing of fishery data in this assessment in an area-specific fashion, especially Japanese longline fisheries, and therefore contain spatial inference (Section 3.3).

4.2.7 Stock structure

The current stock assessment assumes a single stock of albacore in the north Pacific Ocean from the equator to 55°N latitude and between 120°E and 100°W longitude (Fig. 3.2). This assumption is supported by evidence from tagging, and seasonal fishing pattern studies (Suzuki et al. 1977; Ichinokawa et al. 2008; Childers et al. 2011). Studies of albacore population genetics (Chow and Ushiama 1995; Takagi et al. 2001; Montes et al. 2012) support the hypothesis of two stocks in the Pacific Ocean, but do not provide conclusive results on finer scale structure. More recently, a study of single nucleotide polymorphisms of north Pacific albacore from a wide range of locations suggested that the north Pacific albacore stock is best thought of as a single, well-mixed stock with limited amounts of mixture from the south Pacific albacore stock (Vaux et al. 2021).

4.2.8 Recruitment and reproduction

North Pacific albacore were assumed to have one spawning and recruitment period in the second quarter of the year (April – June) based on recent histological assessments of gonadal status and maturity from the western Pacific Ocean (Chen et al. 2010; Ashida et al. 2016). Although historical circumstantial evidence supported spawning in the central Pacific Ocean near Hawaii through the third quarter of the year (e.g., Otsu and Uchida 1959), there is no recent confirmation of this spawning segment so it was not considered in the assessment. Ashida et al. (2016) also recently estimated the length at 50% maturity for female north Pacific albacore at 86 cm, which was approximately the expected length at age-5. Based on this finding, the ALBWG assumed that 50% of the albacore at age-5 were mature and that all fish age-6+ were mature (Fig. 4.3). This maturity ogive has been used in the previous assessments since 2006 (ALBWG 2014).

A standard Beverton-Holt stock recruitment relationship was used in this assessment. The expected annual recruitment was a function of spawning biomass with steepness (h), virgin recruitment (R_0), and unfished equilibrium spawning biomass (SSB_0) corresponding to R_0, and was assumed to follow a lognormal distribution with standard deviation σ_R (Methot 2000; Methot and Wetzel 2013). Annual recruitment deviations were estimated based on the information available in the data and the central tendency that penalizes the log (recruitment) deviations. A log-bias adjustment factor was used to assure that the estimated log-normally distributed recruitments were mean unbiased (Methot and Taylor 2011).

Recruitment variability (σ_R) was tuned and fixed at 0.46 to approximate the expected variability of preliminary models, which had recruitment variability ranging from 0.4 to 0.5 depending on model configuration. The log of R_0, annual recruitment deviates, and the offset for the initial recruitment relative to virgin recruitment, R_1, were estimated in the base case model. The choice of estimating years with information on recruitment was based on a preliminary model run with all recruitment deviations estimated (1994 – 2021). The first few years of size composition data often contain some information on recruitment from early cohorts before 1994 and the variability of recruitment deviations often increases as the information content decreases the further back in time prior to the starting year examined (Methot and Taylor 2011). The number of years for which recruitments may be observed from the early cohorts was set at 10, and these initial recruitment deviances were estimated in the model. Ten annual deviations were estimated prior to the start of the model in 1994 (i.e., 1984-1993). The 10-year period was chosen because early model runs showed negligible information on deviates more than 10 years prior to the beginning of the data. Bias adjustment was used to account for the reduction in information content from the data on recruitment deviations during the early and late periods. This adjustment mostly affects the estimation of uncertainty and not the population trajectory.

Steepness of the stock-recruitment relationship (h) was defined as the fraction of recruitment from a virgin population (R_0) when the spawning stock biomass is 20% of its unfished level (SSB_0). Recently, Lee et al. (2012) concluded that if the model is correctly specified, then steepness is estimable for relatively low productivity stocks with good contrast in spawning stock biomass. However, estimating h within the assessment model for north Pacific albacore is likely to be imprecise and biased because contrast in the spawning biomass over the assessment period is relatively poor. Two independent estimates of steepness for north Pacific albacore (Brodziak et al. 2011; Iwata et al. 2011), based on the life history approach of Mangel et al. (2010), reported values of h ranging from 0.84 to 0.95. Therefore, the ALBWG assumed a h of 0.9 in this assessment, which was the same as for previous assessments during 2014 – 2020, and performed sensitivity analyses within a plausible range of h, and estimating h with a prior (Section 5.6). Nevertheless, the ALBWG notes that these steepness estimates are subject to considerable uncertainty and further work is needed to evaluate steepness estimates.

4.2.9 Initial conditions

A model must assume something about the period prior to the start of the main population dynamics period. Typically, two approaches are used to achieve this assumption. The first approach starts the model as far back as necessary to satisfy the notion that the period prior to the estimation of dynamics was in an unfished or near unfished state. However, this approach is not viable for this assessment because the base case model started in 1994 (Section 3.2). Instead, a second approach was used in which initial conditions were estimated (where possible) assuming equilibrium catch.

The equilibrium catch is the catch taken from a fish stock when it is in equilibrium with fishery removals and natural mortality balanced by stable recruitment and growth. The initial fishing mortality rates in the assessment model that remove these equilibrium catches were estimated to allow the model to start at an appropriate depletion level. Initial fishing mortality rates were estimated for the F28 (TWLL in Areas 3 & 5) because it captures a wide size range of albacore, but the initial fishing mortality rates were not fitted to historical catches prior to 1994. This approach allowed the model to start in 1994 at a depletion level that was consistent with the adult abundance index and size composition data without being overly constrained. In addition, the model included estimation of 10 recruitment deviations prior to 1994 to develop a non-equilibrium age structure at the start of the model time frame.

4.3 Fishery Dynamics

4.3.1 Selectivity

The base case model has a sex-specific structure, with sex-specific growth curves. However, it was assumed that female and male albacore have identical size selectivity for each fleet because sex-specific size composition data were not available. Selectivity curves were fleet-specific and assumed to be a function of only size for all but five fisheries (Table 4.1). Preliminary model runs indicated that size composition data of the JPPL fleets in Areas 3 and 5 (F21 – 24) and the EPO surface fishery (F34) had very strong modes corresponding to juvenile age classes and could not be adequately fit using only size selectivity curves. Therefore, the selectivity curves of these five fleets were assumed to be a product of size and age, which improved model fits. The age-based selectivity was intended to capture differences in the availability of juvenile fish to the fishing gear based on movement patterns, which may vary between seasons and years. Selectivity curves were estimated for all fisheries with representative size composition data while selectivity curves for fisheries without representative size composition data were assumed to be the same as fisheries with similar operating characteristics (season, area, gear) and estimated selectivity curves. If specific fisheries had changes in fishery operations or exhibited changes in size composition data consistent with changes in movement patterns, then selectivity was allowed to vary with time to account for these changes. Highlights of the parameterization of the selectivity curves are briefly described below but more details can be found in Tables 4.2, 4.3, 4.4, and 4.5.

Selectivity curves for longline fleets and the JPPL fleet in Area 2 (F25) were assumed to be dome-shaped, and were modeled using either double-normal functions (F03, F05, F11, F12, F13, F14, F20, F25, F26, F27, and F28) or spline functions (F01, F02, F04, and F19), depending on the size data and model fit (Table 4.2). Fleets were first fitted with double-normal functions but F01, F02, F04, and F19 were found to have inadequate model fits with this approach. These four fleets were subsequently fit with spline functions, which are substantially more flexible. The double-normal selectivity functions were configured to use four parameters: 1) peak, which is the initial length at which albacore were fully selected; 2) width of the plateau at the top; 3) width of the ascending limb of the curve; and 4) width of the descending limb of the curve. If the estimated width of the plateau at the top was negligible and tended to hit the lower bounds, then that parameter was fixed at a small value. The spline selectivity functions were configured to be three knot splines. The first and third knots were generally located near the edges of the respective size compositions, while the second knot was typically located near the midpoint between the first and third knots. However, the locations of the knots were subject to some trial and error. The values of two of the three knots were estimated relative to the value of the third knot, which was fixed at an arbitrary value. The gradients before the first knot and after the third knot were also estimated.

Selectivity curves of the JPPL fleets in Areas 3 and 5 (F21, F22, F23, and F24) and the EPO surface fishery (F34) were assumed to be a product of size and age selectivities because their size composition data exhibited very strong modes corresponding to juvenile age classes (Tables 4.3 and 4.4). The size selectivity curves for these fleets were assumed to be dome-shaped and were modeled using double normal functions, which were configured as described above. The F21, F22, F23, and F24 fleets were assumed to share a size selectivity because the size selectivity was assumed to represent gear selectivity and these fleets shared the same fishing vessels and gear. The age selectivity of the juvenile age-classes (age-1 through age-5) of these five fleets were assumed to represent availability and were estimated as free parameters. If the age selectivity parameter of an age class hit the upper or lower bound, that parameter was fixed at the upper or lower bound during the final model run to stabilize the optimization of the model. The interactions between the age and size selectivity functions for these five fleets were difficult to visualize but resulted in substantially improved fits to their size composition data.

The selectivity curves for fleets lacking representative size composition data (F06, F07, F08, F09, F10, F15, F16, F17, F18, F29, F30, F31, F32, F33, and F35) were assumed to be the same as (i.e., mirrored to) closely related fleets or fleets operating in the same area (Table 4.5). For example, the selectivity of F06 was assumed to be the same as F01 because F05 was identical to F01 except for their catch units (Table 3.1).

Selectivity curves for relative abundance indices were assumed to be the same as the fleet from which each respective index was derived. For example, size selectivity for the F12 index was assumed to be the same as the F12 fleet.

Selectivity curves were allowed to vary over time for fleets exhibiting important changes in fishery operations or if large changes in fish availability during certain periods were observed as changes in the size composition data. The USLL fleets (F26 and F27) had major regulatory changes during 2001 to 2005 to mitigate turtle bycatch, which likely affected fishing operations after 2005 (Table 4.2). The fishing operations of the EPO surface fishery (F34) were found to have changed after 1998, with the fishery moving closer to the US West Coast during and after 1999 (Xu et al. 2013) (Table 4.4).

The JPPL fleets exhibited highly variable size composition data, which was thought to be due to the variability in fishery operations and/or availability of different age classes of albacore in different areas at different times. An important feature of the 2020 assessment was highly time-varying selectivity patterns for the two most important JPPL fleets (F22 and F23). These two fleets caught the largest amounts of albacore and had highly variable and multimodal size compositions. It was considered important to fit the observed removals (i.e., catch-at-age) well and found that doing so improved model diagnostics (ALBWG 2020b). However, for the 2023 assessment, preliminary models with highly time-varying age-selectivities for F22 and F23 resulted in models without positive, definite Hessian matrices, which indicated potentially poor model convergence and unreliable uncertainty estimates. However, preliminary models without any time varying age-selectivities matched the expected catch-at-age poorly and had poor ASPM diagnostics. Therefore, a model with a single age-selectivity time block for F22 and F23 near the end of the historical period was developed. This model adequately matched the catch-at-age and had good ASPM diagnostics. The ALBWG performed sensitivity analyses to evaluate the effect of changing this selectivity assumption (Section 5.6).

4.3.2 Catchability

Catchability, *q*, was estimated (solved analytically) assuming the abundance index was proportional to vulnerable biomass with a scaling factor of *q*. It was assumed that *q* was constant over time for each index.

4.4 Data Observation Models

The current assessment model fitted three data components: 1) total catch, 2) relative abundance indices, and 3) size composition data. The observed total catches were assumed to be unbiased and relatively precise, and were fitted assuming a lognormal error distribution with standard error (SE) of 0.05.

The relative abundance indices were assumed to have lognormally distributed errors with SE in log space, which is approximately equivalent to CV (SE/estimate) in natural space. The CVs of each index are shown in Tables 3.2 and 3.3. The reported CVs from the standardization model of an abundance index only captures observation errors within the standardization model and do not reflect process errors that are inherent in the link between the unobserved vulnerable population and observed abundance indices. Therefore, an additional constant was added to the CVs of the indices, such that the average CV for any index was equivalent to 0.2. Importantly, the WG considered the estimated CVs from the standardization model of the F12 index to be unreliable, and instead assumed a constant CV of 0.2 for 1996 - 2019. In addition, the WG considered the F12 index for 2020 and 2021 to be more uncertain than other years, and represented this increased uncertainty by assuming CVs of 0.3 for these two years (Section 2.4.1).

The size composition data were assumed to have multinomial error distributions with the error variance determined by the effective sample size (*effN*). Size measurements of fish are usually not random samples of fish from the entire population, but are instead highly correlated within each set or trip (Pennington et al. 2002). The effective sample size is usually substantially lower than the actual number of fish measured because the variance within each set or trip is substantially lower than the variance within a population. The WG considered setting the initial effective sample size to the number of trips from which fish were measured to account for the lower variance within a trip relative to the population. However, most albacore fisheries only record the number of fish sampled. Therefore, an analysis of the EPO surface fishery (F34) was used to relate the number of fish sampled to the number of trips. Based on this analysis, we assumed that 100 fish sampled were equivalent to a sampled trip. Size composition records with sample size of <1 were considered unrepresentative and removed. In addition, the WG considered the size composition data for 2020 and 2021 to be more uncertain than other years, and represented this increased uncertainty by multiplying the sample sizes of all fleets by 0.1 for these two years (Section 2.4.1). The input sample sizes for each fishery were further rescaled by a multiplier (0.274) so that the average input sample size for fishery with the most fish sampled (F28) was approximately 30. Therefore, the input sample sizes varied between fleet and over time, depending on the sampling that occurred for that fleet and period.

4.5 Data Weighting

Integrated stock assessment models fit a variety of data components, including abundance indices and size composition data. The results of these models can depend substantially on the relative weighting between different data components (Francis 2011). A statistical approach using the maximum likelihood estimates of variances or effective sample sizes to weight each data component by model fit (Deriso et al. 2007; Maunder 2011) tends to put too much weight on size composition data because numerous important processes such as variability in movements and selectivity are often not modeled or mis-specified. As a result, many assessments now weight different components based on expert knowledge of the data sampling, fishery operations, and biology of the stock, in order to balance or prioritize information from various data components.

Relative abundance indices were prioritized in this assessment based on the principle that relative abundance indices should be fitted well and that other data components such as size composition data should not induce poor fits to the abundance indices because abundance indices are a direct measure of population trends and scale (Francis 2011). Preliminary models indicated that the size composition data from the F11 fleet degraded the fit of the F12 abundance index, especially relative to the ASPM model fit to the index (ALBWG 2023). The weighting to the size composition data from the F11 fleet was down-weighted by reducing the size composition sample size multiplier from 0.274 (Section 4.4) to 0.0274, which is in effect multiplying the likelihoods of these data by 0.1. Down-weighting these size compositions resulted in improved model fits to the F12 abundance index. The effect of these data weightings on model results was investigated using sensitivity runs.

In addition, the ALBWG used the Francis data weighting method (TA1.8 in Francis 2011) to examine the weighting of each fleet's size composition data relative to how well the model fitted to the data. Results from preliminary models indicated that four fleets (F02, F05, F22, and F28) had size composition data that were over-weighted (i.e., Francis weighting multiplier of <1.0). The weighting to the size composition data from the F02, F05, F22, and F28 fleets were down-weighted by reducing the size composition sample size multiplier from 0.274 (Section 4.4) to 0.170, 0.2626, 0.210, and 0.160, respectively. These sample size multipliers correspond to down-weighting the size composition data of these fleets by 38, 4, 23, and 42%, respectively, resulting in Francis weighting multipliers of these four fleets in the base case model of approximately 1.

4.6 Model Diagnostics

Model diagnostics (Carvalho et al. 2021) were used to assess issues associated with convergence, model structure, parameter mis-specification, and data conflicts in the 2023 base case model. The following diagnostic tools were employed in this assessment: 1) model convergence tests, 2) ASPM diagnostic, 3) R_0 likelihood profiles, 4) residual analysis, 5) retrospective analysis, 6) catch-curve analysis, and 6) prediction skill.

4.6.1 Model convergence

Convergence to the global minima was examined by changing initial parameter values and the order of phases used in the optimization procedure. Particular attention was placed on the initial value and estimation phase of parameters, such as R_0, that influence population scale because these changes force the model to search over a vastly expanded portion of the likelihood surface. In addition, all initial parameter values were randomly jittered by sampling from a uniform distribution centered at input parameter values with upper and lower bounds of ±10%. The optimized likelihoods, R_0 values, and important management quantities, were examined from 50 such model runs to ensure that these model runs did not find a solution with better likelihoods.

4.6.2 ASPM diagnostic

Following the proposal by Maunder and Piner (2015), the base case model was modified into an ASPM and ASPM-R (ASPM with recruitment deviates) to identify whether the catch and F12 abundance index were consistent with the estimated scale and trends in the population. Maunder and Piner (2015) stated that "When catch does explain indices with good contrast (e.g., declining and increasing trends), it suggests that a production function is apparent in the data, therefore providing evidence that the index is a reasonable proxy of stock trend". In this assessment, the base case model was modified into an ASPM by fixing the stock-recruitment relationship, sex-specific growth curves, and selectivities of all fleets to those estimated in the base case model, not estimating annual recruitment deviates so that recruitment follows the stock recruitment curve, and not fitting to the size composition data. The ASPM was subsequently modified into an ASPM-R by estimating annual recruitment deviates.

4.6.3 Likelihood profile on virgin recruitment (R_0)

Likelihood profiling over virgin recruitment (R_0) was used to examine the influence of each data component on the overall population scale (Lee et al. 2014). The unfished level of recruitment (R_0) is a global scaling parameter in an SS model because it is proportional to unfished biomass. This process is used to assess whether the relative data weightings are appropriate and/or whether the model is mis-specified. The likelihood profile consisted of running a series of models with the $\ln(R_0)$ parameter fixed at a range of values above and below that estimated within the model, and examining the likelihoods of the various data components. The estimated annual recruitment deviates were also changed from random deviates to a vector of deviates that summed to zero, which minimized the ability of the model to compensate for a lower fixed R_0 by raising the recruitment deviates.

4.6.4 Residual analysis

Model residuals (i.e., differences between observed data and expected values) were examined to evaluate model fit and performance. The residuals were first visually examined for patterns. The variances of residuals were also compared to evaluate the statistical assumptions of the observation model. If the variance of the residuals differs substantially from the assumed variance, then the relative data weightings likely were not appropriate. However, a lack of residual patterns does not ensure that the model is not mis-specified because parameter estimates can change to compensate for the mis-specification (Maunder and Punt 2013).

4.6.5 Retrospective Analysis

Retrospective analysis was used to identify systemic inconsistencies in population estimates given increasing or decreasing data periods. In this assessment, we performed a within-model retrospective analysis by systematically removing the terminal year of data from successive models (1 to 5 years), while maintaining the same model structure between models.

4.6.6 Catch Curve Analysis

Catch curve analyses are used to determine if the information from the size composition data on the population scale and trends are consistent with that from the other data in the model (Minte-Vera et al. 2021). Catch curve analyses are set up by fitting the model only to the size composition data and estimating all parameters except those associated with the index (i.e., catchability).

4.6.7 Prediction Skill

The prediction skill of the 2023 base case model was evaluated by hindcasting the model and calculating the MASE of the F12 index. Following Kell et al. (2021), the MASE of a model with time 1 to T for a prediction horizon of h time steps and $n+1$ predictions from replicate models with 0 to n time steps removed from the terminal end (i.e., a retrospective peel of n time steps), was calculated as:

$$MASE = \frac{\frac{1}{n+1}\sum_{t=T-n}^{T}\left|y_t - \hat{y}_{t|t-h}\right|}{\frac{1}{n+1+h}\sum_{t=T-n-h}^{T}\left|y_t - y_{t-h}\right|}$$

where, the mean absolute prediction error (i.e., the numerator) was calculated as the mean of the absolute differences between the observations y at time t (y_t) and the predictions of the observations made h steps previously ($\hat{y}_{t|t-h}$) for all the predictions made ($n+1$); and scaled by the mean absolute naive prediction error (i.e., the denominator) calculated as the mean of the absolute differences between the observations y at time t (y_t) and the naive predictions of the observations made h steps previously (y_{t-h}) for all the observations ($n+1+h$) between the first time step used (T-n-h) and time step T.

A series of SS model were developed from the 2023 base case model, with a retrospective peel of 0 to 5 years and a prediction horizon of 1 to 5 years. The prediction horizons of 2 and 5 years are of special importance to this study because the terminal years of data are typically 2 years prior to the year when the assessments are performed, and the assessments are currently conducted on a 3-year cycle. For example, the terminal year for the 2023 base case model was 2021, and the next NPALB assessment is expected to be conducted in 2026. A MASE of <1 indicates that the model is able to predict the SSB trends better than a naïve prediction. For the 2020 assessment, the MASE for models with horizons of one or two years were <1 but gradually increased to approximately 2.1 with a horizon of five years (Teo and Minte-Vera 2022).

4.7 Sensitivity to Model Assumptions

A series of sensitivity runs were performed to examine the effects of plausible alternative model assumptions on the assessment results, and to help identify the major axes of uncertainty in this assessment. The sensitivity analyses conducted in this assessment (Table 4.6) can be categorized into three main themes: 1) biology (e.g., natural mortality, steepness); and 2) data (e.g., data weighting, start year, alternative indices); and 3) model structure (e.g., selectivity, equilibrium catch). For each sensitivity run, female spawning stock biomass (SSB), fishing intensity (1-SPR) trajectories, and where appropriate, model fits to the data, were compared.

The model structure of the base case model for this assessment had several important changes from the 2020 base case model (Section 2.3). A sensitivity model was developed to represent the model structure of the 2020 base case model and used as a bridging analysis. This sensitivity model is similar to but not identical to the 2020 base case model due to changes in data preparation and model structure.

4.8 Fishery Impact Analysis

The impact of the surface and longline fisheries on SSB was evaluated. The fishery impact analysis was conducted using the parameterization and assumptions of the base case model and dropping the annual catches (1994-2021) from the SS base case data file one-by-one and calculating the SSB time series for each scenario. The magnitude of differences in the simulated SSB trajectories with and without fishing indicates the impact of the major fishery types on the female SSB. Due to the assumed selectivity of the gillnet and miscellaneous fleet (F35), it was included as part of the surface fisheries.

4.9 Future Projections

Stock projections were used to assess the impact of current and historical fishing intensity on the management objectives of IATTC and WCPFC for this stock. In this assessment, a new version of the software package (SSfuture C++; ssfcpp; ssfcpp_simple_2023.cpp) was developed to perform the future projections (Ijima et al. 2023). The ssfcpp software package is similar in principle to the SS base case model and is highly similar to the ssfcpp package used in the 2020 assessment (Ijima 2020). In general, ssfcpp used the estimated sex-specific N-at-age and biological parameters from the base case model and projected the population forward using either a fixed F-at-age (constant F scenario) or randomly resampled F-at-age from 2005 – 2019 (randomly resampled F scenario), and a recruitment deviate vector sampled from a distribution consistent with the σ_R in the base case model. It should be noted that ssfcpp incorporated three main sources of uncertainty in the projections: 1) uncertainty of N-at-age estimates in the terminal year of the base case model; 2) uncertainty in the F-multipliers; and 3) uncertainty in the average virgin recruitment. Thus, ssfcpp incorporates most of the estimated uncertainty from the base case model into projections and is an improvement over the projections from previous assessments. However, it should also be noted that ssfcpp did not incorporate estimation uncertainties of the selectivity and recruitment deviate estimates. The ALBWG considered these projections to be an improvement over projections from previous assessments but more improvements will still be needed in the future.

Two 10-yr projection scenarios, constant $F_{2018\text{-}2020}$ and randomly resampled F scenarios, were used to evaluate the impacts of fishing on the management objectives of IATTC and WCPFC. The randomly resampled F scenarios had F-at-age that were randomly sampled from 2005 – 2019. This 2005 – 2019 period was chosen as representative of the variability in F-at-age on north Pacific albacore, after both IATTC and WCPFC put in place current management measures (WCPFC CMM 2019-03; IATTC Resolution C-05-02) that maintain albacore fishing effort at or below the average effort levels during 2002 – 2004.

Future recruitment was sampled from a distribution consistent with the expected recruitment variability (σ_R = 0.46) of the recruitment time series (1994 – 2021) in the base case model. The sex-specific F-at-age time series was estimated from the base case model and used to remove albacore from the appropriate age and sex in the projected populations. Projections started in 2022 and continued for 10 years through 2031. The projected female SSB, fishing intensity, $SSB/14\%SSB_{current,F=0}$ ratios, and total biomass (age-1+) were calculated for each projection. 400 initial populations were simulated by sampling from a multivariate normal distribution consistent with the estimated N-at-age in 2021 and its variance-covariance matrix. Each initial population was subsequently projected using 400 runs for 10 years. Each run used a random 10-year recruitment vector that was resampled from the distribution of expected future recruitment, which incorporated uncertainty in the stock-recruitment relationship, and expected recruitment variability. Depending on scenario, the F-at-age used was either based on the average F-at-age during 2018 – 2020, or randomly resampled from 2005 – 2019. The projected F-at-age included the uncertainty in the F-multipliers but not the estimated selectivity. A total of 160,000 (400 x 400) runs were performed for each projection scenario.

5.0 STOCK ASSESSMENT MODELLING RESULTS

5.1 Model Convergence

All estimated parameters in the base case model were within the set bounds and the final gradient of the model was 3.591E-5, which is consistent with a model that converged onto a local or global minimum. Preliminary models results showed that the likelihood surface around the model convergence zone was bumpy and prone to converging onto local minima. The base case model was therefore run from the SS 'par' file, with highly precise initial values for parameters. Based on the results of 50 model runs with different phasing and initial values, the base case model likely converged to a global minimum (i.e., there was no evidence of a lack of convergence to a global minimum) (Fig. 5.1). Total negative log-likelihood from the model run using the phasing and initial parameters from the base case model was 785.702 and the lowest (best) among these runs, and 0 out of 50 model runs also obtained the same negative log-likelihood. In addition, the estimated virgin recruitments in log-scale [ln(R_0)], average fishing intensities during 2018 – 2021, and the estimated female SSB in 2021 relative to the 30%$SSB_{current, F=0}$ ThRP were also similar from runs with total negative log-likelihoods similar to the base case model (Fig. 5.1). Importantly, all 50 model runs had estimated current fishing intensities lower than the $F45_{\%SPR}$ TRP and had SSB_{2021}/30%$SSB_{current, F=0}$ ratios that were >1. Therefore, even if the base case model had not converged onto the global minima, the results of a model that converged onto the global minima would be highly similar to the base case model presented here.

5.2 Model Diagnostics

5.2.1 Model fit of abundance indices

The base case model fitted the F12 adult abundance index adequately (Fig. 5.2 and Table 5.1). The root-mean-squared-error (RMSE) between observed and predicted abundance indices for the F12 index were 0.23, which was approximately the sum of the input CV and variance adjustment for these indices (Table 5.1). This was important because the F12 index was the primary data source that provided information on the spawning stock biomass trends. The catchability coefficient (q) was solved analytically in the base case model as a single value for each index (Table 5.1).

5.2.2 Model fit of size composition data

Base case model fits to the size composition data were adequate. Overall, the model predicted size compositions matched the observations (Fig. 5.3). Examination of the input sample size (input N) and model estimated effective sample size (*effN*) also show adequate model fits (Table 5.2). A higher *effN* is consistent with better model fit and a mean *effN* of >30 is a sign of good overall model fit. In addition, the ratios of the harmonic mean of *effN* to the mean of input N were all >1, which is interpreted to mean that the base case input N did not assume less error than is evident in the model fits. The model fits to the size composition data of several fleets (F01, F03, F22, and F24), although adequate, had a ratio of the harmonic mean of *effN* to the mean of input N that was <2 and could be improved upon in the next assessment. Importantly, the lack of annually varying selectivity for the JPPL fleets in this assessment resulted in degraded fits to the size composition data compared to the 2020 assessment. Given the large amounts of catch by these JPPL fleets, it would be important to improve the fits at the next assessment. Francis weighting multipliers for all fisheries were ≥1, indicating that the weighting for all fisheries were not greater than suggested by model fits (Table 5.2). Pearson residual plots of the model fit to the size composition data did not reveal substantial patterns in residuals (Fig. 5.4). Where patterns were evident visually, the scale of the residuals was generally small, mostly lying within ± 2 standard deviations.

5.2.3 Age-structured production model (ASPM) diagnostic

The ASPM-R model had very similar scale and populations trends to the base case model, while the ASPM model had a slightly larger scale (Fig. 5.5). Model fit of the ASPM to the F12 index was also similar to the base case model, with both the RMSE and negative log-likelihood of the F12 index of the ASPM (0.234 RMSE; -26.8 log-likelihood units) being similar to the base case model (0.231 RMSE; -26.9 log-likelihood units), while the model fit of the ASPM-R to the F12 index (0.189 RMSE; -31.4 log-likelihood units) was better than the base case model. These results showed that the estimated catch-at-age and fixed productivity parameters (i.e., growth, natural mortality, and spawner-recruit relationship) were able to explain overall trends in the F12 index but the addition of process error in the form of annual recruitment deviates improves the model fit. This finding in turn means that the base case model was able to estimate the stock production function and the effect of fishing on the abundance of the north Pacific albacore stock. Similar to the 2017 and 2020 assessments, the connection between catch-at-age and the F12 index adds confidence to the model and data used.

5.2.4 Likelihood Profiles on Virgin Recruitment (R_0)

Results of the likelihood profiling on virgin recruitment, R_0, for the abundance indices and size composition data components of the model are shown in Fig. 5.6. Changes in the likelihood of each data component are a measure of how informative that data component is to the overall estimated population scale.

The ASPM diagnostic showed that the F12 index was informative on the estimated population scale, especially the status of the stock with respect to the 30%$SSB_{current, F=0}$ ThRP. However, due to the moderate exploitation levels of this stock, the R_0 profile of the F12 index showed that the changes in log-likelihood over the range of R_0 examined was relatively small, which means that the estimated population scale was relatively uncertain. Nevertheless, it is important to note that the negative log-likelihood profile of the F12 index was asymmetrical, with increasing negative log-likelihoods when R_0 was low and relatively little change when R_0 was high. This finding is consistent with a F12 index that is particularly useful for providing information on whether the population is lower than a certain minimum level but less informative on the upper limit to the population scale (i.e., uncertainty was primarily on the high R_0 side). The primary aim of estimating the SSB in this assessment was to determine whether the estimated SSB is lower than the LRP (i.e., determine whether the stock was in an overfished condition). Since the R_0 profiles show that the lower bound is better defined, it adds confidence to the ALBWG's evaluation of stock condition relative to the limit reference point.

The information from the size composition data appeared to be relatively consistent with the index data. Importantly, the minima of the likelihood profile of the size composition data occurred around the same range of R_0 as the minima of the likelihood profile of the index data, which suggests that estimated population scales from both data sources were relatively consistent. In addition, the range of changes in the negative log-likelihood of the size composition data were only slightly larger than the range of the F12 index, which suggests that the size composition data are appropriately weighted.

However, it should be noted that the interpretation of the R_0 profile is complicated because the recruitment deviates in the model allow the model to compensate, at least partially, for the fixed changes in R_0. As the R_0 is fixed at lower values, the estimated recruitment deviates go higher to compensate. Even though the estimated recruitment deviates for these profiles are forced to sum to zero, there is minimal information on recruitment in the terminal years of the model and the recruitment deviates in the terminal years go lower so that the recruitment deviates still sum to zero (Fig. 5.6). Therefore, the effect of fixing R_0 is only partial and limited.

Overall, notwithstanding the difficulties in interpretation, the R_0 likelihood profile showed that there was substantial uncertainty in the estimate of population scale of this assessment, which was reflected in the uncertainty in biomass estimates. Nevertheless, the R_0 likelihood profile also showed that the estimated ln(R_0) in the base case model was consistent with all the data components, especially the F12 index, that the ALBWG considered to be important for defining population scale in the assessment model and for defining the status of the stock.

Importantly, even when the fit to the F12 index was degraded (increase in log-likelihood of about 2.74) with a ln(R_0) fixed at 11.8 , the ratio of the estimated female SSB relative to unfished SSB remained higher than the 14%$SSB_{current, F=0}$ LRP and slightly lower than the 30%$SSB_{current, F=0}$ ThRP (Fig. 5.7). Thus, the results of this assessment with respect to the status of the stock, are relatively robust.

5.2.5 Retrospective Analysis

Successive elimination of terminal year data resulted in retrospective patterns in the estimates of spawning biomass and recruitment. Removing one to five years of terminal data resulted in changes in the results of the model (Fig. 5.8). The annualized Mohn's rho (Mohn 1999) for female SSB, recruitment, and SSB depletion of the retrospective models were calculated using the method described by Hurtado-Ferro et al. (2014b) and found to be 0.19, -0.14, and 0.08 y^{-1}, respectively. Analysis of preliminary models indicated that the cause of this retrospective pattern was likely the data from 2020 – 2021. The ALBWG considered the data from this period to be more uncertain due to COVID-19 safety protocols but more work is need to understand the data from this period (Section 2.4.1). Importantly, the estimated female SSB from all the models from this analysis remained above the 30%$SSB_{current,F=0}$ ThRP, which is consistent with the conclusion that the results of this assessment are relatively robust.

5.2.6 Catch Curve Analysis

The catch curve model resulted in similar estimated female SSB scale and trends to the base case model (Fig. 5.9). However, the fit to the F12 index was degraded in the catch curve analysis relative to the base case model (Fig. 5.9). It is useful to compare the results of the catch curve analysis with that of the ASPM analysis (Fig. 5.5). The catch curve analysis resulted in a highly similar estimated population scale to the ASPM-R model but was slightly lower than the ASPM model. The catch curve model also had inferior fits to the F12 index compared to the ASPM and ASPM-R models. Overall, the catch curve analysis indicated that the information on population scale from the size composition data was consistent with that from the abundance index, and adds confidence to the results of this assessment. However, it also indicates that the estimated population trends are also strongly influenced by the size composition data and may be in conflict with the fine-scale trends in the adult index. Future work would be needed to reduce this conflict with the adult index.

5.2.7 Prediction Skill

The 2020 base case model exhibited some prediction skill over one and two years, exhibiting a MASE of 0.86 and 0.91 respectively (Teo and Minte-Vera 2022). However, the prediction skill of the 2023 base case model was poorer over horizons of 1 – 5 years, with MASE of 1.16 – 1.56 (Table 5.3). The MASE has a relatively simple interpretation, with a score of 0.5 indicating that the model has forecasts that are twice as accurate as naive forecasts. Therefore, given that the MASE for all horizons were >1, the base case model did not exhibit any prediction skill over naive forecasts. The poorer MASE of the 2023 base case model may be due to the uncertain data for 2020 and 2021 (Section 2.4.1). Given these results, it may be useful to update the F12 abundance index during the intervening years to monitor the relative status of the SSB.

5.3 Model Parameter Estimates

5.3.1 Selectivity

The estimated selectivity of fisheries assumed to have size-only selectivity or a product of size and age selectivity (F21, F22, F23, F24 and F34) are shown in Fig. 5.10 and 5.11, respectively. All but one fleet with size-only selectivity have dome-shaped selectivity. The USLL fleet in Area 2 and 4 (F27), which catches the largest fish, is assumed to have asymptotic selectivity (Fig. 5.10). The selectivity of the F21, F22, F23, F24 and F34 fleets were relatively non-intuitive, especially the age selectivity, because the overall selectivities were products of both size and age selection.

The peak and width of the ascending slope parameters for the fisheries with dome-shaped selectivity are typically precisely estimated while the width of the plateau and descending slope parameters have high uncertainty (Table 4.2 and 4.3). The differences in uncertainty of parameters in a double normal selectivity curve is expected because the width of the plateau and descending slope parameters are highly correlated, which increases the uncertainty in these parameters. It should also be noted that most of the age selectivity parameters of the F21, F22, F23, F24 and F34 fisheries were also highly uncertain due to correlation between parameters (Table 4.4).

5.3.2 Catch-at-Age

Juvenile albacore aged 2, 3, and 4 were the largest components of north Pacific albacore catch (Figure 5.12) due to the importance of surface fisheries (primarily troll, pole-and-line, and including other miscellaneous gears).

5.3.3 Sex Ratio

The fraction of females in the population changes by age and length (Fig 5.13). Sex ratio is approximately 1:1 until albacore reach age-3+, after which males becomes more common due to the higher M in females at ages-3+. This change in sex ratio is further accentuated by the differences in growth such that the sex ratio is heavily biased for albacore >100 cm FL. The heavy bias towards males at large sizes (>100 cm) has been observed in this stock (Fig. 3.8) and in the south Pacific albacore stock (Farley et al. 2013). Although the heavily biased sex ratio of large albacore may have consequences in the estimated population dynamics of this stock, the implications of this bias on estimates of management quantities, stock status determinations or the development of conservation advice, are not known.

5.4 Stock Assessment Results

5.4.1 Biomass

The estimated female SSB fluctuated between 1994 and 2021, with a high of 96,031 ± 20,569 t (±SE) in 1999 and a low of 61,770 ± 15,122 t in 2007 (Fig. 5.14 and Table 5.4). Estimated female SSB exhibited an initial decline until 2007 followed by fluctuations without a clear trend through 2021 (Fig. 5.14). In the terminal year of the assessment (2021), female SSB was estimated to be 70,229 ± 20,552 t. The ThRP (30%$SSB_{current, F=0}$) adopted by the IATTC and WCPFC is based on dynamic SSB_0 and has fluctuated between 37,300 to 56,179 t during the assessment period (Table 5.4). The maximum likelihood estimate of female SSB has therefore been above the ThRP throughout the assessment period. However, it should be noted that uncertainties in the estimates of female SSB were relatively large. This was because the virgin recruitment parameter (R_0), which largely determines the population scale, was estimated with a relatively large uncertainty.

Estimated summary biomass (males and females at age-1+) declined at the beginning of the time series until 2004 (Fig. 5.14 and Table 5.4). Subsequently, the summary biomass fluctuated without a trend until 2018, after which the biomass rapidly increased to historically high levels (Fig. 5.14 and Table 5.4). It should be noted that the high summary biomass estimates during 2018 – 2021 were highly uncertain and should be treated with caution. These high summary biomass estimates were due to historically high recruitment estimates in 2017.

5.4.2 Recruitment

Estimated recruitment was generally consistent with the biology of the stock and assumptions in the base case model. Recruitment estimates did not show a substantial trend with respect to female SSB (Fig. 5.14), which was expected because albacore and other tunas have recruitment variability largely driven by environmental conditions, and a steepness of 0.9 was assumed in this assessment. The estimated recruitments were consistent with the expected distribution of recruitment deviations (σ_R = 0.46), where all recruitment estimates were within the expected distribution.

The estimated recruitments have fluctuated widely during the assessment period (1994 – 2021), ranging from historical lows of 107.9 ± 27.6 million fish (± SD) in 2015 to a high of 432.5 ± 121.7 million fish in 2017 (Figure 5.14 and Table 5.4). The high summary biomass estimates during 2018 – 2021 were due to the historically high but highly uncertain recruitment estimates in 2017. The average recruitment during the 1994 – 2021 period was 203.2 million fish, which was slightly below virgin recruitment (217.9 million fish).

Uncertainty in the recruitment estimates was relatively large because uncertainty estimated for the virgin recruitment parameter, which largely determines the population scale, was relatively large. Uncertainty in the recruitment estimates also increase towards the end of the time series because the amount of information on recruitment declines towards the end of a model. It is important to note that the recruitment estimates in the last 5 years (2017-2021) were highly uncertain and should be treated with caution.

5.4.3 Fishing intensity

Fishing intensity in this assessment is based on SPR and calculated as $F_{\%SPR}$. SPR is the ratio of the equilibrium female SSB per recruit that would result from the estimated F-at-age relative to that of an unfished population. Spawning potential ratio (SPR) was used to describe the fishing intensity on this stock. Therefore, $F_{\%SPR}$ can be used to describe the overall fishing intensity on a fish stock, with a lower $F_{\%SPR}$ indicating a higher fishing intensity (Goodyear 1993). The average fishing intensity during 2018 – 2020 was estimated to be $F59_{\%SPR}$ (95% CI: $F72_{\%SPR}$ – $F46_{\%SPR}$), which was relatively moderate and resulted in a population with an SPR of approximately 59%. The fishing intensity on the north Pacific albacore stock has fluctuated between $F72_{\%SPR}$ and $F35_{\%SPR}$ during the assessment period (1994 – 2021) (Table 5.4).

Instantaneous fishing mortality-at-age (F-at-age) was estimated for female and male albacore in the base case model (Fig. 5.15). The F-at-age of juveniles was higher than most of the adult age classes, which corresponds to the larger catches of the surface fisheries. The F-at-age is highly similar in both sexes through age-5, peaking at age-4 and declining to a low at age-6, after which males experience higher F-at-age than females up to age 12. These sex and age-specific differences in F-at-age are due to sex-specific differences in natural mortality and size-at-age for adult albacore.

5.5 Biological Reference Points

The WCPFC and IATTC are the tuna RFMOs that manage the north Pacific albacore stock in the WCPO and EPO, respectively, and have adopted similar harvest strategies and biological reference points for this stock (WCPFC HS 2022-01; IATTC Resolution C-22-04). These harvest strategies include target, threshold, and limit reference points. The target reference points are $F45_{\%SPR}$, which is the fishing intensity that results in the stock producing a SPR of approximately 45%. The threshold and limit reference points are $30\%SSB_{current, F=0}$ and $14\%SSB_{current, F=0}$, respectively, which are 30% and 14% of the current, dynamic SSB under zero fishing, and hence fluctuates with changes in recruitment. Importantly, three of the management objectives in the harvest strategies are to: 1) maintain SSB above the limit reference point, with a probability of at least 80% over the next 10 years; 2) maintain depletion of total biomass around historical (2006 – 2015) average depletion over the next 10 years; and 3) maintain fishing intensity at or below the target reference point with a probability of at least 50% over the next 10 years. In addition, both RFMOs have current management measures (WCPFC CMM 2019-03; IATTC Resolution C-05-02) that maintain albacore fishing effort at or below the average effort levels during 2002 – 2004.

Stock status is depicted in relation to the target ($F45_{\%SPR}$,), threshold ($30\%SSB_{current, F=0}$), and limit ($14\%SSB_{current, F=0}$) reference points (Fig. 5.16; Table 5.5). The estimated female SSB has never fallen below the threshold and limit reference points since 1994, albeit with large uncertainty in the terminal year (2021) estimates. However, the estimated fishing intensity for five years (1999, 2002, 2003, 2004, and 2007) have exceeded the target reference point. Even when alternative hypotheses about key model uncertainties such as growth were evaluated, the point estimate of female SSB in 2021 (SSB_{2021}) did not fall below the threshold and limit reference points, although the risk increases with this more extreme assumption (Fig. 5.16). However, estimated average fishing intensity during 2018-2020 ($F_{2018-2020}$) did exceed the target reference point under one of these alternative hypotheses but did not exceed the average fishing intensity during 2002 – 2004 (Fig. 5.16; Table 5.5).

Biological reference points were computed from the base case model (Table 5.5). The point estimate (±SE) of maximum sustainable yield (MSY – which includes male and female juvenile and adult fish) was 121,880 ± 18,318 t and the point estimate of female SSB to produce MSY (SSB_{MSY}) is 23,154 ± 3,434 t. Current F ($F_{\%SPR, 2018-2020}$) was defined as the average $F_{\%SPR}$ for the years 2018-2020 because terminal year estimates of fishing intensity were generally considered to be uncertain. Current SSB (SSB_{2021}) was defined as the female SSB in 2021. The ratio of $F_{\%SPR, 2018-2020}/F45_{\%SPR}$ was estimated to be 1.22, which indicates that current fishing intensity is slightly lower than the TRP. The ratio of $SSB_{2021}/30\%SSB_{current, F=0}$ was estimated to be 1.81, which indicates that SSB_{2021} is well above the ThRP and LRP (Table 5.5).

5.6 Sensitivity to Model Assumptions

The following sensitivity analyses were performed to examine the effects of plausible alternative model assumptions on the assessment results, and help identify the major axes of uncertainty in this assessment (see Table 4.6 for details).

5.6.1 Sensitivity 01 – Natural mortality

Natural mortality is typically considered to be a major axis of uncertainty in most stock assessments. Sensitivity model runs were performed using: 1) a fixed and constant *M* of 0.3 y^{-1} for both sexes and all ages (as in the 2014 assessment); 2) a fixed and constant *M* of 0.38 and 0.49 y^{-1} for males and females, respectively, of all ages; 3) an estimated, single parameter, female *M* for all ages, with the prior from Teo (2017), $M_{female} \sim \log N[-0.7258, (0.457)^2]$, and a constant logscale offset (-0.21258) between male and female M; and 4) a fixed, sex- and age-specific M based on a Lorenzen size-M relationship before maturity, and a logistic-shaped transition to adult M (0.48 and 0.39 y^{-1} for females and males) linked to the maturity ogive (experimental M option similar to the South Pacific albacore assessment).

Changing the M from the sex-specific M-at-age vector in the base case model to the constant 0.3 y^{-1} in the 2014 assessment or estimating M with a prior resulted in major differences in the estimated dynamic SSB depletion, and fishing intensity of the assessment (Fig. 5.17). The estimated female M was 0.875 y^{-1} with a corresponding male M of 0.707 y^{-1}. The results of the model estimating female M with a prior suggests that there may be information on M in the data but the estimated population dynamics appear to be unreasonable and substantial work needs to be done before estimating M in the base case model. The other two M sensitivity models (see #2 and #4 above) resulted in similar estimated population dynamics to the base case model.

5.6.2 Sensitivity 02 – Steepness

Steepness of the Beverton-Holt stock-recruitment relationship is also often considered a major axis of uncertainty in most stock assessments. Sensitivity model runs were performed using: 1) alternative steepness values (h = 0.75; 0.80; and 0.85) to the base case model (h = 0.90); 2) an estimated h using a prior of $h \sim N[0.9, (0.1)^2]$; and 3) an estimated M (see #2 in Section 5.6.1) and h using the same priors. Changing the steepness values had very limited effect on the estimated scale or trends in female SSB, dynamic SSB depletion, and fishing intensity (Fig. 5.18). A similar result was reported in previous assessments. The estimated h in #2 was 0.904, which suggests that there was a negligible amount of information on h in the data. This was not surprising because the north Pacific albacore stock is on the relatively flat part of the stock-recruitment curve and h is generally not well estimated in such cases (Lee et al. 2012). When both M and h were estimated with priors, the estimated female M and h were 0.66 y^{-1} and 0.855, respectively. The estimated SSB for this sensitivity run was substantially lower than the base case model but the dynamic SSB depletion and fishing intensity were highly similar (Fig. 5.18).

5.6.3 Sensitivity 03 – Growth

Growth was considered an important axis of uncertainty in previous assessments because of uncertainty in the age and growth of this stock, as well as conflicts in the size composition data. The same sex-specific growth model from the 2014 - 2020 assessments was used in this assessment. The model fits to the size composition data were adequate but there remained uncertainty in the growth model, especially the CV of the L_{inf} parameter. Two sensitivity runs were performed with the CVs of the L_{inf} parameter (CV = 0.06; and 0.08) that were larger than those parameter values in the base case model (CV = 0.04). In addition, two sensitivity models were developed that estimated growth (with and without estimating CVs) and fitted to the conditional age-at-length data from Xu et al. (2014). Changing the CVs on the L_{inf} parameter had major effects on the scale of estimated female SSB, dynamic SSB depletion, and fishing intensity, with larger CVs leading to lower estimated SSB (Fig. 5.19). Similarly, estimating growth with CVs also resulted in major effects on the estimated population dynamics but estimating growth without estimating the CVs do not (Fig. 5.19). Growth was considered by the ALBWG to be the most important axis of uncertainty in this assessment.

5.6.4 Sensitivity 04 – Fit alternative adult index

In this assessment, the base case model was fitted to the F12 index, which was based on the JPLL fleet in Area 2 and Quarter 2. However, the 2020 base case model was fitted instead to the index from the JPLL fleet in Area 2 and Quarter 1. A sensitivity model run was performed by fitting to the F11 index, which was based on the JPLL fleet in Area 2 and Quarter 1. Fitting to the F11 index resulted in a similar population scale but different trends, especially after 2020 (Fig. 5.20). The F11 index had a downwards trend after 2010 and the 2020 value was unusually low.

5.6.5 Sensitivity 05 – Fit juvenile index

The base case model of this assessment was fitted only to the F12 index as an adult abundance index. Two sensitivity models were developed that fitted to the F12 index and candidate indices for juvenile abundance trends: 1) the F22 index based on the JPPL fleet in Quarter 2; or 2) the F34 index based on the EPO Surface fleet. The sensitivity model that fitted to the F12 and F22 indices did not converge. Fitting to the F34 index resulted in slightly higher estimates of female SSB, and slightly lower estimates of fishing intensity (Fig. 5.21).

5.6.6 Sensitivity 06 – Size composition data weighting

In the base case model of this assessment, the size composition data of the F11 fleet were downweighted (0.1x) to minimize the conflict between the size composition data and the F12 index. In addition, the size composition data of four fleets (F02, F05, F22, and F28) were downweighted, such that the size composition data weightings for these fisheries were consistent with their model fit (i.e., Francis multiplier of ~1). A sensitivity model was developed where the size composition data for F11 were fully weighted (1.0x). In addition, a series of sensitivity models were developed where the size composition data for each fleet, except for F11, were downweighted in turn by 0.1x to understand the effect of data weighting on the size composition data. Allowing the size composition data of the F11 fleet to be fully weighted (1.0x) did not substantially affect either population trends or scale (Fig. 5.22). Similarly, downweighting each fleet (0.1x) did not substantially affect either population trends or scale (Fig. 5.22). The ALBWG concluded that the results of the assessment were robust to the weighting of the size composition data.

5.6.7 Sensitivity 07 – Uncertainty of 2020 and 2021 data

In the base case model of this assessment, the size composition and abundance index data for 2020 and 2021 were downweighted (2.4.1). Sensitivity models were developed with: 1) fully weighted size composition data; 2) fully weighted F12 abundance index; and 3) fully weighted size composition and abundance index data for 2020 and 2021. Fully weighting the data for 2020 and 2021 did not substantially affect either population trends or scale (Fig. 5.23). The ALBWG concluded that the results of the assessment were robust to the weighting of the 2020 and 2021 data.

5.6.8 Sensitivity 08 – US longline selectivity

In this assessment, the F27 USLL fleet was assumed to have an asymptotic selectivity. In the 2020 base case model, all fisheries were allowed to have a dome-shaped selectivity and all estimated size selectivity appeared to be dome-shaped. A sensitivity model was developed where the F27 US longline fishery, which catches the largest albacore, was allowed to estimate a dome-shaped selectivity. Assuming a dome-shaped selectivity for the F27 USLL fleet resulted in negligible differences in the scale and trends of estimated female SSB, spawning depletion, and fishing intensity (Fig. 5.24).

5.6.9 Sensitivity 09 – Japan pole-and-line selectivity

In the 2020 base case model, the two largest JPPL fleets (F22 and F23) had annually time varying selectivities. However, in this assessment, the F22 and F23 fleets did not have annually time varying selectivities because of a lack of a positive, definite Hessian matrix (Section 2.4.4). A sensitivity model was developed where the F22 and F23 fleets had annually time varying selectivities. Having annually varying selectivites for the F22 and F23 fleets resulted in slightly lower estimated population scale but similar population trends (Fig. 5.25).

5.6.10 Sensitivity 10 – Alternative initial equilibrium fleets

Initial conditions of the model in this assessment were relatively freely estimated from the data in the main model period (1994 – 2021). Although the initial fishing mortality of a fishery (F28) was estimated to represent the equilibrium catches, the choice of this initial equilibrium fleet was somewhat arbitrary. Four sensitivity models were developed with different combinations of initial equilibrium fleets: 1) F28 and F34; 2) F22 and F28; 3) F22 and F27; and 4) F02 and F22. These sensitivity models resulted in either slightly larger or highly similar estimated population scales and trends (Fig. 5.26). The ALBWG concluded that the results of the assessment were robust to the choice of initial equilibrium fleet.

5.6.11 Sensitivity 11 – 2020 base case model structure

The model structure of the base case model for this assessment had several important changes from the 2020 base case model (Section 2.4). A sensitivity model was developed that followed the model structure of the 2020 base case model. Importantly, this sensitivity model had: 1) fully weighted 2020 and 2021 data; 2) fitted to the F11 index instead of the F12 index; and 3) annually time varying selectivities for the F22 and F23 fleets. However, this sensitivity model could not follow the 2020 assessment in terms of the JPLL fleet structure due to the data preparation required (Section 2.4.2). Following the model structure of the 2020 base case model resulted in a slightly lower female SSB and dynamic SSB depletion, and a decreasing population trend (Fig. 5.27). The ALBWG noted that this sensitivity model had a non positive definite Hessian matrix, and considered the uncertainty for this sensitivity model to be unreliable. Nevertheless, the ALBWG decided that information from this model would be useful for comparative purposes with the base case model.

5.7 Fishery Impact Analysis

Surface fisheries (primarily troll, and pole-and-line, but including gillnet and other miscellaneous gears), which tend to catch juvenile fish, have generally had a larger impact (approximately 2:1 ratio) on the north Pacific albacore stock than longline fisheries, which tend to remove adult fish (Fig. 5.28).

5.8 Future Projections

The constant fishing intensity scenario showed that the current fishing intensity ($F_{2018\text{-}2020}$) is expected to result in female SSB increasing to 90,098 t (95% CI: 23,218 – 156,978 t) and a $SSB/SSB_{current,\ F=0}$ ratio of 0.54 by 2031. Over the next 10 years, there was: 1) a 97.7% probability of the female SSB remaining above the $14\%SSB_{current,\ F=0}$ LRP for all 10 years; 2) a 72.0% probability of the total biomass (age-1+) being above the average of 2006 – 2015 for any year; and 3) a 95.5% probability of the fishing intensity remaining at or below the $F45_{\%SPR}$ TRP for any year (Fig. 5.29).

The randomly resampled fishing intensity scenario showed that if future fishing intensity is similar to the 2005 – 2019 period, it is expected to result in female SSB increasing to 87,669 t (95% CI: 22,219 – 153,119 t) and a $SSB/SSB_{current, F=0}$ ratio of 0.52 by 2031. Over the next 10 years, there was: 1) a 98.1 % probability of the female SSB remaining above the $14\%SSB_{current, F=0}$ LRP for all 10 years; 2) a 69.5 % probability of the total biomass (age-1+) being above the average of 2006 – 2015 for any year; and 3) a 79.6 % probability of the fishing intensity remaining at or below the $F45_{\%SPR}$ TRP for any year (Fig. 5.30).

6.0 STOCK STATUS

6.1 Current Status

Estimated summary biomass (males and females at age-1+) declined at the beginning of the time series until 2004 (Fig. 5.14). Subsequently, the summary biomass fluctuated without a trend until 2018, after which the biomass rapidly increased to historically high levels. It should be noted that the high summary biomass estimates during 2018 – 2021 were highly uncertain and should be treated with caution (Fig. 5.14). These high summary biomass estimates were due to historically high recruitment estimates in 2017 (~433 million fish; 95% CI: 194 – 671 million fish) (Fig. 5.14). However, it should be noted that the recruitment estimates in the last 5 years (2017-2021) were highly uncertain and should be treated with caution. Estimated female SSB exhibited a similar population trend to the summary biomass, albeit with a lag of several years, and showed an initial decline until 2007 followed by fluctuations without a clear trend through 2021 (Fig. 5.14).

The average fishing intensity during 2018 – 2020 was estimated to be $F59_{\%SPR}$ (95% CI: $F72_{\%SPR}$ – $F46_{\%SPR}$), which was relatively moderate and resulted in a population with an SPR of approximately 59%. Instantaneous fishing mortality at age (F-at-age) was similar in both sexes through age-5, peaking at age-4 and declining to a low at age-6, after which males experienced higher F-at-age than females up to age 12 (Fig. 5.15). Juvenile albacore aged 2 to 4 years comprised approximately 64% of the annual catch-at-age in numbers between 1994 and 2021 (Fig. 5.12) due to the larger fishery impact of surface fisheries (primarily troll, pole-and-line), which remove juvenile fish, relative to longline fisheries, which primarily remove adult fish (Fig. 5.28).

Stock status is depicted in relation to the target ($F45_{\%SPR,}$), threshold ($30\%SSB_{current, F=0}$), and limit ($14\%SSB_{current, F=0}$) reference points (Fig. 5.16; Table 5.5). The estimated female SSB has never fallen below the threshold and limit reference points since 1994, albeit with large uncertainty in the terminal year (2021) estimates. However, the estimated fishing intensity for five years (1999, 2002, 2003, 2004, and 2007) have exceeded the target reference point. Even when alternative hypotheses about key model uncertainties such as growth were evaluated, the point estimate of female SSB in 2021 (SSB_{2021}) did not fall below the threshold and limit reference points, although the risk increases with this more extreme assumption (Fig. 5.16). However, estimated average fishing intensity during 2018-2020 ($F_{2018-2020}$) did exceed the target reference point under one of these alternative hypotheses but did not exceed the average fishing intensity during 2002 – 2004 (Fig. 5.16; Table 5.5).

The SSB_{2021} was estimated to be approximately 54% (95% CI: 40 – 68%) of $SSB_{current, F=0}$ and 1.8 (95% CI: 1.3 – 2.3) times greater than the estimated threshold reference point (Fig. 5.31 and Table 5.5). The estimated current fishing intensity ($F_{2018-2020}$) was estimated to be $F59_{\%SPR}$ (95% CI: $F72_{\%SPR}$ – $F46_{\%SPR}$) and was lower than both the $F45_{\%SPR}$ target reference point and the average fishing intensity during 2002 – 2004 (Fig. 5.31 and Table 5.5).

Based on these findings, the following information on the status of the north Pacific albacore stock is provided:

1. The stock is likely not overfished relative to the threshold ($30\%SSB_{current, F=0}$) and limit ($14\%SSB_{current, F=0}$) reference points adopted by the WCPFC and IATTC, and
2. The stock is likely not experiencing overfishing relative to the adopted target reference point ($F45_{\%SPR}$).
3. Current fishing intensity ($F_{2018\text{-}2020}$) is lower than the fishing intensity from the 2002-2004 period (the reference level for IATTC Resolution C-05-02 and WCPFC CMM-2019-03).

6.2 Conservation Information

Two harvest scenarios were projected to evaluate impacts on the management objectives of IATTC and WCPFC for this stock: 1) maintain SSB above the limit reference point, with a probability of at least 80% over the next 10 years; 2) maintain depletion of total biomass around historical (2006 – 2015) average depletion over the next 10 years; and 3) maintain fishing intensity at or below the target reference point with a probability of at least 50% over the next 10 years (WCPFC HS 2022-01; IATTC Resolution C-22-04).

The constant fishing intensity scenario showed that the current fishing intensity ($F_{2018\text{-}2020}$) is expected to result in female SSB increasing to 90,098 t (95% CI: 23,218 – 156,978 t) and a $SSB/SSB_{current, F=0}$ ratio of 0.54 by 2031. Over the next 10 years, there was: 1) a 97.7% probability of the female SSB remaining above the $14\%SSB_{current, F=0}$ LRP for all 10 years; 2) a 72.0% probability of the total biomass (age-1+) being above the average of 2006 – 2015 for any year; and 3) a 95.5% probability of the fishing intensity remaining at or below the $F45_{\%SPR}$ TRP for any year.

The randomly resampled fishing intensity scenario showed that if future fishing intensity is similar to the 2005 – 2019 period, it is expected to result in female SSB increasing to 87,669 t (95% CI: 22,219 – 153,119 t) and a $SSB/SSB_{current, F=0}$ ratio of 0.52 by 2031. Over the next 10 years, there was: 1) a 98.1 % probability of the female SSB remaining above the $14\%SSB_{current, F=0}$ LRP for all 10 years; 2) a 69.5 % probability of the total biomass (age-1+) being above the average of 2006 – 2015 for any year; and 3) a 79.6 % probability of the fishing intensity remaining at or below the $F45_{\%SPR}$ TRP for any year.

Based on these findings, the following conservation information is provided:

1. If fishing intensity over the next ten years is maintained at the current fishing intensity ($F_{2018\text{-}2020}$), then female SSB is expected to remain around $54\%SSB_{current, F=0}$ (90,098 t), with a 97.7% probability of the female SSB remaining above the 14% $SSB_{current, F=0}$ LRP for all ten years, and the management objectives of IATTC and WCPFC will likely be met.

2. If fishing intensity over the next ten years is similar to the 2005 – 2019 period, then female SSB is expected to decrease to $52\%SSB_{current, F=0}$ (87,669 t), with a 98.1% probability of the female SSB remaining above the 14% $SSB_{current, F=0}$ LRP for all ten years, and the management objectives of IATTC and WCPFC will likely be met.

7.0 EXCEPTIONAL CIRCUMSTANCES

The adopted harvest strategies of WCPFC and IATTC for north Pacific albacore tuna included the identification of exceptional circumstances during the stock assessment. The ALBWG developed and considered the preliminary criteria for identifying exceptional circumstances for north Pacific albacore tuna, and did not find any strong evidence of exceptional circumstances with respect to the conservation and management of this stock. At this time, the ALBWG stresses that the preliminary criteria are still incomplete and without implementation indicators based on adopted HCRs, the application of these incomplete criteria may bias results and introduce uncertainty.

8.0 KEY UNCERTAINTIES AND RESEARCH RECOMMENDATIONS

The ALBWG noted that the lack of sex-specific size data, uncertainty in growth and natural mortality, uncertainty in the impacts of COVID safety protocols on fishery operations and data collection, and the simplified treatment of the spatial structure of north Pacific albacore population dynamics are important sources of uncertainty in the assessment.

The following recommendations were developed to improve the future iterations of the stock assessment model:

1. Further investigation of the data, especially CPUE, from 2020 and 2021 to better understand if and how COVID-19 safety protocols affected these data;
2. Further investigation of appropriate adult abundance index for the NPALB stock especially with respect to expanding the spatial domain of the CPUE standardization model to reduce the effect of time-varying availability on the standardized abundance index, which in the model is assumed to be proportionally influenced solely by population abundance;
3. Re-examine the fleet structure for the NPALB stock assessment;
4. Evaluate potential juvenile indices from the Japanese longline fisheries in northern areas (Areas 1, 3 and 5), the Japanese pole-and-line and/or EPO surface fisheries;
5. Investigate the sensitivity of model estimates to the variability in L_{inf};
6. Investigate how to better model variability in availability in size and/or age to the juvenile fisheries (JPPL and EPO fisheries selectivities);
7. Investigate the conflict in size composition data between fleets;
8. Collect sex-specific age-length samples using a coordinated biological sampling plan to improve current growth curves, and examine regional and temporal differences in length-at-age;
9. Collect sex ratio data by fleet;
10. Estimate and document historical high seas drift gillnet removals by member countries;
11. Explore ocean productivity as drivers of albacore trends and dynamics.

9.0 LITERATURE CITED

ALBWG. 2014. Stock assessment of albacore tuna in the North Pacific Ocean in 2014. Page 132.

ALBWG. 2016. Report of the Albacore Working Group Workshop, 8-14 November 2016, Nanaimo, British Columbia, Canada.

ALBWG. 2017. Stock assessment of albacore tuna in the North Pacific Ocean in 2017. Page 103. International Scientific Committee for Tuna and Tuna-like Species in the North Pacific Ocean.

ALBWG. 2019. Report of the Albacore Working Group, 12-18 November 2019, NRIFSF/FRA, Shimizu, Shizuoka, Japan.

ALBWG. 2020a. Report of the Albacore Working Group, 5-14 April, 2020, Webinar.

ALBWG. 2020b. Stock assessment of albacore tuna in the North Pacific Ocean in 2020. Page 109. International Scientific Committee for Tuna and Tuna-like Species in the North Pacific Ocean, Stock Assessment.

ALBWG. 2022. Report of the Albacore Working Group Workshop, 6-12 December 2022, Yokohama, Japan.

ALBWG. 2023. Report of the Albacore Working Group Workshop, 20-27 March 2023, La Jolla, California, USA.

Aoki, Y., T. Senda, H. Ijima, N. Matsubara, J. Matsubayashi, and Y. Tsuda. 2023. Sex specific size data for North Pacific albacore (Thunnus alalunga) in Japanese research/training vessels. ISC/23/ALBWG-01/04. Working paper submitted to the ISC Albacore Working Group Workshop, 6-12 March, 2023. Southwest Fisheries Science Center, La Jolla, California, USA (March 2023).

Ashida, H., T. Gosho, and H. Kiyofuji. 2016. Sex ratio, spawning season, spawning fraction and size at maturity of North Pacific albacore (*Thunnus alalunga*) caught in subtropical western North Pacific. ISC/16/ALBWG-02/05. Working document submitted to the ISC Albacore Working Group Meeting, 8 - 14 November, 2016, Pacific Biological Station, Nanaimo, BC, Canada.

Brodziak, J., H. H. Lee, and M. Mangel. 2011. Probable values of stock-recruitment steepness for north Pacific albacore tuna. ISC/11/ALBWG/11. Working Paper submitted to the ISC Albacore Working Group Stock Assessment Workshop, 4-11 June 2011, National Research Institute of Far Sea Seas Fisheries, Shimizu, Japan.

Carvalho, F., H. Winker, D. Courtney, M. Kapur, L. Kell, M. Cardinale, M. Schirripa, T. Kitakado, D. Yemane, K. R. Piner, M. N. Maunder, I. Taylor, C. R. Wetzel, K. Doering, K. F. Johnson, and R. D. Methot. 2021. A cookbook for using model diagnostics in integrated stock assessments. Fisheries Research 240:105959.

Chen, K.-S., P. R. Crone, and C.-C. Hsu. 2010. Reproductive biology of albacore *Thunnus alalunga*. Journal of Fish Biology 77(1):119–136.

Chen, K.-S., C.-C. Hsu, C.-Y. Chen, F.-C. Cheng, and H. Ijima. 2016. Estimation of sexual maturity-at-length of the North Pacific albacore. Working document submitted to the ISC Albacore Working Group Meeting, 8 - 14 November, 2016, Pacific Biological Station, Nanaimo, BC, Canada.

Chen, K.-S., T. Shimose, T. Tanabe, C.-Y. Chen, and C.-C. Hsu. 2012. Age and growth of albacore *Thunnus alalunga* in the North Pacific Ocean. Journal of Fish Biology 80(6):2328–44.

Childers, J., S. Snyder, and S. Kohin. 2011. Migration and behavior of juvenile North Pacific albacore (*Thunnus alalunga*). Fisheries Oceanography 20(3):157–173.

Chow, S., and H. Ushiama. 1995. Global population structure of albacore (*Thunnus alalunga*) inferred by RFLP analysis of the mitochondrial ATPase gene. Marine Biology 123(1):39–45.

Clemens, H. B. 1961. The migration, age, and growth of Pacific albacore (*Thunnus germo*), 1951-1958. Fish Bulletin California Department of Fish and Game 115:1–128.

Craig, M. T., and J. R. Hyde. 2020. PCR-based sex determination for North Pacific Albacore (*Thunnus alalunga*). ISC/20/ALBWG-01/08. Working document submitted to the ISC Albacore Working Group Meeting, 6-15 April 2020, by Webinar.

Deriso, R., M. N. Maunder, and J. Skalski. 2007. Variance estimation in integrated assessment models and its importance for hypothesis testing. Canadian Journal of Fisheries and Aquatic Sciences 64(2):187–197.

Farley, J. H., A. J. Williams, S. D. Hoyle, C. R. Davies, and S. J. Nicol. 2013. Reproductive Dynamics and Potential Annual Fecundity of South Pacific Albacore Tuna (*Thunnus alalunga*). PLoS ONE 8(4).

Fitzgerald, S. M., H. McElderry, H. Hatanaka, Y. Watanabe, J. S. Park, Y. Gong, and S.-Y. Yeh. 1993. 1990-1991 North Pacific High Seas Driftnet Scientific Observer Program. Bulletin of the International North Pacific Fisheries Commission 53(1):77–90.

Francis, R. I. C. C. 2011. Data weighting in statistical fisheries stock assessment models. Canadian Journal of Fisheries and Aquatic Science 68:1124–1138.

Fujioka, K., D. Ochi, H. Ijima, and H. Kiyofuji. 2019. Update standardized CPUE of North Pacific albacore caught by Japanese longline data from 1976 to 2018. ISC/19/ALBWG-02/01. Working document submitted to the ISC Albacore Working Group Meeting, 12-18 November 2019, National Research Institute of Far Seas Fisheries, Shimizu, Shizuoka Japan.

Fujioka, K., D. Ochi, H. Ijima, and H. Kiyofuji. 2020. Estimation of adult and immature abundance indices of North Pacific albacore caught by Japanese longline fisheries over a long period of time, from 1976 to 2018. ISC/20/ALBWG-01/01. Working document submitted to the ISC Albacore Working Group Meeting, 6-15 April 2020, by Webinar.

Gong, Y., Y. S. Kim, and S. J. Hwang. 1993. Outline of the Korean Squid Gillnet Fishery in he North Pacific. Bulletin of the International North Pacific Fisheries Commission 53(1):45–69.

Hamel, O. S. 2015. A method for calculating a meta-analytical prior for the natural mortality rate using multiple life history correlates. ICES Journal of Marine Science 72(1):62–69.

Hsu, J., C.-H. Yi, C.-W. Chang, and Y.-J. Chang. 2022. Catch, length composition, and standardized CPUE of the North Pacific albacore caught by the Taiwanese distant-water longline fisheries in North Pacific Ocean from 1995 – 2021. ISC/22/ALBWG-02/08. Working paper submitted to the ISC Albacore Working Group Workshop, 6-12 December, 2022. National Research Institute of Fisheries Science, Yokohama, Japan (December 2022).

Hurtado-Ferro, F., A. E. Punt, and K. T. Hill. 2014a. Use of multiple selectivity patterns as a proxy for spatial structure. Fisheries Research 158:102–115.

Hurtado-Ferro, F., C. S. Szuwalski, J. L. Valero, S. C. Anderson, C. J. Cunningham, K. F. Johnson, R. Licandeo, C. R. McGilliard, C. C. Monnahan, M. L. Muradian, K. Ono, K. A. Vert-Pre, A. R. Whitten, and A. E. Punt. 2014b. Looking in the rear-view mirror: bias and retrospective patterns in integrated, age-structured stock assessment models. ICES Journal of Marine Science 72(1):99–110.

Ichinokawa, M., A. L. Coan, and Y. Takeuchi. 2008. Transoceanic migration rates of young North Pacific albacore, *Thunnus alalunga*, from conventional tagging data. Canadian Journal of Fisheries and Aquatic Sciences 65(8):1681–1691.

Ijima, H. 2020. The test run of future projection for North Pacific albacore stock using the SSfuture C++ and the multivariate normal distribution. ISC/20/ALBWG-01/03. Working document submitted to the ISC Albacore Working Group Meeting, 6-15 April 2020, by Webinar.

Ijima, H., Y. Aoki, and Y. Tsuda. 2023. Revision of future projection software SSfuture C++. ISC/23/ALBWG-01/09. Working paper submitted to the ISC Albacore Working Group Workshop, 6-12 March, 2023. Southwest Fisheries Science Center, La Jolla, California, USA.

Ijima, H., D. Ochi, and H. Kiyofuji. 2017. Estimation for Japanese catch at length data of North Pacific albacore tuna (Thunnus alalunga). ISC/17/ALBWG/04. Working document submitted to the

ISC Albacore Working Group Meeting, 11-19 April 2017, Southwest Fisheries Science Center, La Jolla, California, USA.

Ijima, H., and Y. Tsuda. 2022. Additional analysis for Japanese longline logbook data using finite mixture model. ISC/22/ALBWG-02/03. Working paper submitted to the ISC Albacore Working Group Workshop, 6-12 December, 2022. National Research Institute of Fisheries Science, Yokohama, Japan (December 2022).

Ijima, H., and Y. Tsuda. 2023. Additional Japanese longline logbook data analysis for adult albacore tuna CPUE. IS/23/ALBWG-01/08. Working paper submitted to the ISC Albacore Working Group Workshop, 6-12 March, 2023. Southwest Fisheries Science Center, La Jolla, California, USA.

Ito, J., W. Shaw, and R. L. Burgner, editors. 1993. Symposium on Biology, Distribution and Stock Assessment of Species Caught in the High Seas Driftnet Fisheries in the North Pacific Ocean. Part I: Driftnet Fisheries of the North Pacific Ocean. North Pacific Anadramous Fish Commission, Vancouver, Canada.

Iwata, S., H. Sugimoto, and Y. Takeuchi. 2011. Calculation of the steepness for the north Pacific albacore. ISC/11/ALBWG/18. Working Paper submitted to the ISC Albacore Working Group Stock Assessment Workshop, 4-11 June 2011, National Research Institute of Far Sea Seas Fisheries, Shimizu, Japan.

James, K., H. Dewar, and S. L. H. Teo. 2020a. Review of current status of North Pacific albacore (*Thunnus alalunga*) age and growth. ISC/20/ALBWG-01/07. Working document submitted to the ISC Albacore Working Group Meeting, 6-15 April 2020, by Webinar.

James, K., H. Dewar, and S. L. H. Teo. 2020b. Ideas for future sampling programs of North Pacific albacore (*Thunnus alalunga*). ISC/20/ALBWG-01/09. Working document submitted to the ISC Albacore Working Group Meeting, 6-15 April 2020, by Webinar.

Kell, L. T., R. Sharma, T. Kitakado, H. Winker, I. Mosqueira, M. Cardinale, and D. Fu. 2021. Validation of stock assessment methods: is it me or my model talking? ICES Journal of Marine Science 78(6):2244–2255.

Kimura, S., M. Nakai, and T. Sugimoto. 1997. Migration of albacore, *Thunnus alalunga*, in the North Pacific Ocean in relation to large oceanic phenomena. Fisheries Oceanography 6(2):51–57.

Kinney, M. J., and S. L. H. Teo. 2016. Meta-analysis of north Pacific albacore tuna natural mortality. ISC/16/ALBWG-02/07.

Kiyofuji, H., and K. Uosaki. 2010. Revision of standardized CPUE for albacore caught by the Japanese pole and line fisheries in the northwestern North Pacific albacore. ISC/10-3/ALBWG/07. Working paper presented at the ISC Albacore Working Group Workshop, 12-19 October 2010, Southwest Fisheries Science Center, NOAA, La Jolla, USA.

Kobayashi, M. 2022. The COVID-19 impacts and challenges to achieving sustainability in Japan's fisheries and aquaculture. Marine Policy 143:105161.

Lee, H. H., M. N. Maunder, K. R. Piner, and R. D. Methot. 2012. Can steepness of the stock-recruitment relationship be estimated in fishery stock assessment models? Fisheries Research 125–126:254–261.

Lee, H. H., K. R. Piner, R. D. Methot, and M. N. Maunder. 2014. Use of likelihood profiling over a global scaling parameter to structure the population dynamics model: AN example using blue marlin in the Pacific Ocean. Fisheries Research 158:138–146.

Lindgren, F., H. Rue, and J. Lindström. 2011. An explicit link between Gaussian fields and Gaussian Markov random fields: the stochastic partial differential equation approach. Journal of the Royal Statistical Society: Series B (Statistical Methodology) 73(4):423–498.

Link, J. S., F. E. Werner, K. Werner, J. Walter, M. Strom, M. P. Seki, F. Schwing, J. Rusin, C. E. Porch, K. Osgood, K. Moline, R. D. Methot, P. D. Lynch, D. Lipton, K. Koch, E. A. Howell, J. A. Hare, R. J. Foy, D. Detlor, L. Desfosse, J. Crofts, and N. Cabana. 2021. A NOAA Fisheries science perspective on the conditions during and after COVID-19: challenges, observations, and some possible solutions, or why the future is upon us. Canadian Journal of Fisheries and Aquatic Sciences 78(1):1–12.

Liu, Y.-C., R.-L. Kuo, and S.-R. Shih. 2020. COVID-19: The first documented coronavirus pandemic in history. Biomedical Journal 43(4):328–333.

Mangel, M., J. Brodziak, and G. DiNardo. 2010. Reproductive ecology and scientific inference of steepness: A fundamental metric of population dynamics and strategic fisheries management. Fish and Fisheries 11(1):89–104.

Martins, T. G., D. Simpson, F. Lindgren, and H. Rue. 2013. Bayesian computing with INLA: New features. Computational Statistics & Data Analysis 67:68–83.

Matsubara, N., J. Matsubayashi, Y. Aoki, Y. Tsuda, and H. Ijima. 2022a. Standardized CPUE for North Pacific albacore caught by the Japanese pole and line by Geostatistical method. ISC/22/ALBWG-02/06. Working paper submitted to the ISC Albacore Working Group Workshop, 6-12 December, 2022. National Research Institute of Fisheries Science, Yokohama, Japan (December 2022).

Matsubara, N., J. Matsubayashi, Y. Aoki, Y. Tsuda, and H. Ijima. 2022b. Update standardized CPUE for North Pacific albacore caught by the Japanese pole and line from 1972 to 2021. ISC/22/ALBWG-02/07. Working paper submitted to the ISC Albacore Working Group Workshop, 6-12 December, 2022. National Research Institute of Fisheries Science, Yokohama, Japan (December 2022).

Matsubayashi, J., H. Ijima, N. Matsubara, Y. Aoki, and Y. Tsuda. 2022. CPUE standardization for North Pacific albacore caught by Japanese longline fishery from 1996 to 2021: the GLMM analysis using R-INLA. ISC/22/ALBWG-02/04. Working paper submitted to the ISC Albacore Working Group Workshop, 6-12 December, 2022. National Research Institute of Fisheries Science, Yokohama, Japan (December 2022).

Matsubayashi, J., H. Ijima, N. Matsubara, Y. Aoki, and Y. Tsuda. 2023. CPUE standardization for North Pacific albacore caught by Japanese longline fishery from 1996 to 2021 in Area 2 and Quarter 2. ISC/23/ALBWG-01/03. Working paper submitted to the ISC Albacore Working Group Workshop, 6-12 March, 2023. Southwest Fisheries Science Center, La Jolla, California, USA (March 2023).

Maunder, M. N. 2011. Review and evaluation of likelihood functions for composition data in stock-assessment models: Estimating the effective sample size. Fisheries Research 109(2–3):311–319.

Maunder, M. N., and A. E. Punt. 2013. A review of integrated analysis in fisheries stock assessment. Fisheries Research 142:61–74.

Maunder, M., and K. Piner. 2015. Contemporary fisheries stock assessment: many issues still remain. ICES Journal of Marine Science 72(1):7–18.

Methot, R. D. 2000. Technical Description of the Stock Synthesis Assessment Program. NOAA Technical Memorandum NMFS-NWFSC-43.

Methot, R. D., and I. G. Taylor. 2011. Adjusting for bias due to variability of estimated recruitments in fishery assessment models. Canadian Journal of Fisheries and Aquatic Sciences 68(10):1744–1760.

Methot, R. D., and C. R. Wetzel. 2013. Stock synthesis: A biological and statistical framework for fish stock assessment and fishery management. Fisheries Research 142:86–99.

Minte-Vera, C. V., M. N. Maunder, and A. M. Aires-da-Silva. 2021. Auxiliary diagnostic analyses used to detect model misspecification and highlight potential solutions in stock assessments: application to yellowfin tuna in the eastern Pacific Ocean. ICES Journal of Marine Science 78(10):3521–3537.

Mohn, R. 1999. The retrospective problem in sequential population analysis: An investigation using cod fishery and simulated data. ICES Journal of Marine Science 56(4):473–488.

Montes, I., M. Iriondo, C. Manzano, H. Arrizabalaga, E. Jiménez, M. Á. Pardo, N. Goñi, C. A. Davies, and A. Estonba. 2012. Worldwide genetic structure of albacore *Thunnus alalunga* revealed by microsatellite DNA markers. Marine Ecology Progress Series 471:183–191.

Nishikawa, Y., M. Honma, S. Ueyanagi, and KikawaS. 1985. Average distribution of larvae of oceanic species of scrombroid fishes, 1956–1981. Far Seas Fisheries Research Laboratory , Shimizu, S Series 12.

Ochi, D., H. Ijima, J. Kinoshita, and H. Kiyofuji. 2016. New fisheries definition from Japanese longline North Pacific albacore size data. ISC/16/ALBWG-02/03. Working document submitted to ISC Albacore Working Group Meeting, 8 - 14 November, 2016, Pacific Biological Station, Nanaimo, BC, Canada.

Otsu, T., and R. F. Sumida. 1968. Distribution, apparent abundance, and size composition of albacore (Thunnus alalunga) taken in the longline fishery based in American Samoa, 1954-65. Fishery Bulletin 67(1):47–67.

Otsu, T., and R. N. Uchida. 1959. Sexual maturity and spawning of albacore in the Pacific Ocean. Fishery Bulletin 59(148):287–305.

Polovina, J. J., E. Howell, D. R. Kobayashi, and M. P. Seki. 2001. The transition zone chlorophyll front, a dynamic global feature defining migration and forage habitat for marine resources. Progress in Oceanography 49(1–4):469–483.

Ramon, D., and K. Bailey. 1996. Spawning seasonality of albacore, *Thunnus alalunga*, in the South Pacific ocean. Fishery Bulletin 94(4):725–733.

Rue, H., S. Martino, and N. Chopin. 2009. Approximate Bayesian inference for latent Gaussian models by using integrated nested Laplace approximations. Journal of the Royal Statistical Society: Series B (Statistical Methodology) 71(2):319–392.

Schnute, J. 1981. A versatile growth model with statistically stable parameters. Canadian Journal of Fisheries and Aquatic Sciences 38(9):1128–1140.

Smith, S. L., S. Cook, A. Golden, M. A. Iwane, D. Kleiber, K. M. Leong, A. Mastitski, L. Richmond, M. Szymkowiak, and S. Wise. 2022. Review of adaptations of U.S. Commercial Fisheries in response to the COVID-19 pandemic using the Resist-Accept-Direct (RAD) framework. Fisheries Management and Ecology 29(4):439–455.

Suzuki, Z., Y. Warashina, and M. Kishida. 1977. The comparison of catches by regular and deep tuna longline gears in the western and central equatorial Pacific. Bulletin Far Seas Fisheries Laboratory 15:51–89.

Takagi, M., T. Okamura, S. Chow, and N. Taniguchi. 2001. Preliminary study of albacore (*Thunnus alalunga*) stock differentiation inferred from microsatellite DNA analysis. Fishery Bulletin 99(4):697–701.

Teo, S. L. H. 2016. Spatiotemporal definitions of the US albacore longline fleets in the north Pacific for the 2017 assessment. ISC/16/ALBWG-02/08. Working document submitted to ISC Albacore Working Group Meeting, 8 - 14 November, 2016, Pacific Biological Station, Nanaimo, BC, Canada.

Teo, S. L. H. 2017. Meta-analysis of north Pacific albacore tuna natural mortality: an update. ISC/17/ALBWG/07. Working document submitted to the ISC Albacore Working Group Meeting, 11-19 April 2017, Southwest Fisheries Science Center, La Jolla, California, USA.

Teo, S. L. H. 2022a. Candidate relative abundance indices of juvenile albacore tuna for the US surface fishery in the north Pacific Ocean. ISC/22/ALBWG-02/11. Working paper submitted to the ISC Albacore Working Group Workshop, 6-12 December, 2022. National Research Institute of Fisheries Science, Yokohama, Japan (December 2022).

Teo, S. L. H. 2022b. Preliminary catch and size composition time series of the U.S. and Mexico surface fishery for the 2023 north Pacific albacore tuna assessment. ISC/22/ALBWG-02/10. Working paper submitted to the ISC Albacore Working Group Workshop, 6-12 December, 2022. National Research Institute of Fisheries Science, Yokohama, Japan (December 2022).

Teo, S. L. H. 2022c. Preliminary catch and size composition time series of the U.S. pelagic longline fleets for the 2023 north Pacific albacore tuna assessment. ISC/22/ALBWG-02/09. Working paper submitted to the ISC Albacore Working Group Workshop, 6-12 December, 2022. National Research Institute of Fisheries Science, Yokohama, Japan (December 2022).

Teo, S. L. H., J. Holmes, and S. Kohin. 2010. Joint standardized abundance index of US and Canada albacore troll fisheries in the North Pacific. ISC/10-3/ALBWG/01. Working document submitted to the ISC Albacore Working Group Meeting, 12-19 October 2010, Southwest Fisheries Science Center, NOAA, La Jolla, California, USA.

Teo, S. L. H., and C. Minte-Vera. 2022. Re-examining the model diagnostics of the 2020 north Pacific albacore tuna stock assessment. ISC/22/ALBWG-01/01. Working document submitted to the ISC Albacore Working Group Meeting, 9-12 May 2022, held by Webinar.

Then, A. Y., J. M. Hoenig, N. G. Hall, and D. A. Hewitt. 2015. Evaluating the predictive performance of empirical estimators of natural mortality rate using information on over 200 fish species. ICES Journal of Marine Science 72(1):82–92.

Ueyanagi, S. 1957. Spawning of the albacore in the Western Pacific. Report of Nankai Regional Fisheries Research Laboratory 6:113–124.

Ueyanagi, S. 1969. Observations on the distribution of tuna larvae in the Indo-Pacific Ocean with emphasis on the delineation of the spawning areas of albacore, *Thunnus alalunga*. Bulletin Far Seas Fisheries Laboratory 2:177–256.

Uosaki, K., H. Kiyofuji, and T. Matsumoto. 2011. Review of Japanese albacore fisheries as of 2011. ISC/11/ALBWG/13. Working Paper submitted to the ISC Albacore Working Group Stock Assessment Workshop, 4-11 June 2011, National Research Institute of Far Sea Seas Fisheries, Shimizu, Japan.

Vaux, F., S. Bohn, J. R. Hyde, and K. G. O'Malley. 2021. Adaptive markers distinguish North and South Pacific Albacore amid low population differentiation. Evolutionary Applications 14(5):1343–1364.

Watanabe, H., T. Kubodera, S. Masuda, and S. Kawahara. 2004. Feeding habits of albacore *Thunnus alalunga* in the transition region of the central North Pacific. Fisheries Science 70:573–579.

Watanabe, K., K. Uosaki, T. Kokubo, P. R. Crone, A. L. Coan, and C. C. Hsu. 2006. Revised practical solutions of application issues of length-weight relationship for the North Pacific albacore with respect to stock assessment. ISC/06/ALBWG/14. Report of the ISC Albacore Working Group Workshop, 28 November - 5 December, 2006.

Waterhouse, L., D. B. Sampson, M. Maunder, and B. X. Semmens. 2014. Using areas-as-fleets selectivity to model spatial fishing: Asymptotic curves are unlikely under equilibrium conditions. Fisheries Research 158:15–25.

Wells, R. J. D., S. Kohin, S. L. H. Teo, O. E. Snodgrass, and K. Uosaki. 2013. Age and growth of North Pacific albacore (*Thunnus alalunga*): Implications for stock assessment. Fisheries Research 147:55–62.

White, E. R., H. E. Froehlich, J. A. Gephart, R. S. Cottrell, T. A. Branch, R. Agrawal Bejarano, and J. K. Baum. 2021. Early effects of COVID-19 on US fisheries and seafood consumption. Fish and Fisheries 22(1):232–239.

Williams, A. J., J. H. Farley, S. D. Hoyle, C. R. Davies, and S. J. Nicol. 2012. Spatial and sex-specific variation in growth of albacore tuna (*Thunnus alalunga*) across the South Pacific Ocean. PLoS ONE 7(6).

Xu, Y., T. Sippel, S. L. H. Teo, K. Piner, K. Chen, and R. J. Wells. 2014. A comparison study of North Pacific albacore (*Thunnus alalunga*) age and growth among various sources. ISC/14/ALBWG/04. Working paper submitted to the ISC Albacore Working Group Workshop, 14-28 April, 2014. Southwest Fisheries Science Center, La Jolla, California, USA (April 2014).

Xu, Y., S. L. H. Teo, and J. Holmes. 2013. An update of standardized abundance index of US and Canada albacore troll fisheries in the North Pacific (1966-2012). ISC/13/ALBWG-03/06. Working paper submitted to the ISC Albacore Working Group Workshop, 5-12 November, 2013.

Yatsu, A., K. Hiramatsu, and S. Hayase. 1993. Outline of the Japanese Squid Driftnet Fishery with Notes on the By-catch. Bulletin of the International North Pacific Fisheries Commission 53(1):5–24.

Yeh, S.-Y., and I.-H. Tung. 1993. Review of Taiwanese Pelagic Squid Fisheries in the North Pacific. Bulletin of the International North Pacific Fisheries Commission 53(1):71–76.

Yoshida, H. O. 1966. Early life history and spawning of the albacore, *Thunnus alalunga*, in hawaiian waters. Fishery Bulletin 67(2):205–211.

Zainuddin, M., H. Kiyofuji, K. Saitoh, and S. I. Saitoh. 2006. Using multi-sensor satellite remote sensing and catch data to detect ocean hot spots for albacore (*Thunnus alalunga*) in the northwestern North Pacific. Deep-Sea Research Part II: Topical Studies in Oceanography 53(3–4):419–431.

Zainuddin, M., K. Saitoh, and S.-I. Saitoh. 2008. Albacore (*Thunnus alalunga*) fishing ground in relation to oceanographic conditions in the western North Pacific Ocean using remotely sensed satellite data. Fisheries Oceanography 17(2):61–73.

TABLES

Table 3.1. Fleet definitions for the 2023 assessment of north Pacific albacore tuna. Availability of size and abundance index data is indicated in the notes. * indicates that size or index data were available but were not fitted in the base case model. Two letter country codes are used in the fishery name: JP = Japan; US = United States of America; TW = Chinese-Taipei; KR = Korea; and VU = Vanuatu.

ID	Fishery name	Area	Primary gear	Quarter	Catch unit	Notes
F01	F01_JPLL_A13_Q1_J_wt	1 & 3	Longline	1	Tonnes	Size, Index*
F02	F02_JPLL_A13_Q1_A_wt	1 & 3	Longline	1	Tonnes	Size
F03	F03_JPLL_A13_Q2_wt	1 & 3	Longline	2	Tonnes	Size
F04	F04_JPLL_A13_Q3_wt	1 & 3	Longline	3	Tonnes	Size
F05	F05_JPLL_A13_Q4_wt	1 & 3	Longline	4	Tonnes	Size
F06	F06_JPLL_A13_Q1_J_num	1 & 3	Longline	1	1000s	
F07	F07_JPLL_A13_Q1_A_num	1 & 3	Longline	1	1000s	
F08	F08_JPLL_A13_Q2_num	1 & 3	Longline	2	1000s	
F09	F09_JPLL_A13_Q3_num	1 & 3	Longline	3	1000s	
F10	F10_JPLL_A13_Q4_num	1 & 3	Longline	4	1000s	
F11	F11_JPLL_A2_Q1_wt	2	Longline	1	Tonnes	Size, Index*
F12	F12_JPLL_A2_Q2_wt	2	Longline	2	Tonnes	Size, Index
F13	F13_JPLL_A2_Q3_wt	2	Longline	3	Tonnes	Size
F14	F14_JPLL_A2_Q4_wt	2	Longline	4	Tonnes	Size
F15	F15_JPLL_A2_Q1_num	2	Longline	1	1000s	
F16	F16_JPLL_A2_Q2_num	2	Longline	2	1000s	
F17	F17_JPLL_A2_Q3_num	2	Longline	3	1000s	
F18	F18_JPLL_A2_Q4_num	2	Longline	4	1000s	
F19	F19_JPLL_A4_num	4	Longline	All	1000s	Size
F20	F20_JPLL_A5_num	5	Longline	All	1000s	Size
F21	F21_JPPL_A3_Q1	3	Pole & line	1	Tonnes	Size
F22	F22_JPPL_A3_Q2	3	Pole & line	2	Tonnes	Size
F23	F23_JPPL_A3_Q3	3	Pole & line	3	Tonnes	Size
F24	F24_JPPL_A3_Q4	3	Pole & line	4	Tonnes	Size
F25	F25_JPPL_A2	2	Pole & line	All	Tonnes	Size
F26	F26_USLL_A35	3 & 5	Longline	All	Tonnes	Size
F27	F27_USLL_A24	2 & 4	Longline	All	Tonnes	Size
F28	F28_TWLL_A35	3 & 5	Longline	All	Tonnes	Size
F29	F29_TWLL_A24	2 & 4	Longline	All	Tonnes	
F30	F30_KRLL	All	Longline	All	Tonnes	
F31	F31_CNLL_A35	3 & 5	Longline	All	Tonnes	Size*
F32	F32_CNLL_A24	2 & 4	Longline	All	Tonnes	Size*
F33	F33_VU_OTH_LL	All	Longline	All	Tonnes	Size*
F34	F34_EPOSF	3 & 5	Surface	All	Tonnes	Size
F35	F35_JPKRTW_DNMISC	All	Drift net, Miscellaneous	All	Tonnes	

Table 3.2. Standardized values and input coefficients of variation (CVs) of north Pacific albacore annual abundance indices developed for the 2023 base case model (F12 index). Units are number of fish per unit effort. Quarter refers to annual quarters in which the majority of catch was made in the underlying fishery, where 1 = Jan-Mar, 2 = Apr-June, 3 = July-Sept, and 4 = Oct-Dec. A constant of 0.2 was assumed for the CVs of the F12 index in the base case model for all years except for 2020 and 2021, when it was assumed to be 0.3. The CV of the index was tuned by adding a CV of 0.01973 for all years (not shown).

F12 index – Japanese longline in Area 2, Quarter 2		
Year	CPUE	CV
1996	7.097	0.20
1997	9.131	0.20
1998	9.732	0.20
1999	8.732	0.20
2000	11.877	0.20
2001	8.856	0.20
2002	6.123	0.20
2003	5.587	0.20
2004	4.502	0.20
2005	6.200	0.20
2006	7.543	0.20
2007	4.782	0.20
2008	8.863	0.20
2009	7.123	0.20
2010	9.146	0.20
2011	6.825	0.20
2012	8.314	0.20
2013	6.642	0.20
2014	8.281	0.20
2015	8.254	0.20
2016	7.363	0.20
2017	7.871	0.20
2018	7.989	0.20
2019	5.871	0.20
2020	4.065	0.30
2021	10.786	0.30

Table 3.3. Standardized values and input coefficients of variation (CVs) of north Pacific albacore annual abundance indices developed for sensitivity model runs. Quarter refers to annual quarters in which the majority of catch was made in the underlying fishery, where 1 = Jan-Mar, 2 = Apr-June, 3 = July-Sept, and 4 = Oct-Dec. Constant additional CVs of 0.078, 0.164, and 0.083 were added to the CVs of the F11, F22, and F34 indices in sensitivity model runs, to raise the average CV to 0.2. CV values shown here do not include these additional CVs.

	F11 index – JPLL in Area 2, Qtr 1 (numbers)		F22 index – JPPL in Areas 3 and 5, Qtr 2 (weight)		F34 index – EPO Surface in Areas 3 and 5, Qtr 3 (numbers)	
Year	CPUE	CV	CPUE	CV	CPUE	CV
1994			2.394	0.068		
1995			1.806	0.052		
1996	21.140	0.136	1.642	0.037		
1997	24.539	0.133	1.970	0.035		
1998	22.869	0.119	1.747	0.045		
1999	19.467	0.120	2.363	0.040	53.545	0.096
2000	28.449	0.122	0.962	0.022	46.736	0.100
2001	22.901	0.116	1.527	0.025	87.709	0.098
2002	16.160	0.115	2.732	0.043	79.032	0.129
2003	16.180	0.119	1.733	0.031	80.160	0.134
2004	12.423	0.117	1.656	0.040	88.334	0.155
2005	17.584	0.118	0.734	0.018	80.197	0.110
2006	18.591	0.116	0.606	0.020	145.249	0.115
2007	14.206	0.115	1.254	0.032	86.186	0.128
2008	15.594	0.116	0.687	0.029	88.316	0.148
2009	15.879	0.118	1.110	0.046	105.961	0.110
2010	18.409	0.122	1.003	0.036	81.929	0.105
2011	15.017	0.116	0.712	0.052	72.240	0.103
2012	13.194	0.116	1.252	0.033		
2013	14.246	0.126	0.832	0.030	91.387	0.106
2014	10.604	0.117	0.910	0.042	79.406	0.129
2015	16.852	0.118	0.521	0.023	95.661	0.121
2016	11.018	0.117	0.438	0.022	85.931	0.129
2017	12.151	0.122	0.430	0.032	52.122	0.120
2018	14.906	0.123	0.217	0.032	68.447	0.134
2019	12.030	0.127	0.101	0.022	103.291	0.108
2020	6.063	0.127	1.347	0.084	99.448	0.108
2021	17.816	0.170	0.316	0.022	94.721	0.097

Table 4.1. Key life history parameters and model structures used in the base case model.

Parameter	Value	Comments	Source
Natural mortality (M)	Female age-0: 1.36 y^{-1} Female age-1: 0.56 y^{-1} Female age-2: 0.45 y^{-1} Female age-3+: 0.48 y^{-1} Male age-0: 1.36 y^{-1} Male age-1: 0.56 y^{-1} Male age-2: 0.45 y^{-1} Male age-3+: 0.39 y^{-1}	Fixed parameter.	Teo (2017)
Length at age-1 (L_1)	Female: 43.504 cm Male: 47.563 cm	Fixed parameter	Xu et al. (2014)
Asymptotic length (L_{inf})	Female: 106.57 cm Male: 119.15 cm	Fixed parameter	Xu et al. (2014)
Growth rate (k)	Female: 0.29763 y^{-1} Male: 0.20769 y^{-1}	Fixed parameter	Xu et al. (2014)
CV of L_1	0.06	Non sex-specific, fixed parameter	ALBWG (2014)
CV of L_{inf}	0.04	Non sex-specific, fixed parameter	ALBWG (2014)
Weight-at-length – Q1	W_L (kg) = 8.7 * 10^{-5} L (cm) $^{2.67}$	Non sex-specific, fixed parameters	Watanable et al. (2006)
Weight-at-length – Q2	W_L (kg) = 3.9 * 10^{-5} L (cm) $^{2.84}$	Non sex-specific, fixed parameters	Watanable et al. (2006)
Weight-at-length – Q3	W_L (kg) = 2.1 * 10^{-5} L (cm) $^{2.99}$	Non sex-specific, fixed parameters	Watanable et al. (2006)
Weight-at-length – Q4	W_L (kg) = 2.8* 10^{-5} L (cm) $^{2.92}$	Non sex-specific, fixed parameters	Watanable et al. (2006)
Maturity	50% at age-5, 100% age-6+	Fixed parameters	Ueyanagi (1957); Chen et al. (2016);
Fecundity	Proportional to spawning biomass	Fixed parameters	Ueyanagi (1957)
Spawning season	2	Model structure	Ueyanagi (1957); Chen et al. (2010); Ashida et al. (2016)
Spawner-recruit relationship	Beverton-Holt	Model structure	

Parameter	Value	Comments	Source
Spawner-recruit steepness (h)	0.9	Fixed parameter	Brodziak et al. (2011); Iwata et al. (2011); ALBWG (2014)
Log of Recruitment at virgin biomass ln(R_0)	12.2919	Maximum likelihood estimate	
Recruitment variability (σ_R)	0.46	Fixed parameter	
Initial age structure	10 y	Estimated	
Main recruitment deviations	1994-2021	Estimated	
Selectivity	Size selectivity only (splines): F01, F02, F04, & F19 Size selectivity only (dome): F03, F05, F11, F12, F13, F14, F20, F25, F26, F27, & F28 Size and age selectivity: F21, F22, F23, F24, & F34 Shared selectivity: F06, F07, F08, F09, F10, F15, F16, F17, F18, F29, F30, F31, F32, F33, & F35	Estimated (see Table 4.2 – 4.5)	
Catchability		Solved analytically	

Table 4.2. Selectivity parameters used in the base case model for fisheries with only size selectivity. Estimated parameters are shown in bold, with estimated standard deviation in parentheses. The optional initial and final parameters for all double-normal selectivity curves were fixed at -999 and ignored by the model. The value for the first knot for all spline selectivity curves were fixed at 0 and values for the second and third knot were estimated relative to that. Knot locations in cm are indicated in parentheses in the years column.

Size selectivity (double-normal)					
Fishery	Years	Parm 1 – Size at peak	Parm 2 – Plateau width	Parm 3 – Ascending slope	Parm 4 – Descending slope
F03	1994 – 2021	**79.1 (0.6)**	-8	**3.73 (0.17)**	**4.69 (0.16)**
F05	1994 – 2021	**105.5 (2.5)**	**-3.17 (3.94)**	**5.40 (0.16)**	**4.87 (1.71)**
F11	1994 – 2021	**113.1 (2.3)**	**-7.11 (36.38)**	**5.79 (0.22)**	**-0.74 (7.39)**
F12	1994 – 2021	**104.8 (2.1)**	**-2.94 (1.84)**	**4.28 (0.28)**	**3.32 (1.15)**
F13	1994 – 2021	**106.0 (2.0)**	**-4.91 (11.46)**	**4.63 (0.22)**	**3.26 (0.98)**
F14	1994 – 2021	**108.0 (1.7)**	-8	**4.98 (0.16)**	**2.81 (1.06)**
F20	1994 – 2021	**115.7 (38.4)**	**-1.74 (8.75)**	**6.40 (1.37)**	**0.69 (65.62)**
F25	1994 – 2021	**91.4 (4.7)**	-8	**4.54 (0.78)**	**3.63 (2.28)**
F26	1994 – 2004	**100.4 (19.2)**	**0.24 (98.15)**	**6.20 (0.97)**	**4.00 (111.83)**
	2005 – 2021	**90.1 (8.9)**	**0.73 (53.35)**	**5.48 (0.78)**	**2.02 (156.89)**
F27	1994 – 2004	**139.0 (18.3)**	99	**5.82 (0.51)**	99
	2005 – 2021	**126.3 (15.9)**	99	**5.68 (0.68)**	99
F28	1994 – 2021	**91.0 (1.6)**	**0.79 (50.82)**	**5.28 (0.14)**	**4.02 (111.64)**

Size selectivity (3–knot spline)					
Fishery	Years (knot locations in cm)	Gradient Low	Gradient High	Value at 2nd knot	Value at 3rd knot
F01	1994 – 2021 (60, 90, 130)	**1.21 (0.13)**	**-0.99 (0.47)**	**6.87 (0.78)**	**-0.66 (4.83)**
F02	1994 – 2021 (60, 90, 140)	**0.62 (0.19)**	**-0.83 (0.64)**	**6.94 (1.30)**	**-4.64 (8.69)**
F04	1994 – 2021 (70, 95, 140)	**0.85 (0.52)**	**-1.31 (1.09)**	**5.01 (2.72)**	**-8.58 (12.55)**
F19	1994 – 2021 (60, 90, 140)	**0.29 (0.37)**	**-0.78 (0.66)**	**9.76 (5.64)**	**3.83 (12.39)**

Table 4.3. Size selectivity parameters used in the base case model for fisheries with selectivity assumed to be a product of size and age selectivity. Estimated parameters are shown in bold, with estimated standard deviation in parentheses. Size selectivity was assumed to follow a double-normal function. The optional initial and final parameters for all double-normal selectivity curves were fixed at -999 and ignored by the model.

Size selectivity (double-normal)					
Fishery	Years	Parm 1 – Size at peak	Parm 2 – Plateau width	Parm 3 – Ascending slope	Parm 4 – Descending slope
F21, F22, F23, F24	1994 – 2021	**76.3 (1.3)**	-8	**5.28 (0.16)**	**3.36 (0.35)**
F34	1994 – 2021	**58.3 (1.3)**	**-2.80 (0.68)**	**2.53 (0.48)**	**5.30 (0.24)**

Table 4.4. Age selectivity parameters used in the base case model for fisheries with selectivity assumed to be a product of size and age selectivity. Estimated parameters are shown in bold, with estimated standard deviation in parentheses. Age selectivity was modeled as estimated free parameters for ages-1 to 5, with all other ages fixed at a negligible low value (-9 or -12). Estimated age selectivity parameters at the lower (-9 or -12) or upper (9 or 12) bound were fixed at the bound on the final run to improve model optimization.

Age selectivity (free parameters for ages-1 to 5)						
Fishery	**Years**	**Age-1**	**Age-2**	**Age-3**	**Age-4**	**Age-5**
F21	1994 – 2021	**-6.79 (42.3)**	**-8.13 (21.7)**	**-2.53 (16.9)**	**-2.08 (18.7)**	**8.40 (16.8)**
F22	1994 - 2015	**-2.20 (92.1)**	**-4.03 (92.1)**	**-4.57 (92.1)**	**-0.22 (92.2)**	**7.45 (92.1)**
	2016 – 2021	**-7.53 (71.5)**	**-4.97 (63.5)**	**-4.40 (63.5)**	**-0.06 (63.5)**	**9.33 (63.5)**
F23	1994 – 2015	**1.58 (92.1)**	**-4.21 (91.8)**	**-4.77 (91.8)**	**-2.80 (91.8)**	**7.31 (91.8)**
	2016 - 2021	**-7.95 (55.0)**	**-10.1 (41.0)**	**-3.68 (33.5)**	**-0.28 (33.5)**	**10.7 (33.4)**
F24	1994 – 2021	**8.47 (14.5)**	**-5.04 (14.6)**	**-8.13 (18.0)**	**-5.87 (16.5)**	**-6.12 (49.7)**
F34	1994 – 1998	-12	-12	**-11.45 (0.4)**	**-10.26 (0.9)**	**-0.21 (0.7)**
	1999 – 2021	-12	**-10.44 (0.4)**	**-9.38 (0.5)**	**-8.08 (0.6)**	**1.84 (0.4)**

Table 4.5. Fisheries without an estimated selectivity were assumed to have size selectivity identical to other fisheries (mirrored selectivity).

Mirrored selectivity			
Fishery without estimated selectivity	Mirrored to	Fishery without estimated selectivity	Mirrored to
F06	F01	F18	F14
F07	F02	F29	F19
F08	F03	F30	F19
F09	F04	F31	F28
F10	F05	F32	F19
F15	F11	F33	F28
F16	F12	F35	F21
F17	F13		

Table 4.6. Sensitivity analyses conducted on the 2023 base case model for north Pacific albacore.

Sensitivity run number	Sensitivity run name	Description
	Sensitivity to biological assumptions	
01	Natural mortality	1) Fixed constant M of 0.3 y^{-1} for both sexes and all ages (same as 2014 assessment); 2) Fixed constant M of 0.48 and 0.39 y^{-1} for female and male albacore of all ages, respectively; 3) Estimated, single-parameter, female M for all ages, with the prior from Teo et al. (2017), $M_{female} \sim \log N[-0.7258, (0.457)^2]$, and a constant logscale offset (-0.21258) between male and female M; and 4) Fixed, experimental sex-and age-specific M based on a Lorenzen size-M relationship before maturity, and a logistic-shaped transition to adult M (0.48 and 0.39 y^{-1} for females and males) linked to the maturity ogive (similar to South Pacific albacore).
02	Stock-recruitment steepness	1) Use alternative constant values for the steepness parameter (h = 0.75; 0.80; and 0.85); 2) Estimated h with the prior, $h \sim N[0.9, (0.1)^2]$; and 3) Estimated M (see above model 3 for M sensitivity) and h with prior.
03	Growth	1) CV of L_{inf} is fixed at higher (0.06 & 0.08) levels; 2) Estimated L_1, L_{inf}, and k by fitting to conditional age-at-length data from the Xu et al. (2014); and 3) Same as model 2 but estimated CVs as well.
	Sensitivity to data inputs	
04	Fit alternative adult index	1) Fit to F11 index as alternative adult index.
05	Fit juvenile index	1) Fit to JPPL F22 index as a juvenile index; 2) Fit to EPO F34 as a juvenile index.
06	Size composition weighting	1) Change the relative weighting of size composition data. Fit size composition data of JPLL fleet in Area 2 during Quarter 1 (F11) at natural weight (input sample size multiplier = 0.274); and 2) Down-weight size composition data of each fishery (lambda = 0.1).
07	Uncertainty of 2020 and 2021 data	1) No downweight of the 2020 and 2021 data.
	Sensitivity to model structure assumptions	
08	USLL selectivity	1) Assume that the USLL fleet in Areas 2 & 4 (F27) has a dome-shaped size selectivity.
09	JPPL selectivity	1) Annually varying selectivity for F22 and F23 (same as 2020 assessment)

Sensitivity run number	Sensitivity run name	Description
10	Alternative equilibrium catch fleets	1) Use F28 and F34 as fleets for initial equilibrium catch; 2) Use F22 and F28; 3) Use F22 and F27; and 4) Use F2 and F22.
11	2020 base case model structure	1) Model structure follows the 2020 assessment as close as possible (no downweight 2020 and 2021 data, fit to F11 index, annually varying selectivity for F22 and F23).

Table 5.1. Analytical estimates of catchability, mean input variance, variance adjustment, and model fit (root-mean-square-error; RMSE of predictions to observations) for the F12 abundance index in the 2023 base case model.

Index	Years	Catchability	Mean input CV	Variance adjustment	Input CV + Var. Adj.	RMSE
F12	1996 – 2021	6.995E-03	0.208	1.973E-02	0.227	0.231

Table 5.2. Mean input variances (input N after variance adjustment) and model estimated mean variance (*effN*) of the size composition data components. Harmonic means of *effN* and ratio of input N to *effN* are also provided. A higher *effN* indicates a better model fit. Number of observations corresponds to the number of quarters in which size composition data were sampled in a fishery.

Fishery	Number of obs.	Var. adj.	Mean input N after var. adj.	Mean effective N (effN)	Harmonic mean of effN	Harmonic mean effN / mean input N	Francis weighting multiplier
F01	26	0.274	27.9	70.6	37.0	1.3	1.4
F02	26	0.17	13.7	92.0	34.9	2.6	1.0
F03	24	0.274	28.3	76.4	41.6	1.5	2.1
F04	17	0.274	1.3	20.7	13.4	10.0	3.5
F05	24	0.2626	23.1	118.5	64.9	2.8	1.0
F11	26	0.0274	1.3	114.9	73.1	56.9	16.4
F12	22	0.274	12.9	157.4	79.7	6.2	4.3
F13	21	0.274	14.8	186.0	68.0	4.6	3.5
F14	25	0.274	8.2	109.2	66.0	8.0	3.9
F19	53	0.274	2.3	85.3	40.6	18.0	7.6
F20	8	0.274	1.2	48.0	30.5	24.4	7.1
F21	1	0.274	2.8	17.4	17.4	6.3	NA
F22	24	0.21	7.1	57.4	13.8	1.9	1.0
F23	22	0.274	4.9	17.6	11.3	2.3	1.1
F24	7	0.274	5.5	8.6	7.2	1.3	7.5
F25	6	0.274	1.5	48.2	10.6	6.9	2.8
F26	36	0.274	0.9	54.9	29.5	31.5	6.5
F27	74	0.274	1.9	101.0	50.7	26.1	36.3
F28	50	0.16	14.9	69.7	31.6	2.1	1.0
F34	61	0.274	26.6	198.8	64.6	2.4	2.1

Table 5.3. Prediction skill of the 2023 North Pacific albacore base case model on the F12 abundance index over a horizon of 1 to 5 years and a retrospective peel of 0 to 5 years, using mean absolute scaled error (MASE) as the metric of skill.

Horizon (y)	Mean absolute prediction error (index units)	Mean absolute naïve prediction error (index units)	Mean absolute fit error (index units)	Mean absolute scaled error
1	2.02	1.74	1.19	1.16
2	2.15	1.80	1.20	1.19
3	2.10	1.50	1.22	1.40
4	2.25	1.44	1.27	1.56
5	2.30	1.90	1.30	1.21

Table 5.4. Total biomass (Q1, age-1+), female spawning biomass (Q2), limit reference point adopted by the NC of the WCPFC (20%$SSB_{current, F=0}$), recruitment, and fishing intensity (1-SPR) estimated in the base case model. Estimated virgin female spawning biomass (SSB_0) and virgin recruitment are 136,833 t and 180 million fish, respectively.

Year	Total biomass age-1+ (t)	Female spawning biomass (t)	Threshold reference point (30%$SSB_{current, F=0}$) (t)	Recruitment (x1000 fish)	Fishing intensity ($F_{\%SPR}$)
1994	914,370	76,445	56,179	239,937	56.7
1995	976,727	87,564	54,675	149,427	60.0
1996	981,948	91,535	51,869	232,014	53.4
1997	962,017	83,695	47,624	195,155	49.2
1998	927,430	88,690	49,875	127,084	50.7
1999	867,529	96,031	53,923	328,327	35.2
2000	849,253	80,096	50,869	125,091	51.0
2001	860,413	76,987	49,225	214,979	47.7
2002	843,187	75,619	49,166	115,502	37.9
2003	779,063	65,676	44,979	226,092	44.4
2004	747,893	75,466	48,624	258,194	37.5
2005	775,206	69,991	48,950	178,097	53.2
2006	825,670	67,474	46,552	186,195	51.4
2007	844,780	61,770	43,411	162,615	43.5
2008	814,092	61,955	42,931	225,067	55.9
2009	828,163	75,584	47,698	201,792	47.8
2010	839,581	76,581	48,591	230,510	54.0
2011	874,786	74,659	46,916	153,820	50.7
2012	873,779	71,654	44,943	155,274	46.9
2013	824,915	73,245	45,591	221,188	46.7
2014	806,417	75,282	47,030	124,967	48.9
2015	777,703	76,946	48,476	107,914	50.4
2016	722,600	74,271	47,027	235,903	56.0
2017	729,582	69,536	43,530	432,503	56.8
2018	879,850	73,569	44,044	217,506	55.8
2019	1,026,990	70,849	42,374	222,047	65.1
2020	1,109,370	64,592	37,300	212,904	56.0
2021	1,114,260	70,229	38,874	210,015	72.0

Table 5.5. Estimates of maximum sustainable yield (MSY), female spawning stock biomass (SSB), fishing intensity (F), and reference point ratios for north Pacific albacore tuna for: 1) the base case model; 2) two important sensitivity models due to uncertainty in growth parameters; and 3) a model representing an update of the 2020 base case model to 2023 data. SSB_0, $SSB_{current, F=0}$ and SSB_{MSY} are the expected female SSB of a population in the equilibrium, unfished state; in the current, dynamic, unfished state; and at MSY, respectively. The Fs in this table are indicators of fishing intensity based on spawning potential ratio (SPR) and calculated as %SPR. SPR is the ratio of the equilibrium SSB per recruit that would result from the estimated F-at-age relative to that of an unfished population. Depletion is calculated as the proportion of the age-1+ biomass during the specified period relative to an unfished age-1+ equilibrium biomass. The model representing an update of the 2020 base case model is similar to but not identical to the 2020 base case model due to changes in data preparation and model structure. *Model may not have converged and uncertainty estimates were unreliable because of the lack of a positive, definite Hessian matrix. †A value of >1 for the depletion ratio indicates higher age-1+ biomass in 2021 relative to the 2006 – 2015 period. §Higher %SPR values indicate lower fishing intensity levels. ¶Values of >1 for ratios of $F_{\%SPR}$ to $F_{\%SPR}$-based reference points indicate fishing intensity levels lower than the reference points.

Quantity	Base Case	Growth CV = 0.06 for L_{inf}	Growth All parameters estimated	Update of 2020 base case model to 2023 data*
MSY (t)	121,880	93,167	144,792	97,777
SSB_{MSY} (t)	23,154	18,133	30,435	18,756
SSB_0 (t)	165,567	128,155	198,913	132,570
SSB_{2021} (t)	70,229	35,418	101,161	36,909
$SSB_{current, F=0}$ (2021 estimate)	129,581	97,368	155,542	93,808
$SSB_{2021}/SSB_{current, F=0}$	0.54	0.36	0.65	0.39
$SSB_{2021}/30\%SSB_{current, F=0}$	1.81	1.21	2.17	1.31
$SSB_{2021}/14\%SSB_{current, F=0}$	3.87	2.60	4.65	2.81
†$Depletion_{2021}/Depletion_{2006-2015}$	1.34	1.33	1.37	1.30
§ $F_{\%SPR,\ 2018-2020}$ (%SPR)	59.0	41.4	70.4	43.2
§ $F_{\%SPR,\ 2011-2020}$ (%SPR)	55.0	36.6	63.8	37.9
¶ $F_{\%SPR,\ 2018-2020}/F_{\%SPR,\ MSY}$	2.04	1.42	2.78	1.47
¶ $F_{\%SPR,\ 2011-2020}/F45_{\%SPR}$	1.22	0.81	1.42	0.84
¶ $F_{\%SPR,\ 2018-2020}/F45_{\%SPR}$	1.31	0.92	1.56	0.96
¶ $F_{\%SPR,\ 2018-2020}/F_{\%SPR,\ 2002-2004}$	1.48	1.63	1.40	1.25

FIGURES

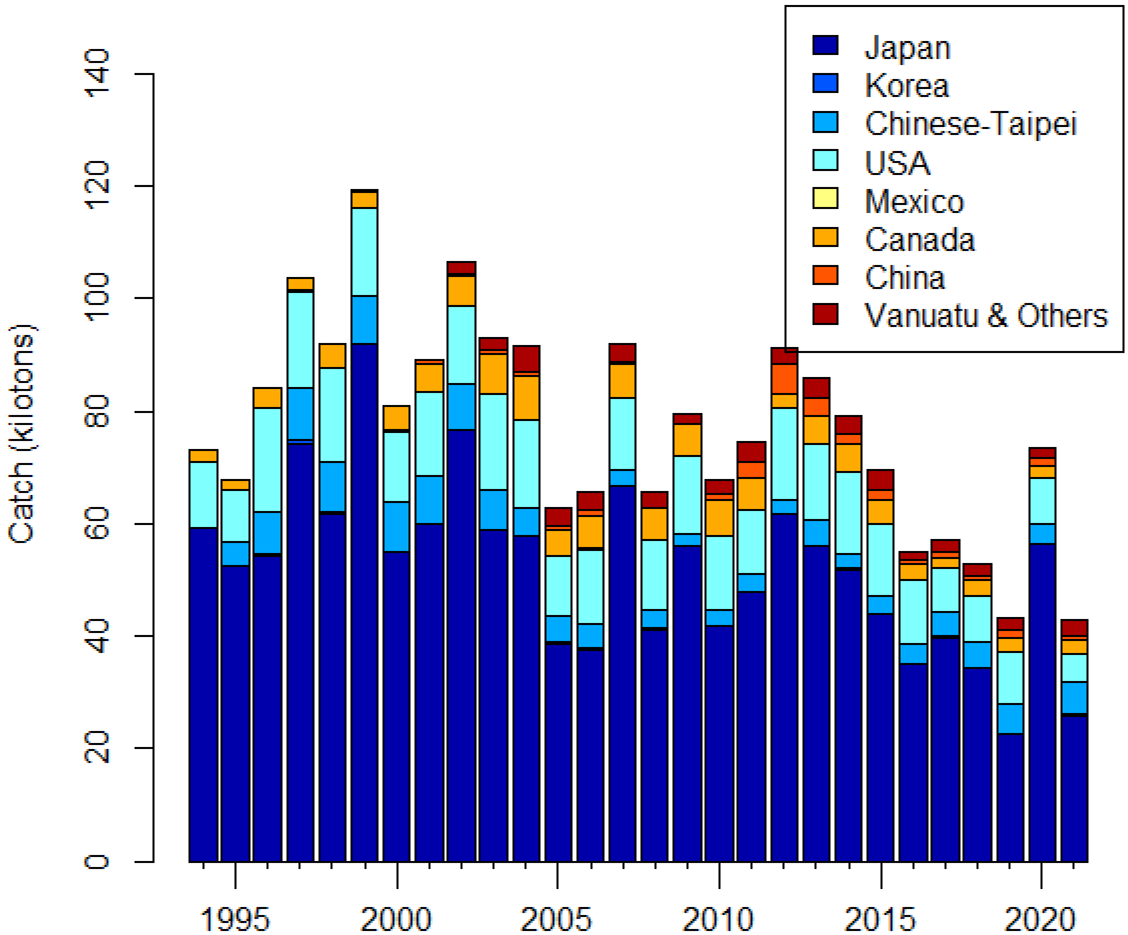

Figure 2.1. Total annual reported catch of north Pacific albacore (*Thunnus alalunga*) by ISC member and non-member countries, 1994-2021. Catches by Vanuatu and other countries includes small amounts of catch by other countries such as Tonga, Belize, Cook Islands, and Marshall Islands.

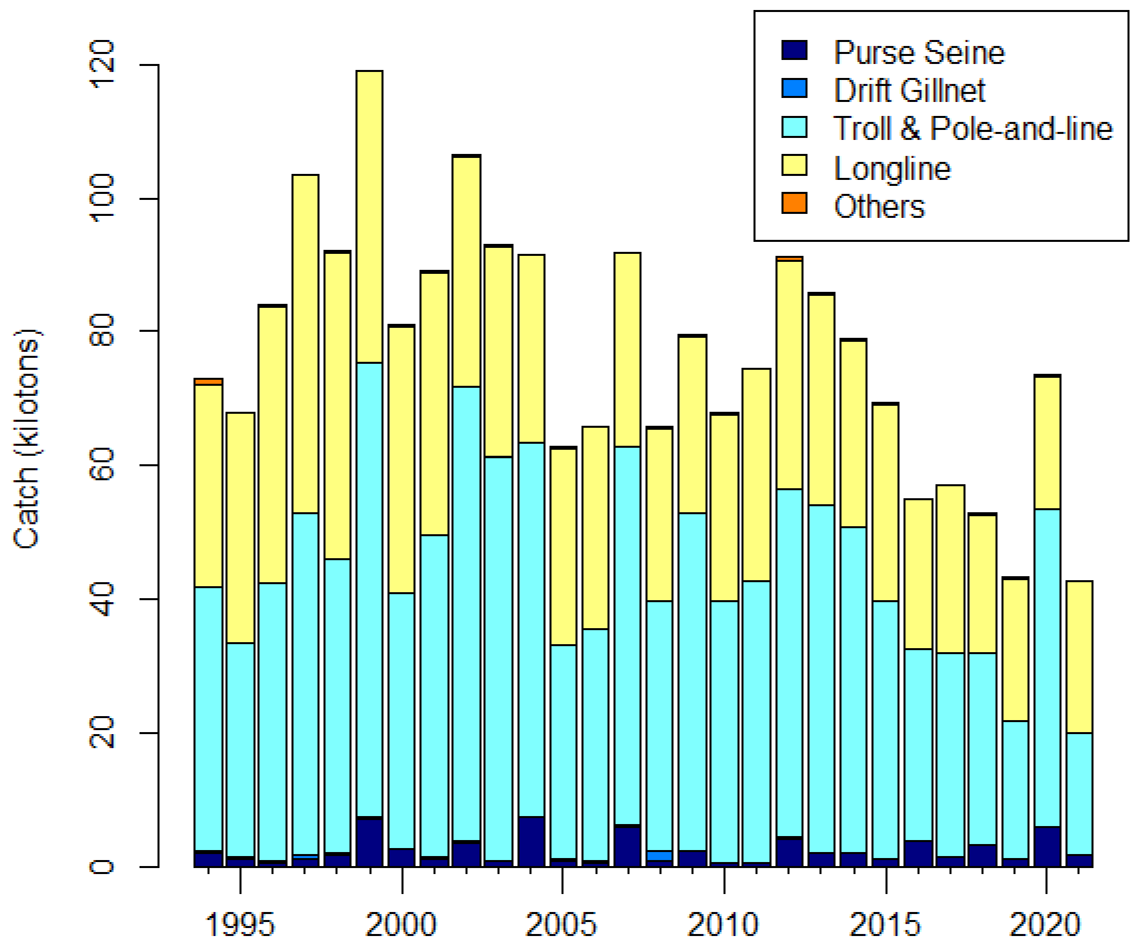

Figure 2.2. Total annual reported catch of north Pacific albacore by major gear types, 1994-2021. The Other Gears category includes set nets, recreational, hand line, and harpoon.

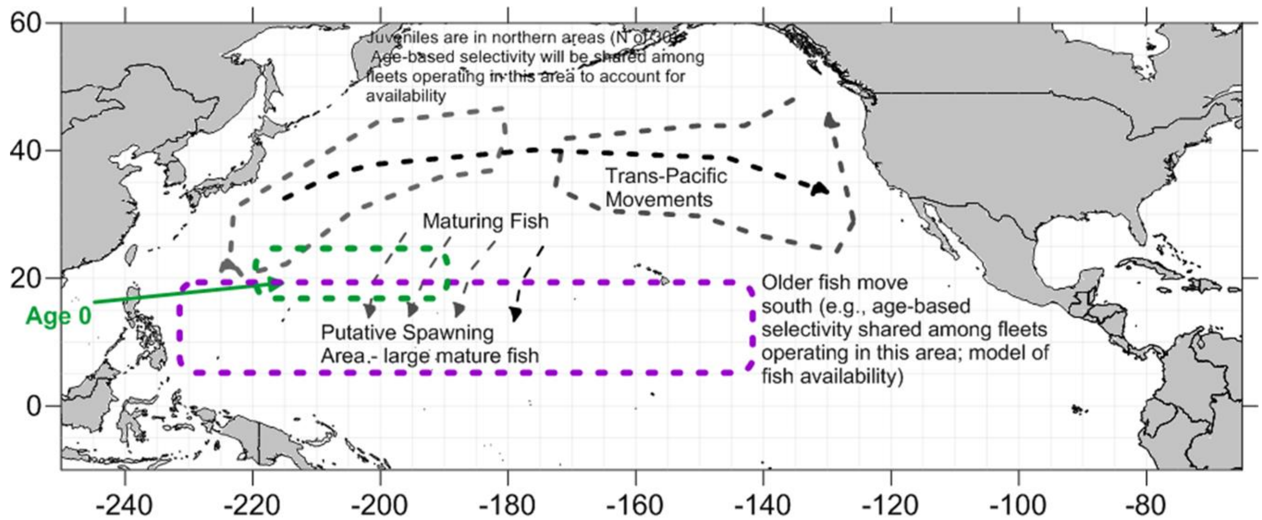

Figure 2.3. Conceptual model of north Pacific albacore biology and population dynamics. See Section 2.3 for details.

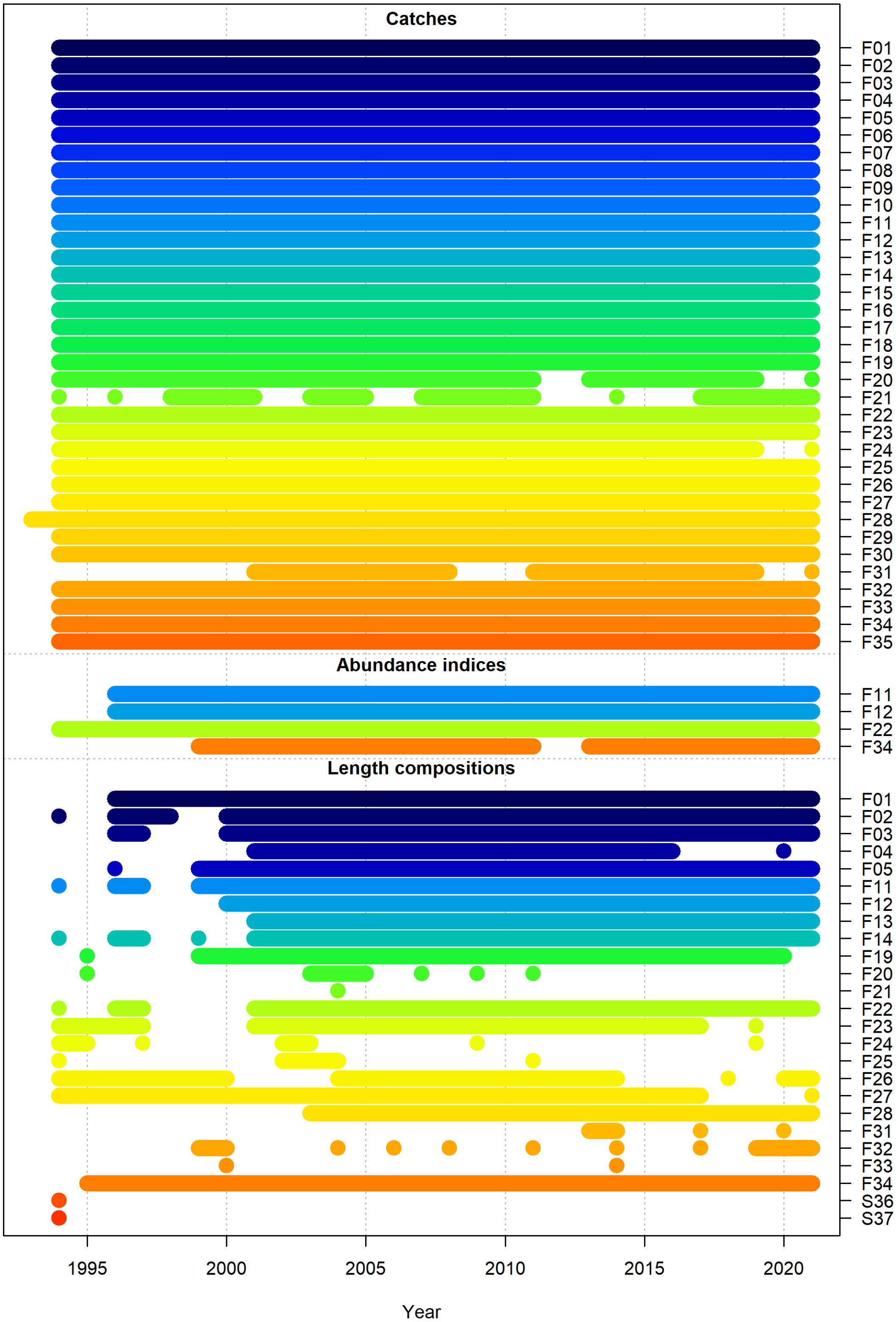

Figure 3.1. Temporal coverage and sources of catch, abundance indices, and length composition data by fleet used in the 2023 assessment of north Pacific albacore tuna. See the text and Table 3.1 for detailed descriptions of fishery codes.

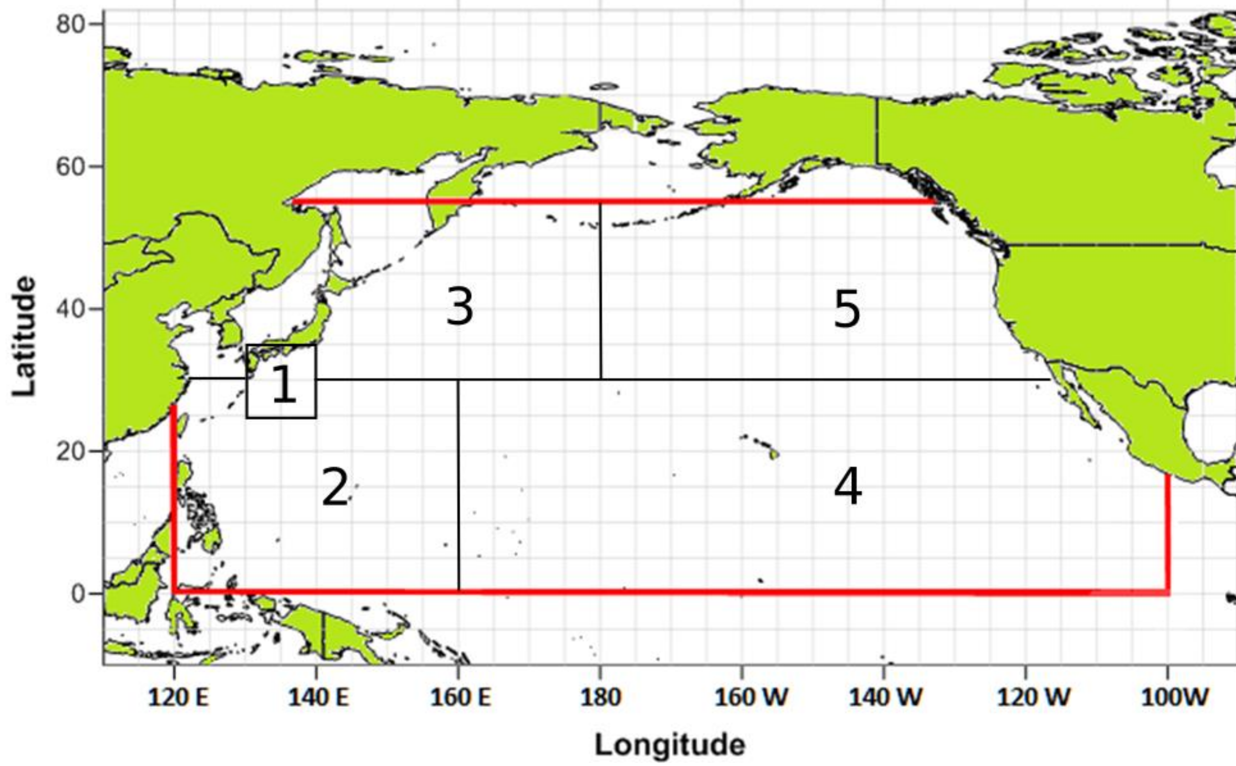

Figure 3.2. Spatial domain (red box) of the north Pacific albacore stock (*Thunnus alalunga*) in the 2023 stock assessment. Fishery definitions were based on five fishing areas (black boxes and numbers) defined from cluster analyses of size composition data.

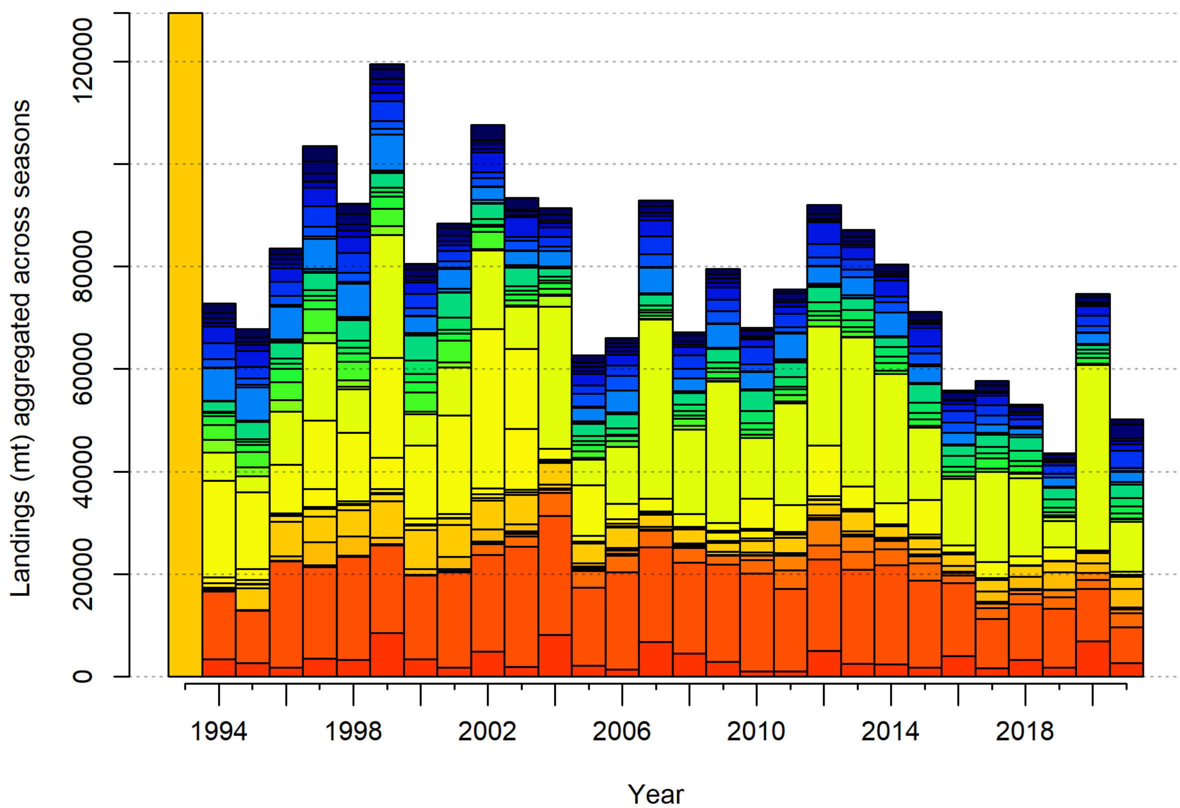

Figure 3.3. Annual catch in weight (t) by fleet in the base case model. Color indicates fleet in base case model (Table 3.1), with F01 in dark blue and F35 in dark red. Catch in weight for some fleets were estimated from catch in numbers. First bar (yellow) indicates the estimated initial catch of F28.

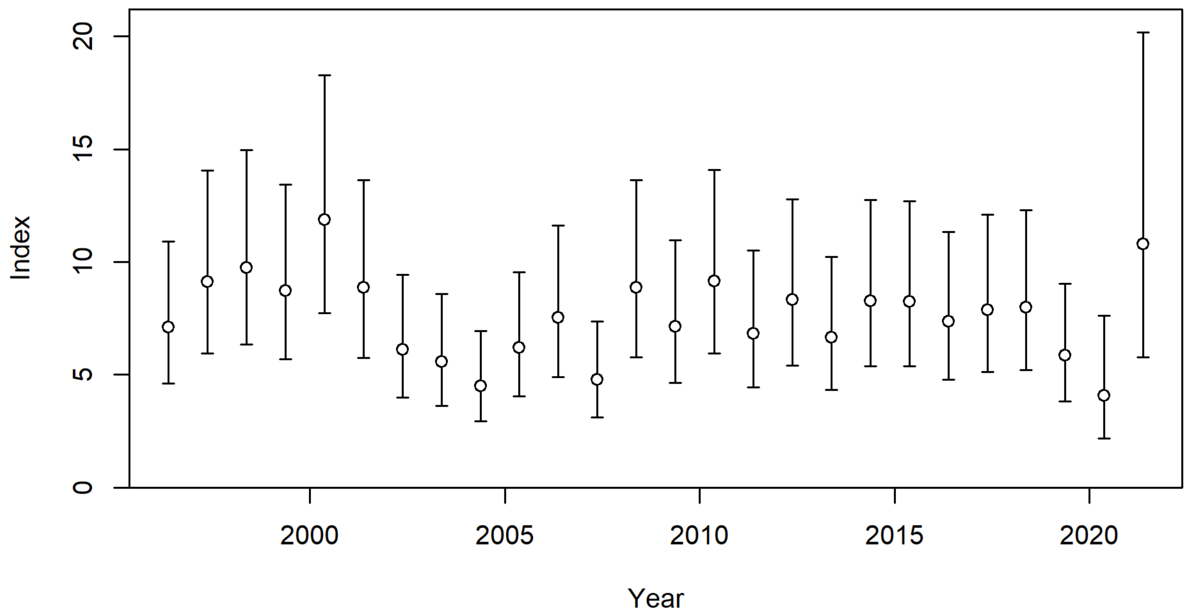

Figure 3.4. Trends and 95% confidence intervals of the adult index (F12) used in the base case model. Note that the 95% confidence intervals are based on the model assumption of lognormal error, and include both input and additional coefficients of variation (CVs). See Table 3.2 for index values and CVs.

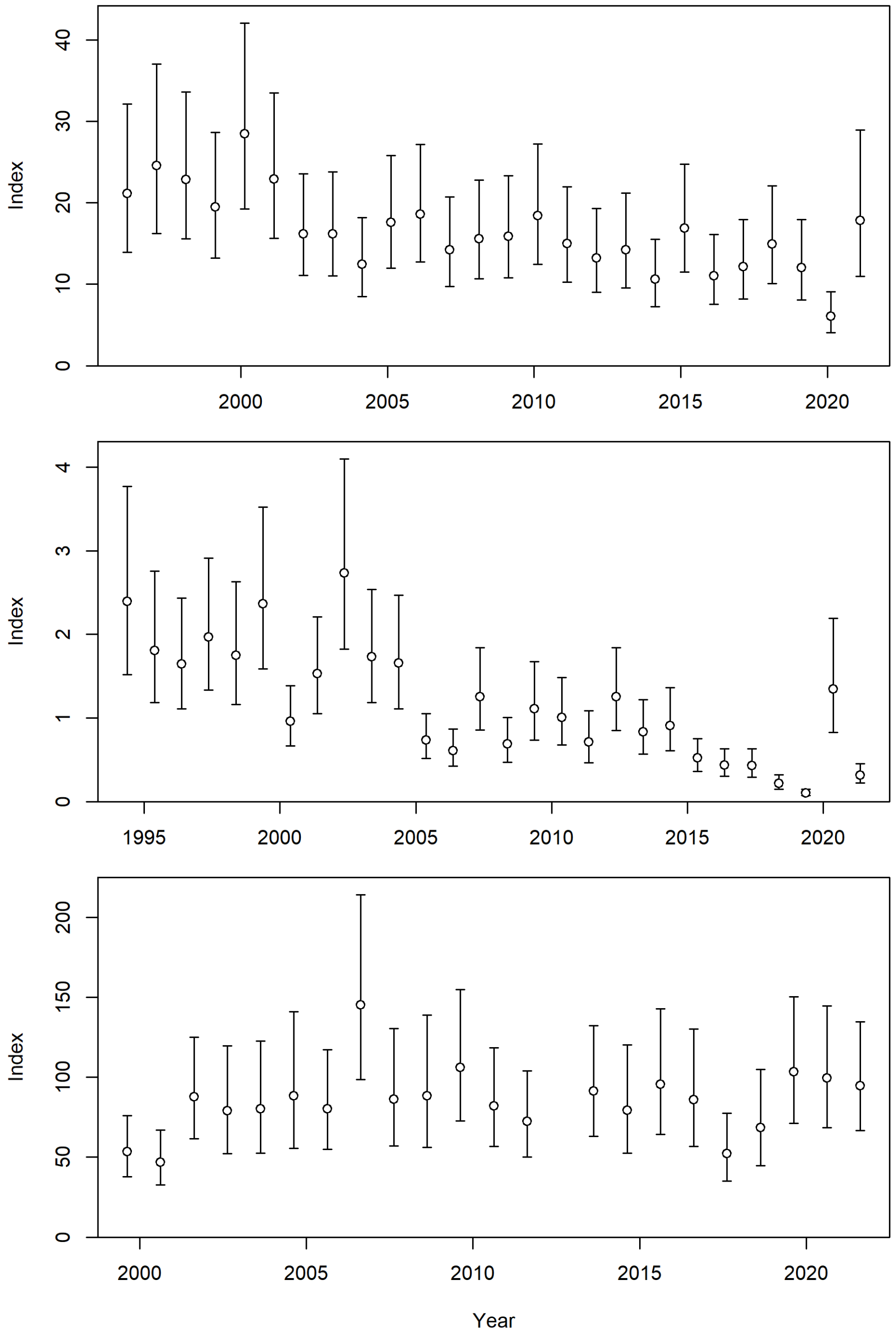

Figure 3.5. Trends and 95% confidence intervals of the indices (F11 – top; F22 – middle; and F34 - bottom) used in sensitivity model runs. Note that the 95% confidence intervals are based on the model assumption of lognormal error, and include both input and additional coefficients of variation (CVs). See Table 3.3 for index values and CVs.

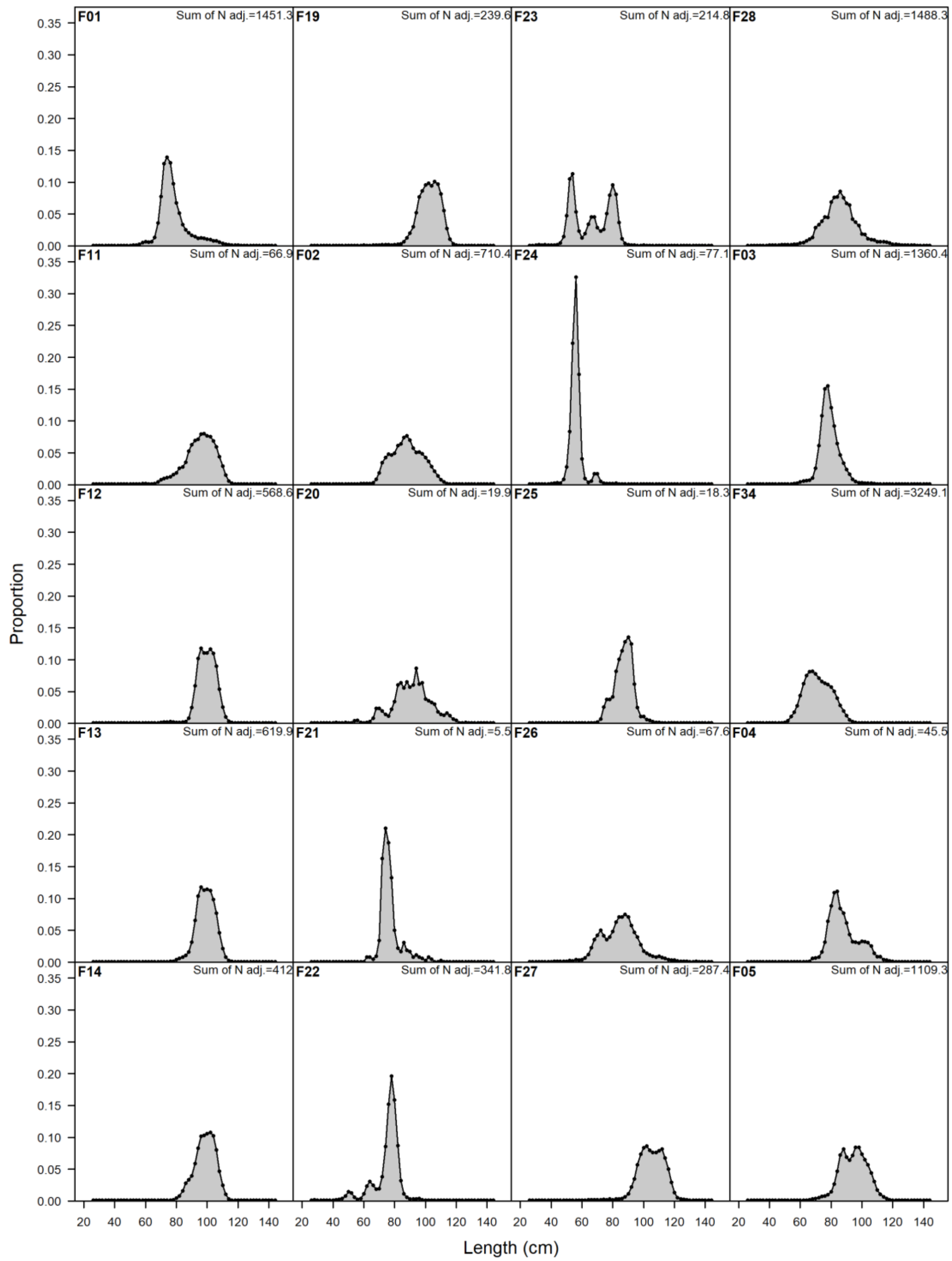

Figure 3.6. Aggregated size composition data fitted in the base case model for the 2023 north Pacific albacore stock assessment. Sum of N adj indicate the total sample size of the size composition data for each fishery after data reweighting. See Table 3.1 for description of fisheries.

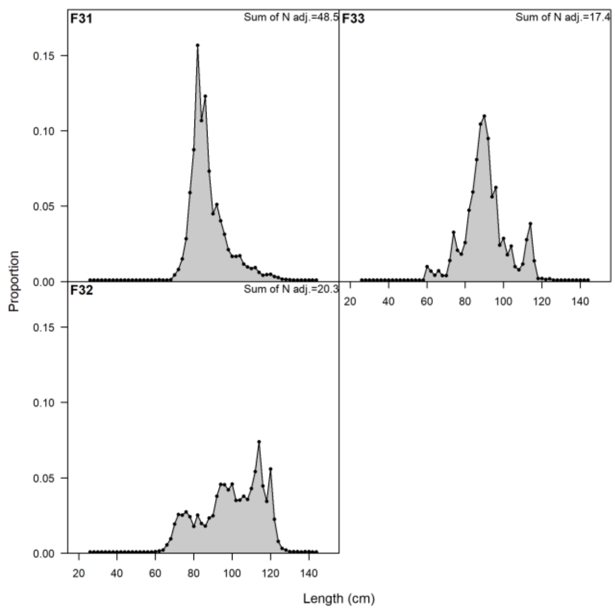

Figure 3.7. Aggregated size composition data that were available but not fitted in the base case model for the 2023 north Pacific albacore stock assessment. Sum of N adj indicate the total sample size of the size composition data for each fishery after data reweighting. See Table 3.1 for description of fisheries.

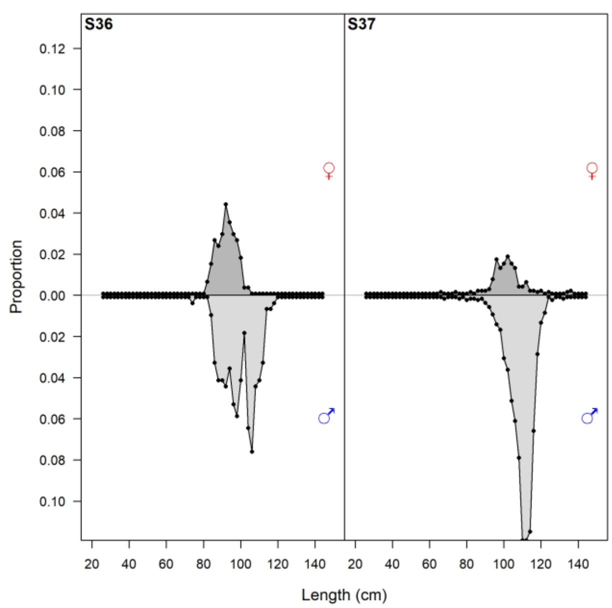

Figure 3.8. Aggregated sex-specific size composition data sampled by Japanese research and training longline vessels in Area 2 (S36) and 4 (S37) but were not fitted in the base case model for the 2023 north Pacific albacore stock assessment. See Section 3.7.

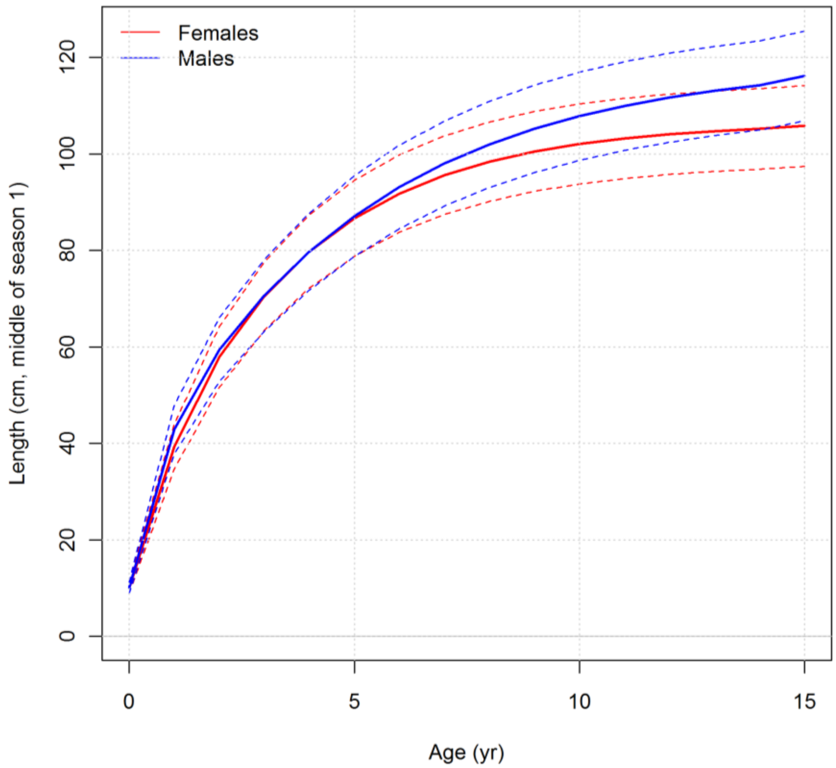

Figure 4.1. Growth model of north Pacific albacore used in the 2023 assessment. Dashed lines indicate 95% confidence intervals. Based on sex-specific growth model by Xu et al. (2014). See Table 4.1 for detailed parameters.

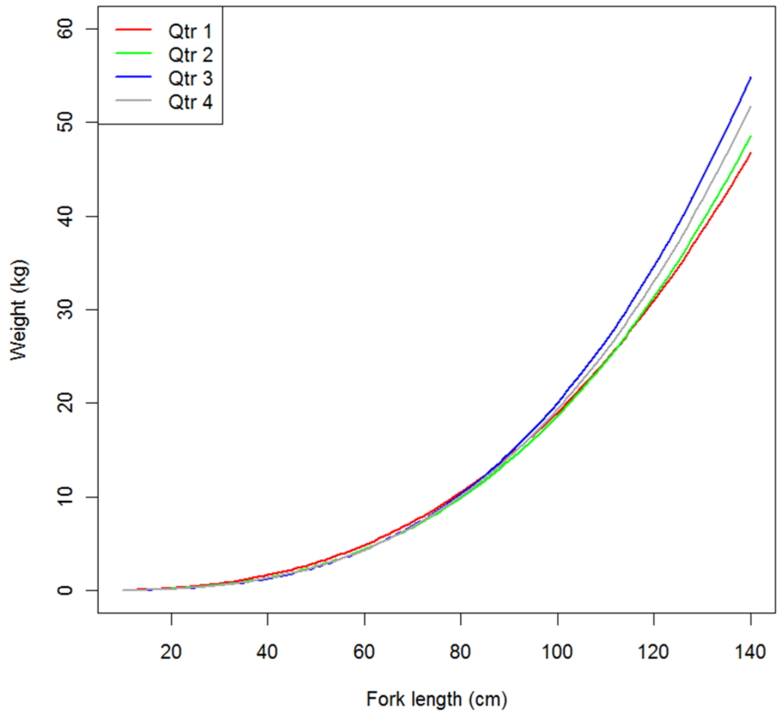

Figure 4.2. Seasonal weight-at-length relationships of north Pacific albacore used in the 2023 assessment. Based on Watanabe et al. (2006). Male and female weight-at-length relationships were assumed to be identical. See Table 4.1 for detailed parameters.

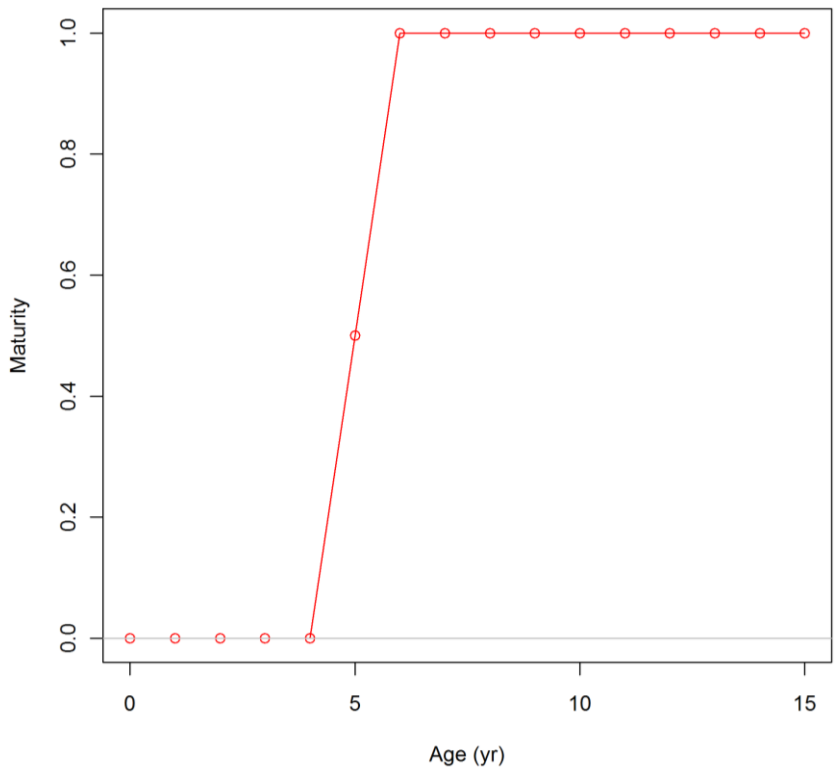

Figure 4.3. Maturity-at-age for female north Pacific albacore used in the 2023 assessment. See Table 4.1 for detailed parameters.

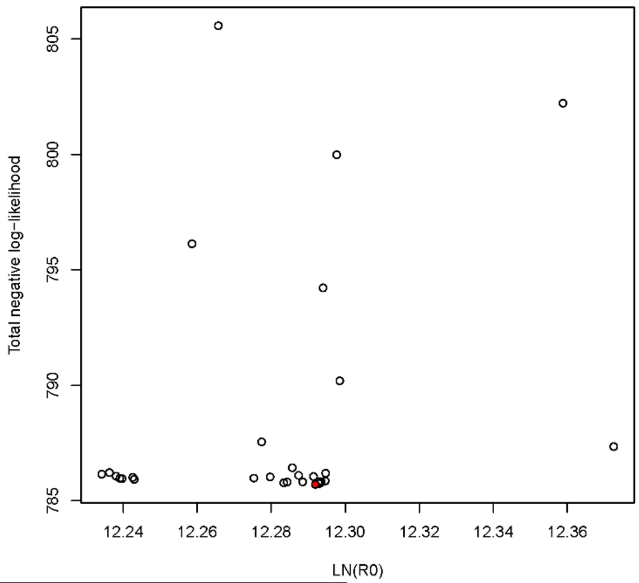
Total negative log−likelihood
805
800
795
790
785
12.24
12.26
12.28
12.30
12.32
12.34
12.36
LN(R0)

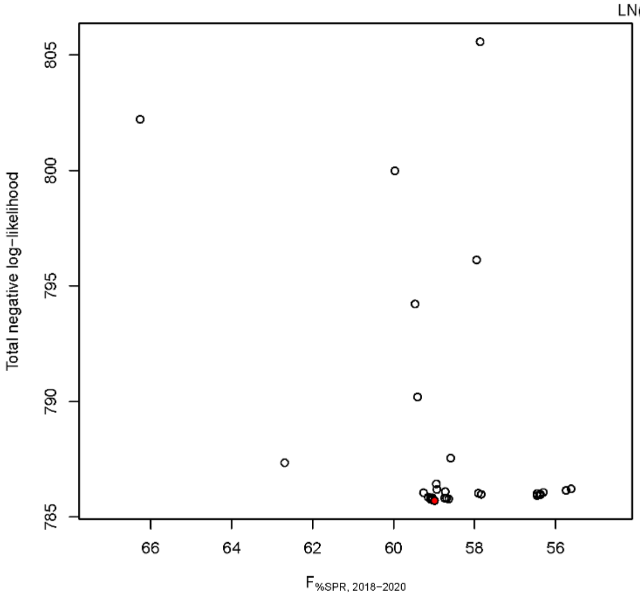
Total negative log−likelihood
805
800
795
790
785
66
64
62
60
58
56
F%SPR, 2018−2020

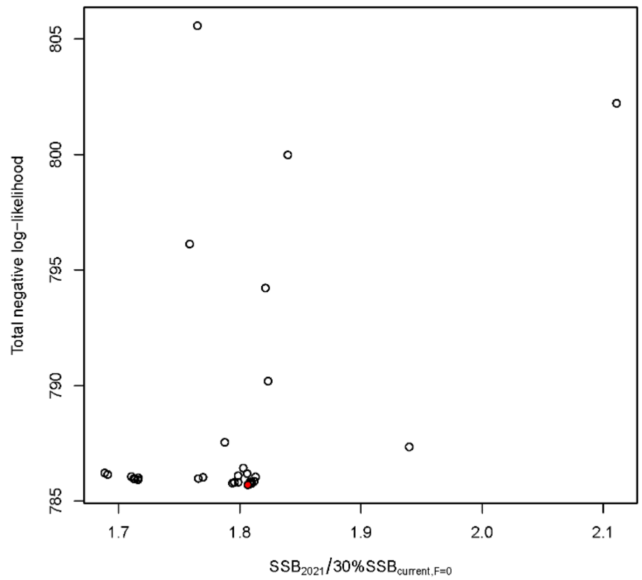

Figure 5.1. Total negative log-likelihood versus estimated virgin recruitment in log-scale [ln(R_0)] (upper panel), the average fishing intensity during 2018 - 2020 ($F_{\%SPR,\ 2018\text{-}2021}$) (lower left panel), and the ratio of female spawning biomass in 2021(SSB_{2021}) to the $30\%SSB_{current,\ F=0}$ threshold reference point (lower right panel) from 50 model runs with different phasing and initial values of ln(R_0) and other important parameters, as well as randomly jittered initial values for all estimated parameters in the base-case model. Red closed circle shows results from the model run using initial parameters and phasing corresponding to the 2023 base case model, which had the lowest total negative log-likelihood (785.702) of all 50 model runs.

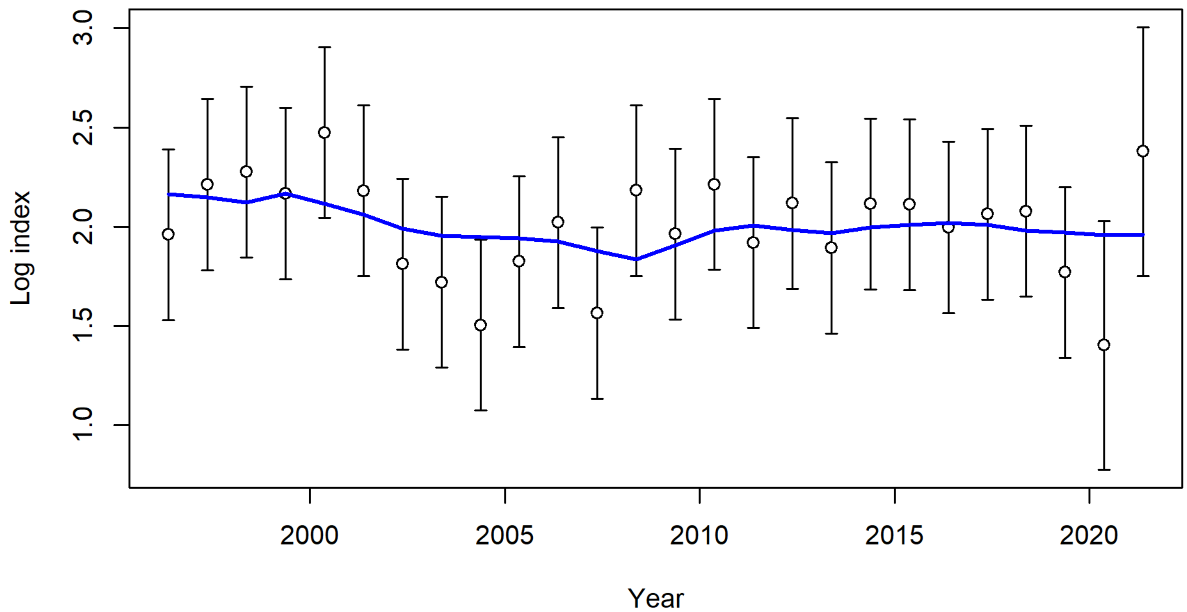

Figure 5.2. Log-scale observed (open circles) and predicted (blue line) relative abundance from the F12 adult abundance index in the 2023 base case model. Error bars are the 95% confidence intervals.

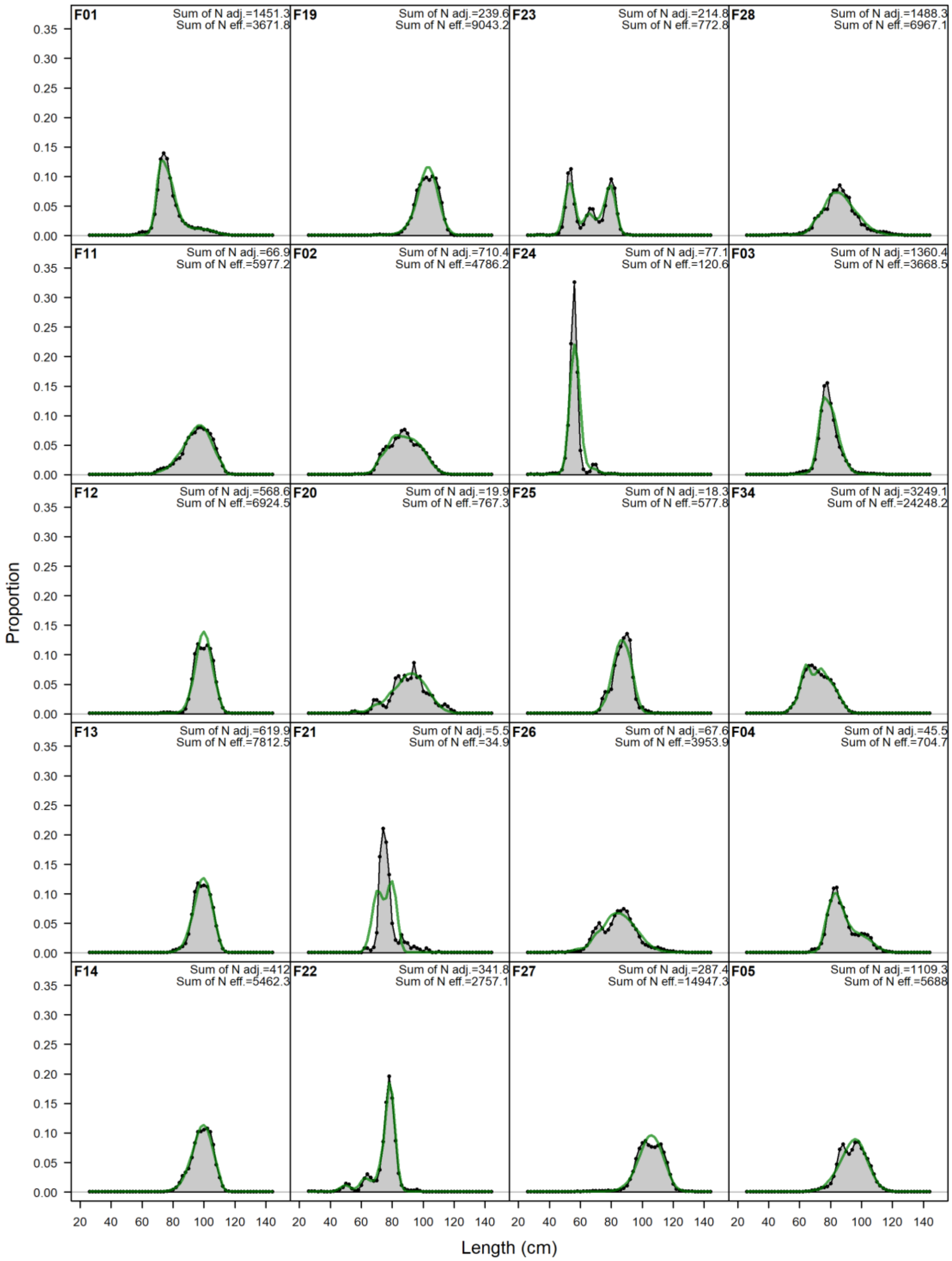

Figure 5.3. Observed (grey) and model predicted (green line) aggregated size compositions for fleets in the 2023 base-case model. Only fleets with fitted size compositions are shown. See Tables 3.1 and 5.2 for description of fleets and details of model fit, respectively.

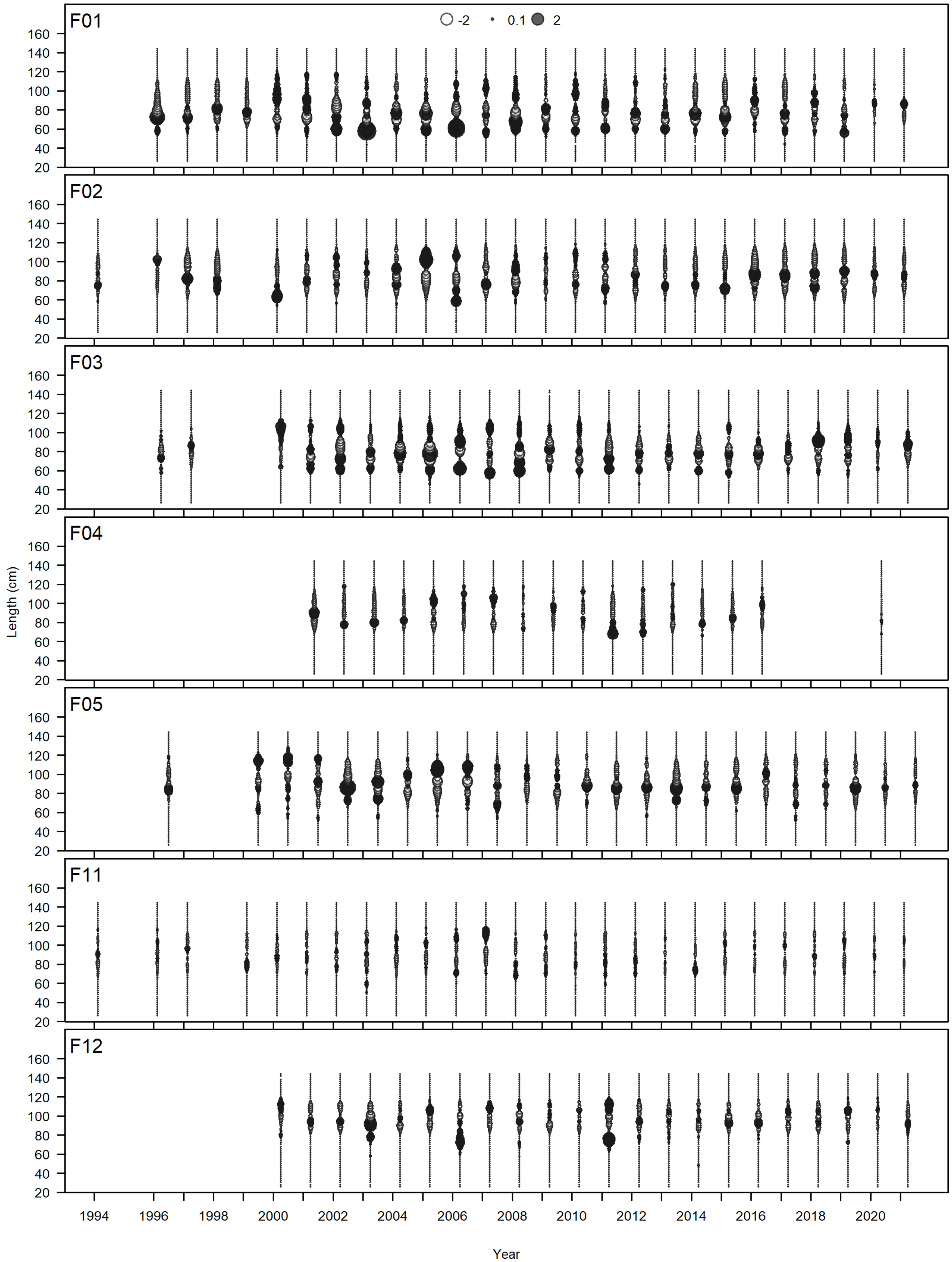

Figure 5.4. Pearson residuals of model fit to size composition data from fisheries in the 2023 base case model. Filled and open circles represent observations (i.e., proportions at size) that are larger and smaller than model predictions, respectively. Area of the circle is proportional to absolute values of residuals.

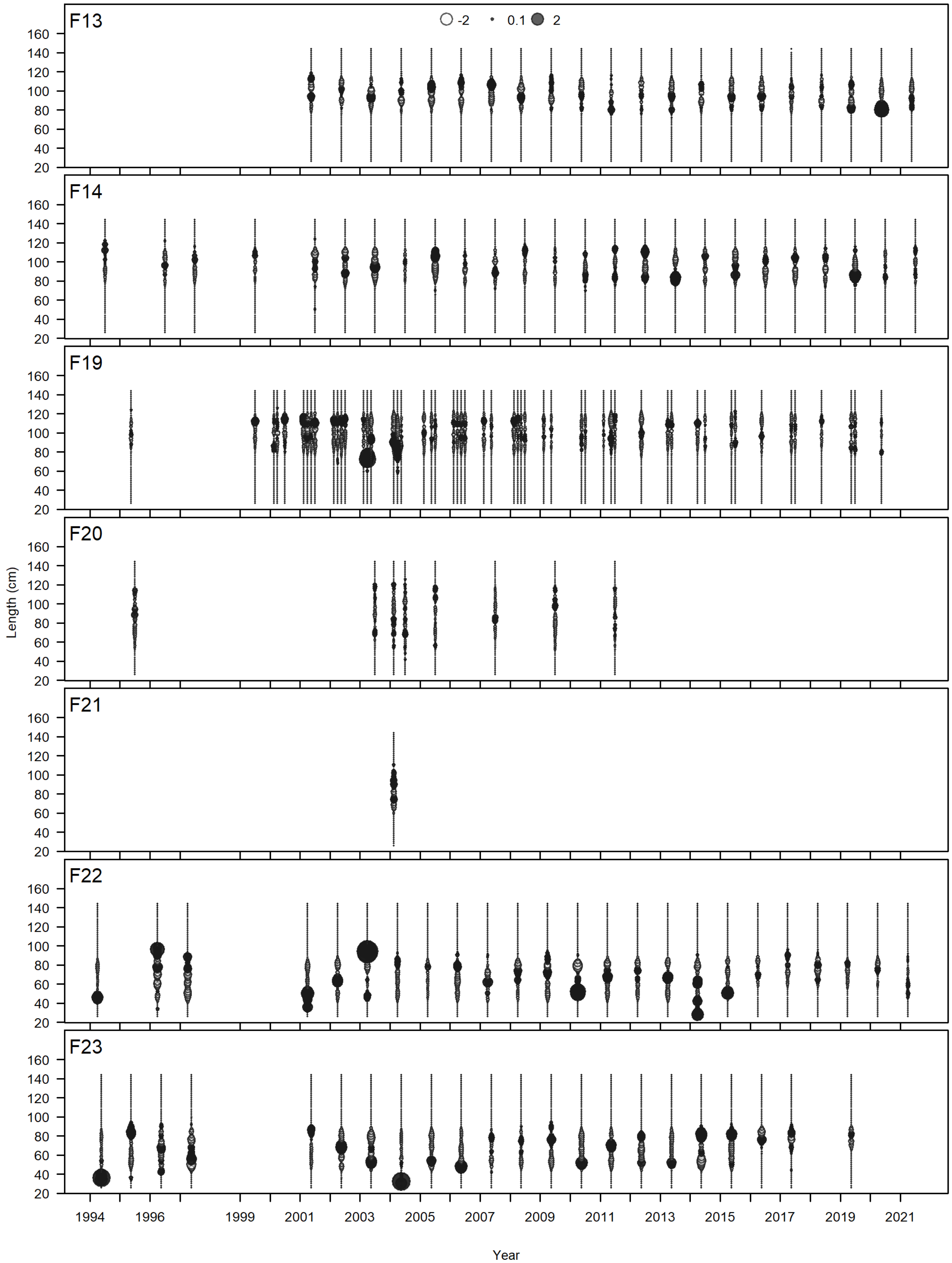

Figure 5.4. continued.

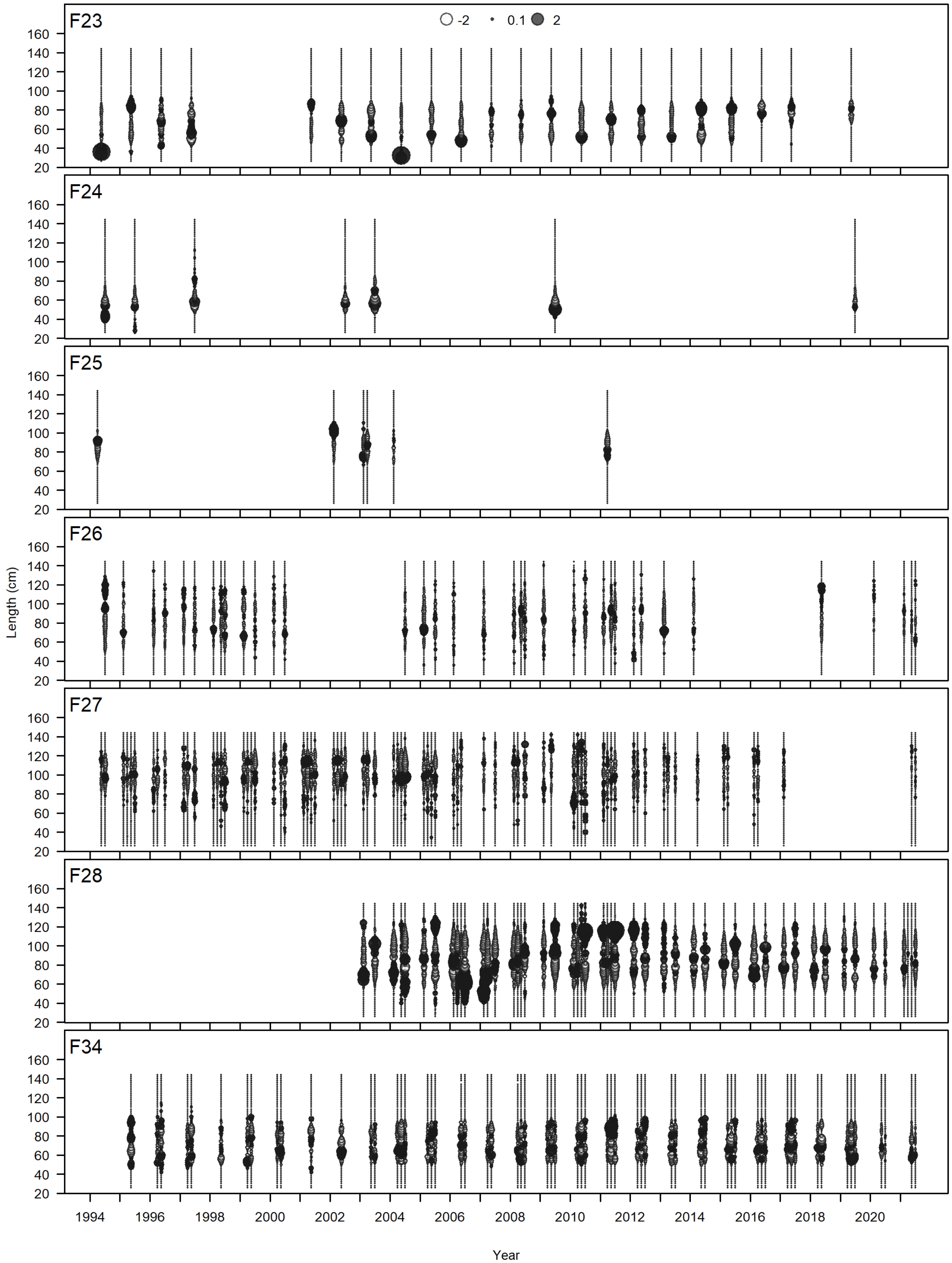

Figure 5.4. continued.

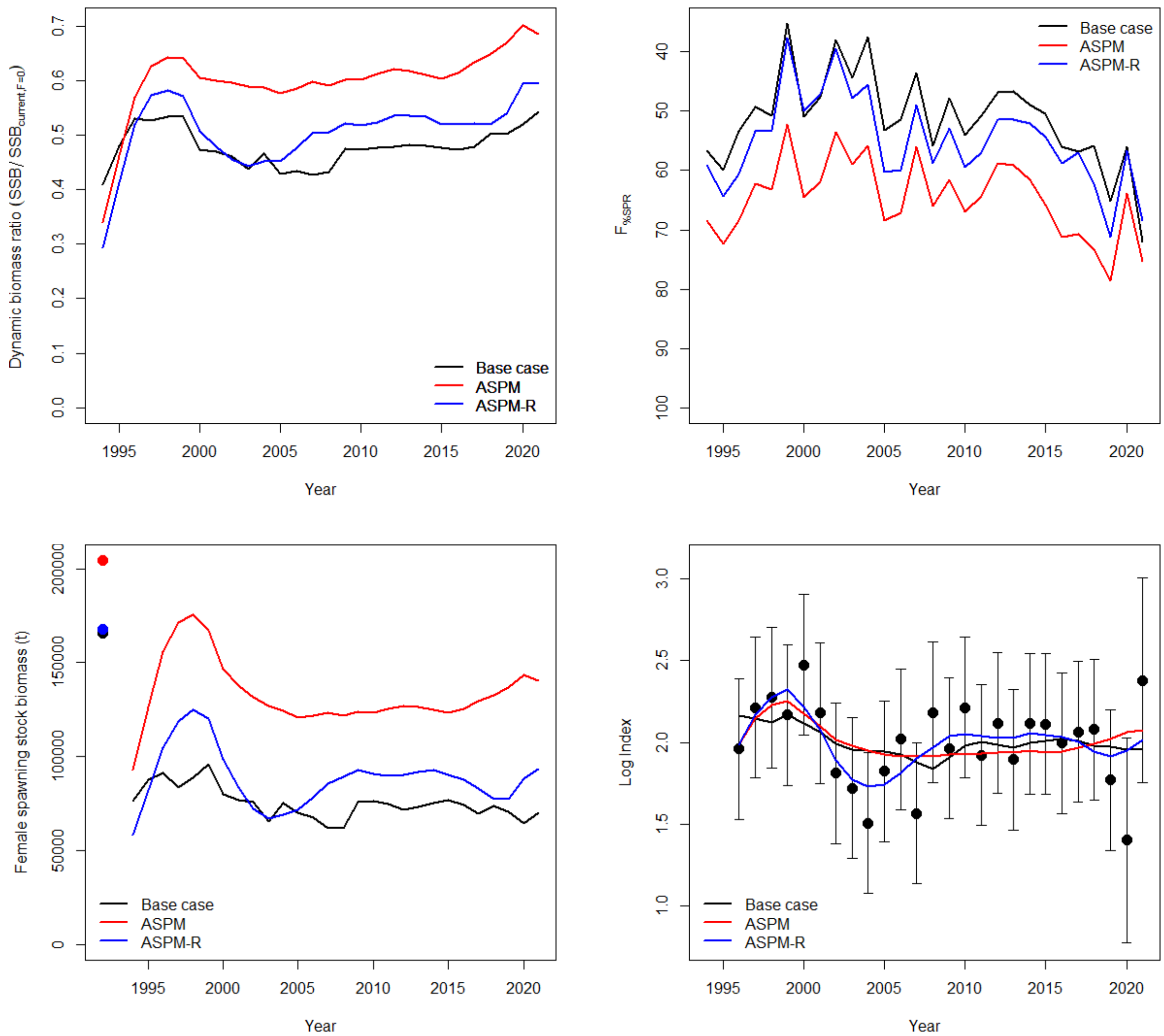

Figure 5.5. Estimated ratio of female spawning stock biomass to dynamic, unfished female spawning stock biomass (upper left panel); fishing intensity ($F_{\%SPR}$; upper right panel); female spawning stock biomass (lower left panel); and fit to the F12 adult abundance index (lower right panel) of the age-structured production model (ASPM; red), ASPM with recruitment deviates (ASPM-R; blue) and the base case model (black). Colored circles in lower left panel indicate the estimated virgin female spawning stock biomass (SSB_0) for each model. Black circles and error bars in the lower right panel indicate observations and 95% confidence intervals of the F12 index.

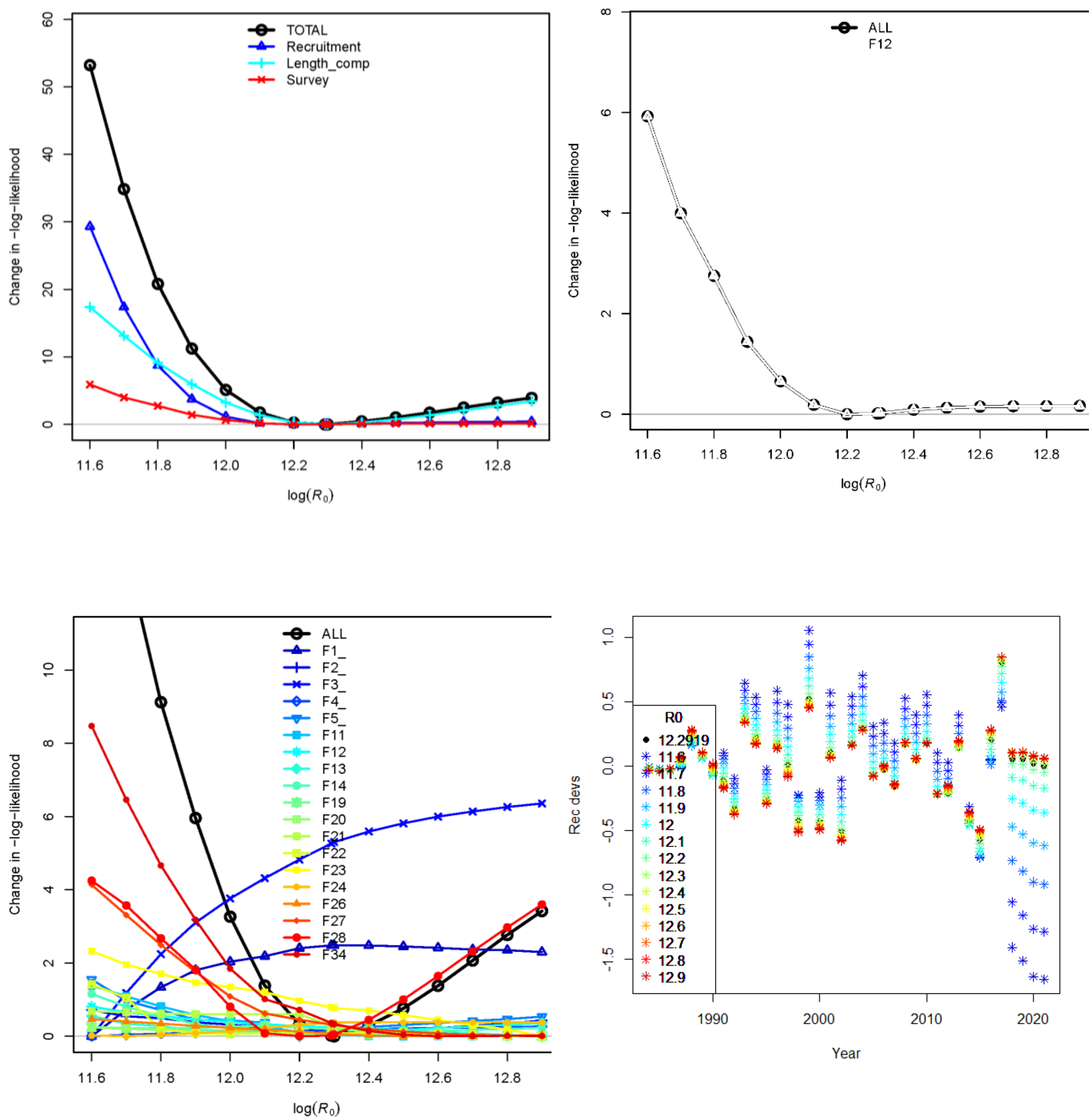

Figure 5.6. Likelihood profiles with respect to virgin recruitment [log(R_0)] of the main data components (upper left), F12 abundance index (upper right), and size compositions (lower left); and recruitment deviate time series of the likelihood profiles (lower right) of the 2023 base case model.

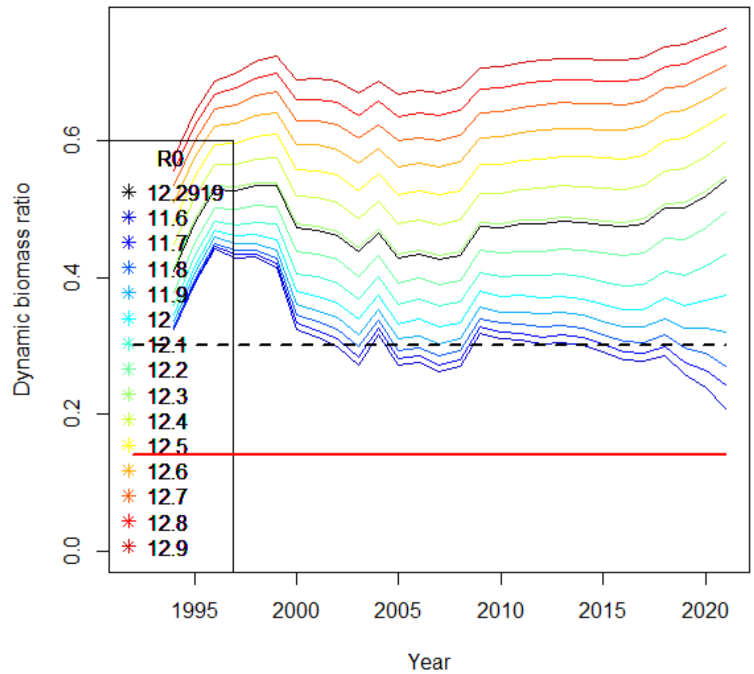

Figure 5.7. Estimated dynamic biomass ratios (i.e., ratios of female spawning stock biomass (SSB) relative to dynamic, unfished SSB) of the base case model (black line) and models with virgin recruitment [log(R_0)] fixed at various values. Horizontal lines indicate the threshold (dashed black line; 30%$SSB_{current,\ F=0}$) and limit (solid red line; 14%$SSB_{current,\ F=0}$) reference points.

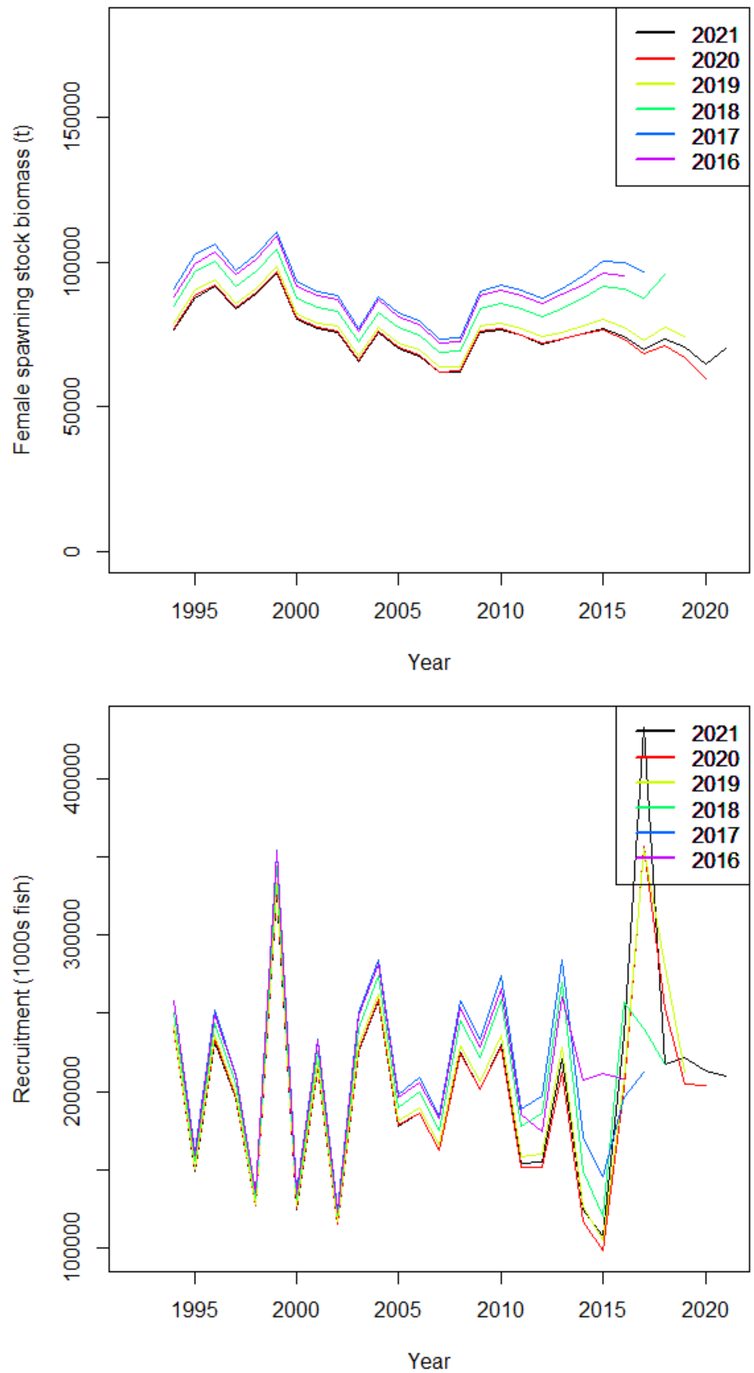

Figure 5.8. Estimated female spawning biomass (SSB) (upper), and recruitment (lower) of the base case model (black; 2021) and models with one to five terminal years of data removed. Legend indicate terminal year of the model.

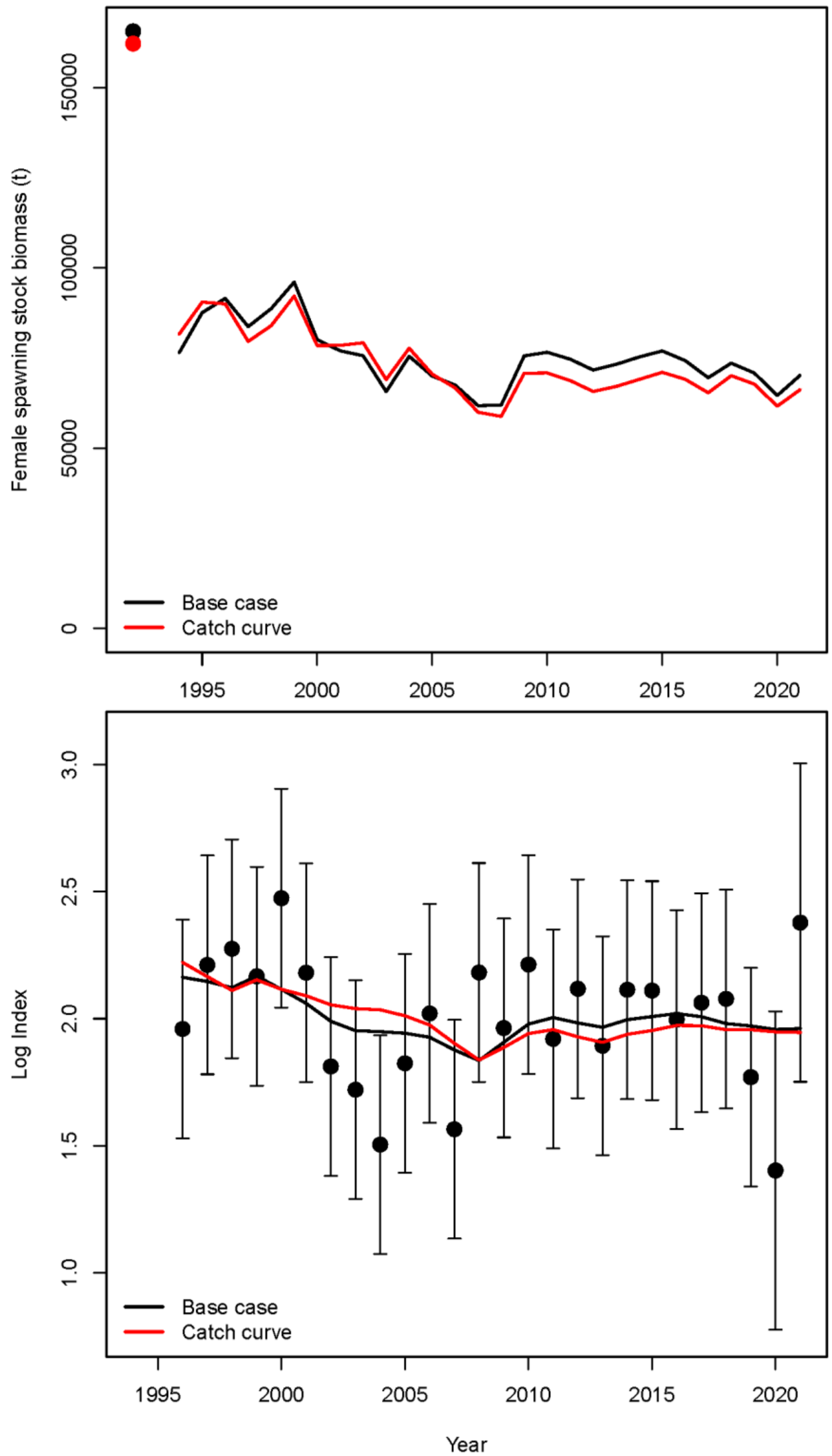

Figure 5.9. Estimated female spawning stock biomass (upper) and fit to the F12 adult abundance index (lower) of the 2023 base case model (black) and the catch curve analysis (red).

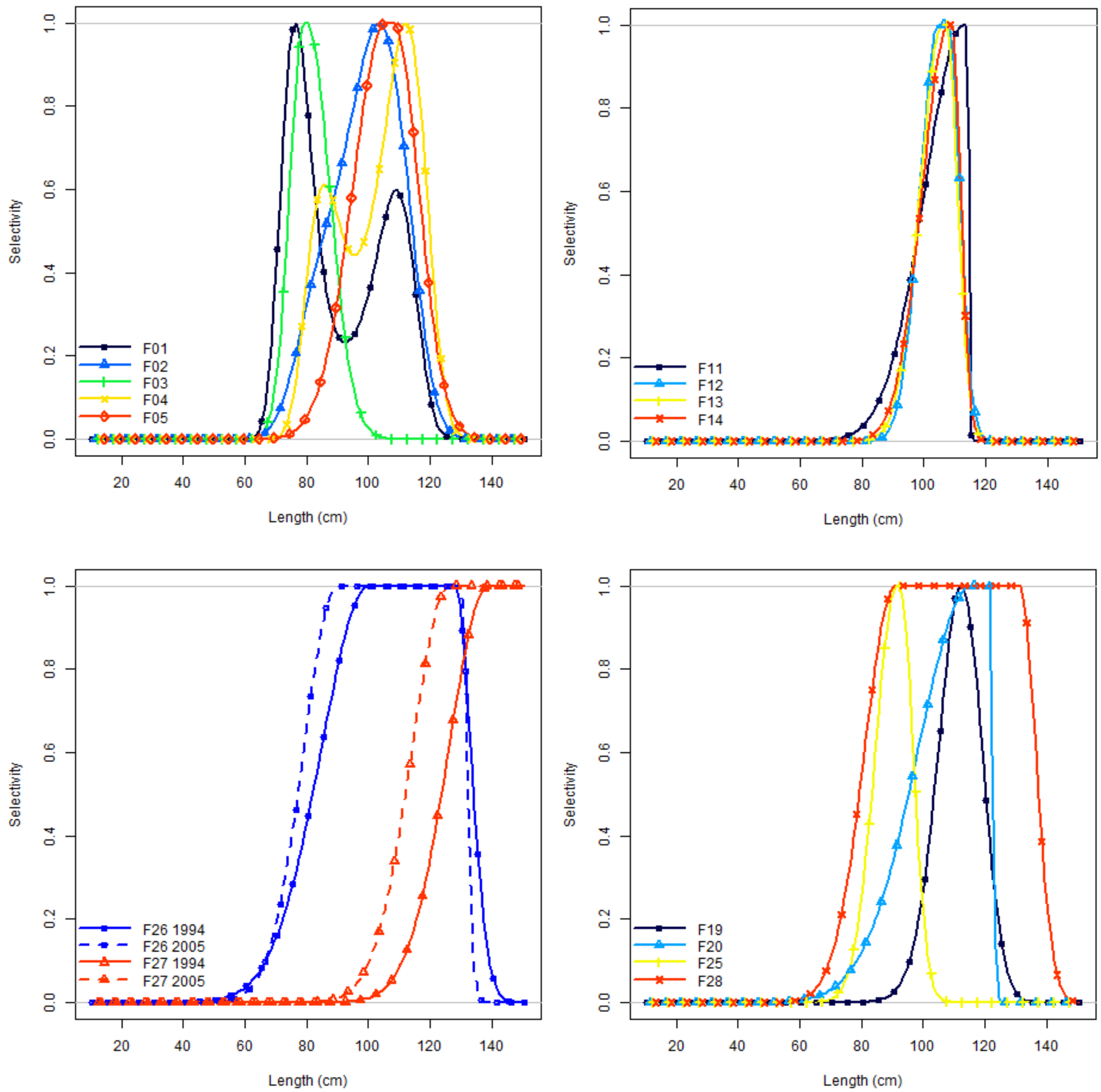

Figure 5.10. Estimated selectivity for fisheries with size-only selectivity in the 2023 base case model. Selectivity patterns are grouped by: 1) Japanese longline fisheries in Areas 1 and 3 (upper left); 2) Japanese longline fisheries in Area 2 (upper right); 3) US longline fisheries (lower left); and 4) all other fisheries with size-only selectivities (lower right). Years in lower left panel indicates first year of time block. All other panels in this figure have constant selectivity through time. Male selectivity is identical to female selectivity in the base case model. Only fisheries with size composition data fitted in the base case model are shown.

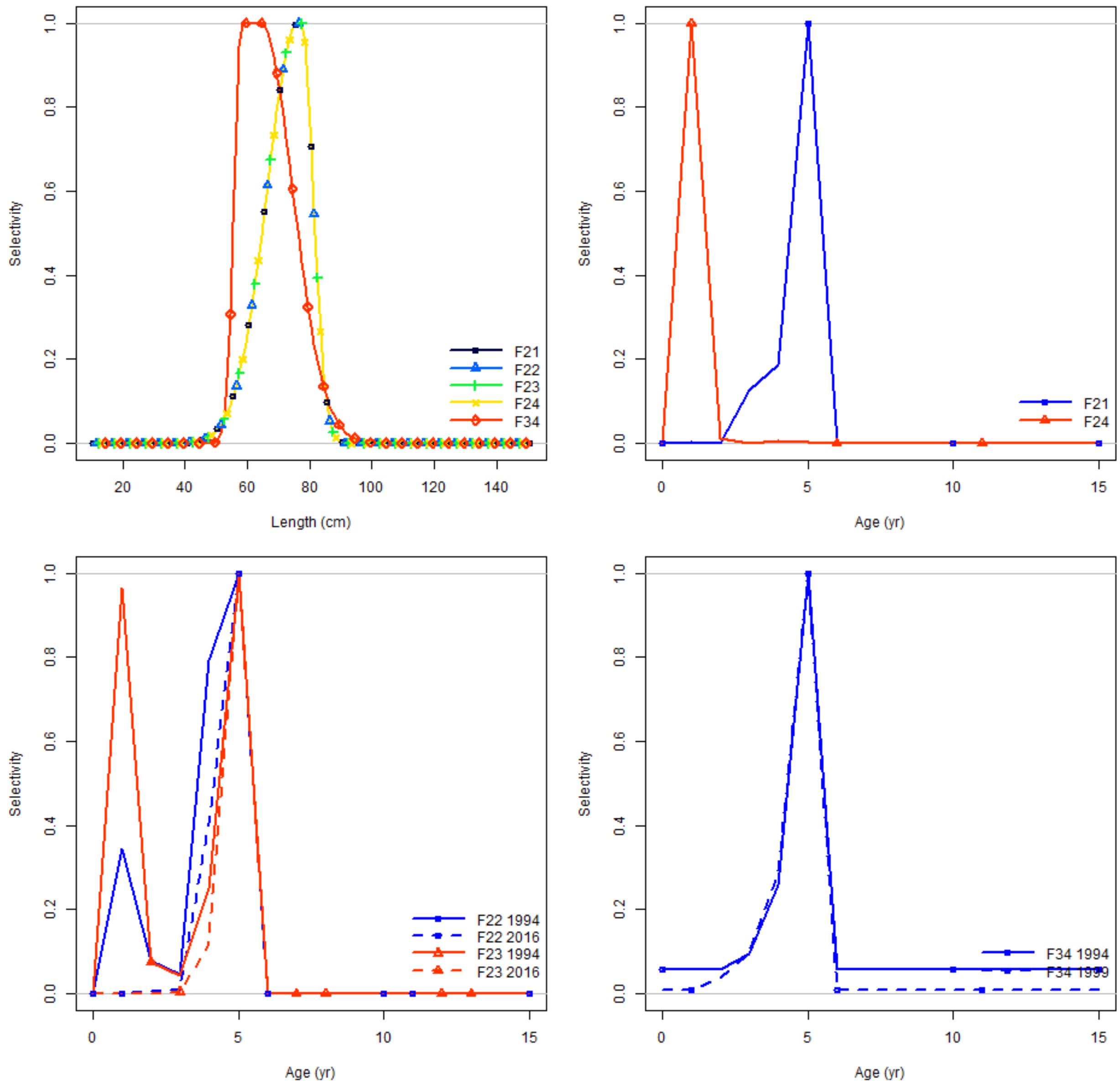

Figure 5.11. Estimated selectivity for fisheries with selectivity assumed to be a product of size (upper left) and age selectivity (upper right: F21 and F24; lower left: F22 and F23; lower right: F34), in the 2023 base case model. F21, F22, F23, and F24 are Japanese pole-and-line fleets in Areas 3 and 5 and share the same size selectivity. Years in lower panels indicates first year of time block. Male selectivity is identical to female selectivity in the base case model. Only fisheries with size composition data fitted in the model are shown.

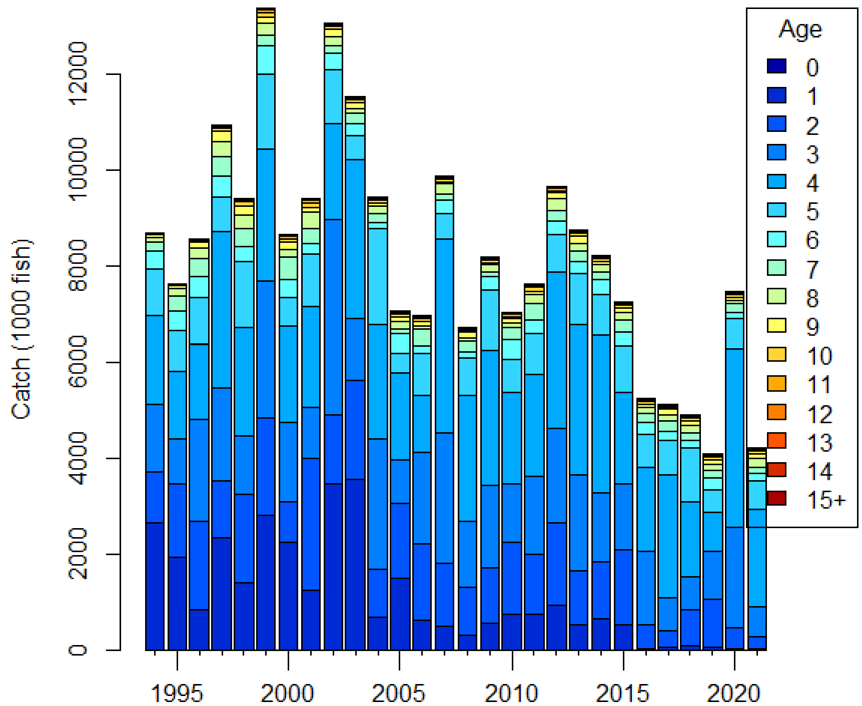

Figure 5.12. Historical catch-at-age of north Pacific albacore (*Thunnus alalunga*) estimated by the 2023 base case model.

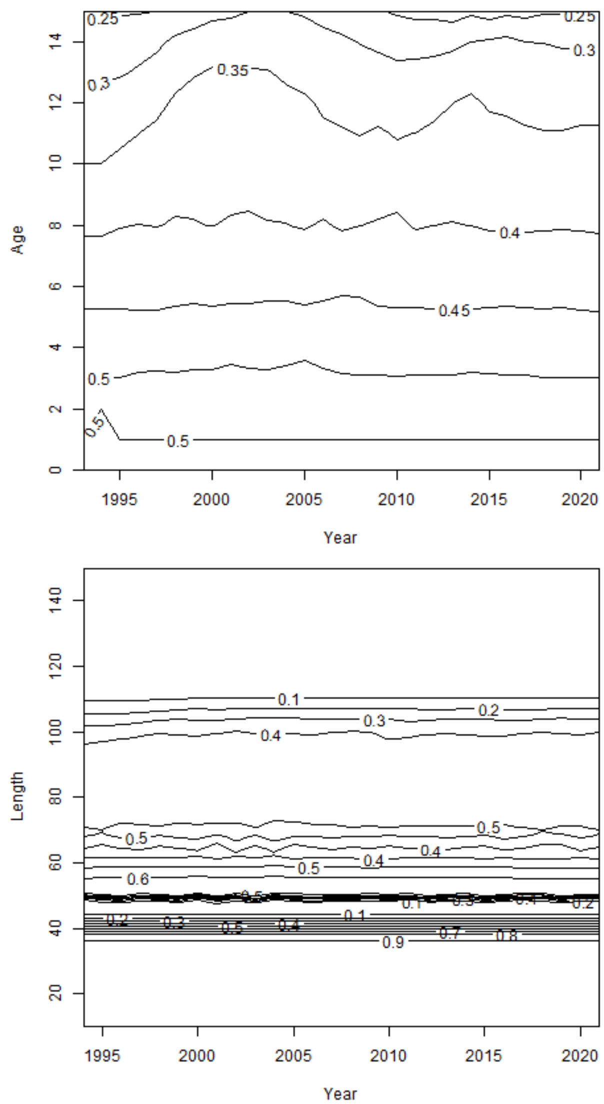

Figure 5.13. Estimated fraction of females in the population by age (upper) and fork length in cm (lower) in the 2023 base case model.

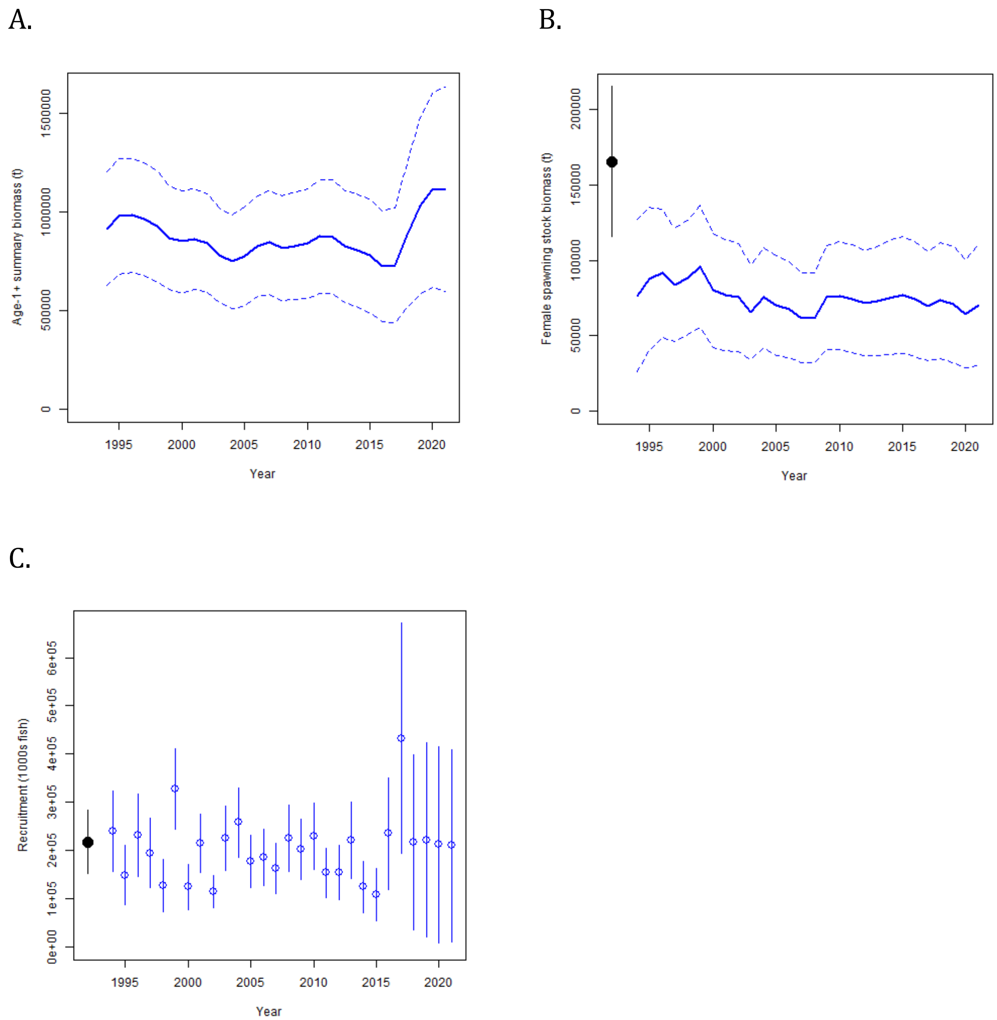

Figure 5.14. Maximum likelihood estimates of (A) age-1+ biomass, (B) female spawning biomass (SSB), and (C) age-0 recruitment of north Pacific albacore tuna (*Thunnus alalunga*). Dashed lines (A and B) and vertical bars (C) indicate 95% confidence intervals. Closed black circle and error bars in (B) and (C) are the maximum likelihood estimate and 95% confidence intervals of unfished female spawning biomass, SSB_0, and unfished recruitment, respectively, at equilibrium.

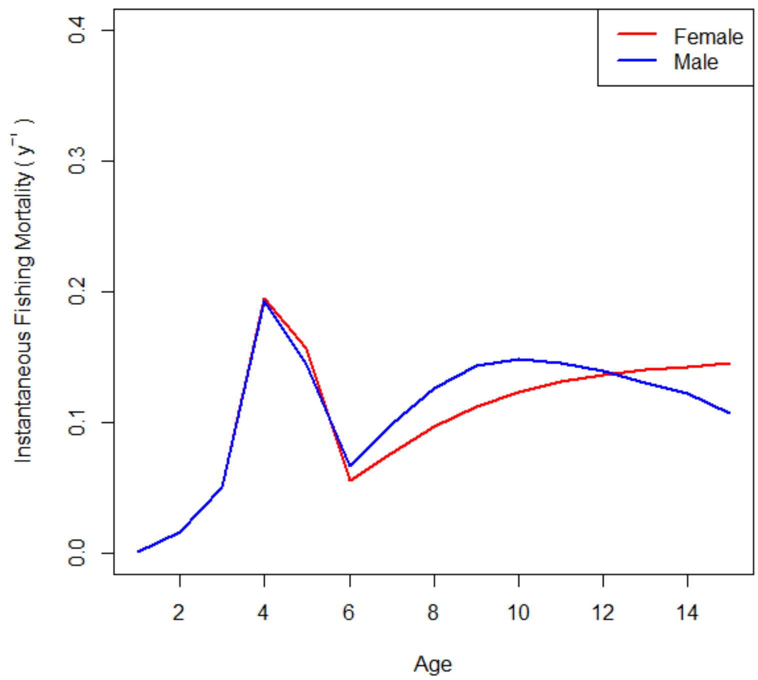

Figure 5.15. Estimated sex-specific instantaneous fishing mortality-at-age (F-at-age) for the 2023 base case model, averaged across 2018-2020.

A

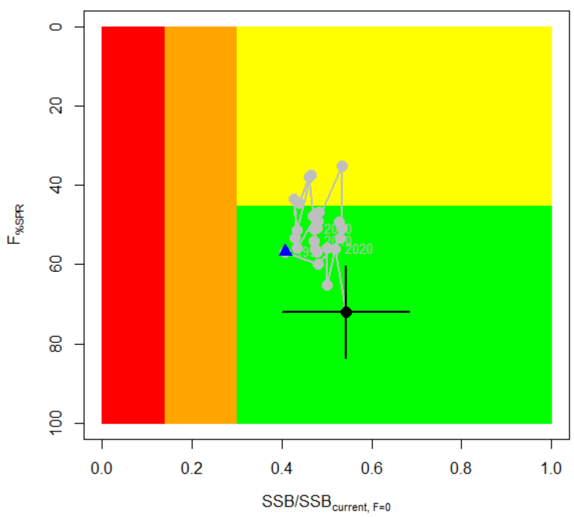

B

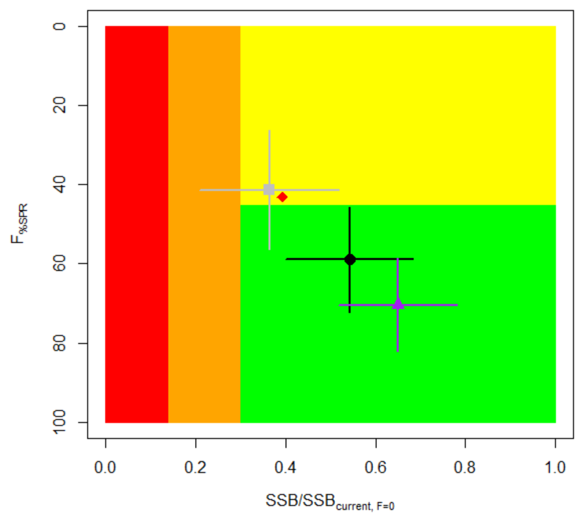

Figure 5.16. (**A**) Stock status phase plot showing the status of the north Pacific albacore (*Thunnus alalunga*) stock relative to the biomass-based threshold (30%$SSB_{current, F=0}$) and limit (14%$SSB_{current, F=0}$) reference points, and fishing intensity-based target reference point ($F45_{\%SPR}$) over the modeling period (1994 – 2021). Blue triangle indicates the start year (1994) and black circle with 95% confidence intervals indicates the terminal year (2021). (**B**) Stock status plot showing current stock status and 95% confidence intervals of the base case model (black circle), an important sensitivity run of CV = 0.06 for L_{inf} in the growth model (gray square), an important sensitivity run with an estimated growth model (purple triangle), and a model representing an update of the 2020 base case model to 2023 data (red diamond). 95% confidence intervals are not shown for the update of the 2020 base case model (red diamond) because the model did not have a positive definite Hessian matrix and uncertainty estimates were unreliable. Red zones in both panels indicate female SSBs falling below the limit reference point while the orange zones indicate female SSBs between the threshold and limit reference points. Green zones indicate female SSBs above the threshold reference point and fishing intensity levels below the target reference point. Yellow areas indicate female SSBs above the threshold reference point and fishing intensity levels above the target reference point. The Fs in this figure are indicators of fishing intensity based on spawning potential ratio (SPR) and calculated as %SPR. SPR is the ratio of the equilibrium SSB per recruit that would result from the estimated F-at-age relative to that of an unfished population. A higher %SPR indicates lower fishing intensity. Current fishing intensity values and $SSB/SSB_{current,F=0}$ ratios in (B) were calculated as the average during 2018-2020 ($F_{\%SPR,\ 2018\text{-}2020}$) and 2021 ($SSB_{2021}/SSB_{current, F=0}$), respectively. The model representing an update of the 2020 base case model is similar to but not identical to the 2020 base case model due to changes in data preparation and model structure.

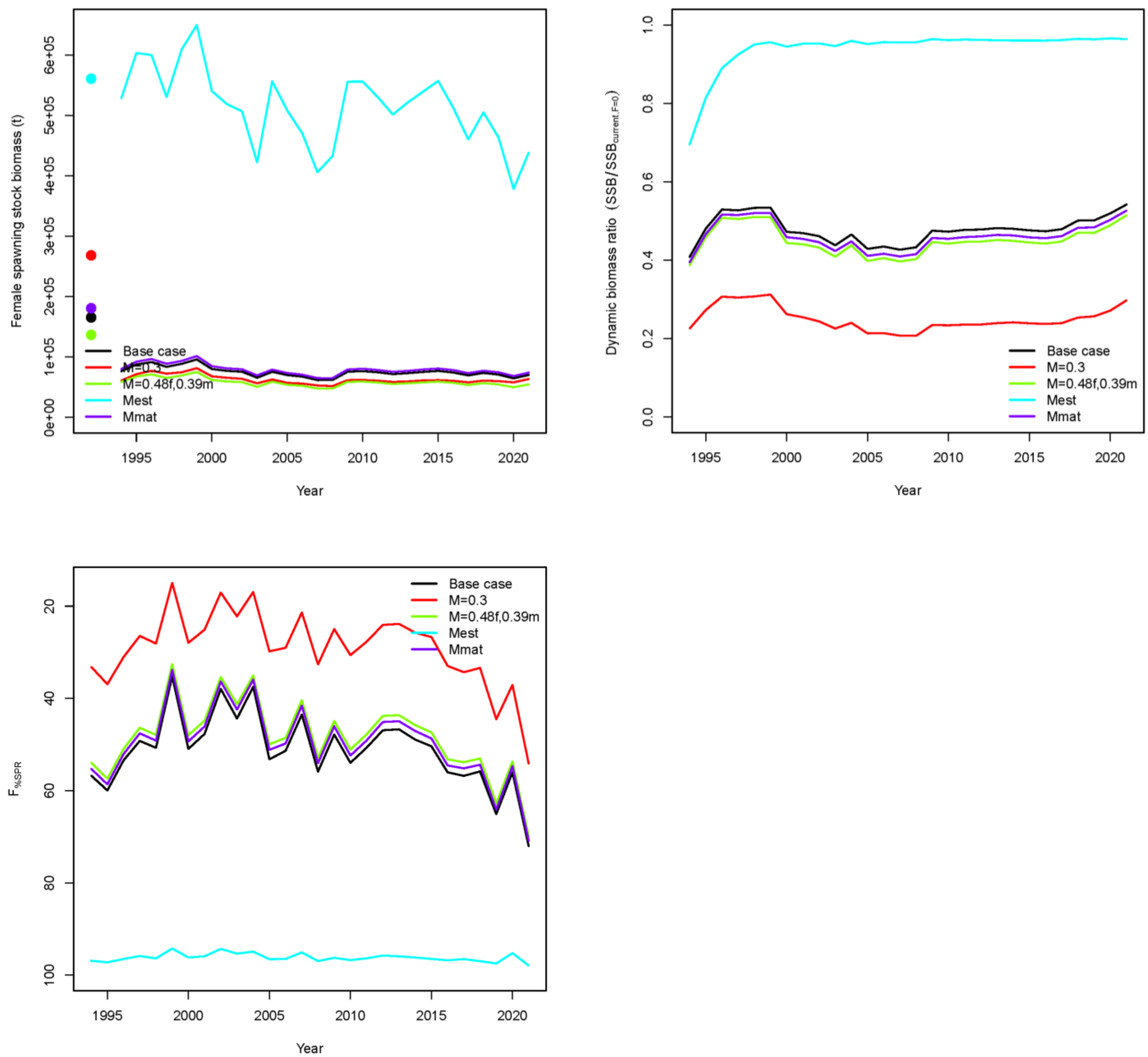

Figure 5.17. Estimated female spawning biomass (upper left), dynamic spawning biomass depletion (upper right), and fishing intensity ($F_{\%SPR}$) (lower left) for the 2023 base case model (black), and four sensitivity runs with alternative natural mortality schedules [constant M of 0.3 y^{-1} for both sexes and all ages (red); constant M of 0.38 and 0.49 y^{-1} for males and females, respectively, of all ages (green); an estimated, single parameter, female M for all ages, with the prior from Teo (2017), $M_{female} \sim \log N[-0.7258, (0.457)^2]$, and a constant logscale offset (-0.21258) between male and female M (cyan); and a fixed, sex- and age-specific M based on a Lorenzen size-M relationship before maturity, and a logistic-shaped transition to adult M (0.48 and 0.39 y^{-1} for females and males) linked to the maturity ogive (purple)]. See Table 4.6 and Section 5.6.1 for details on sensitivity runs.

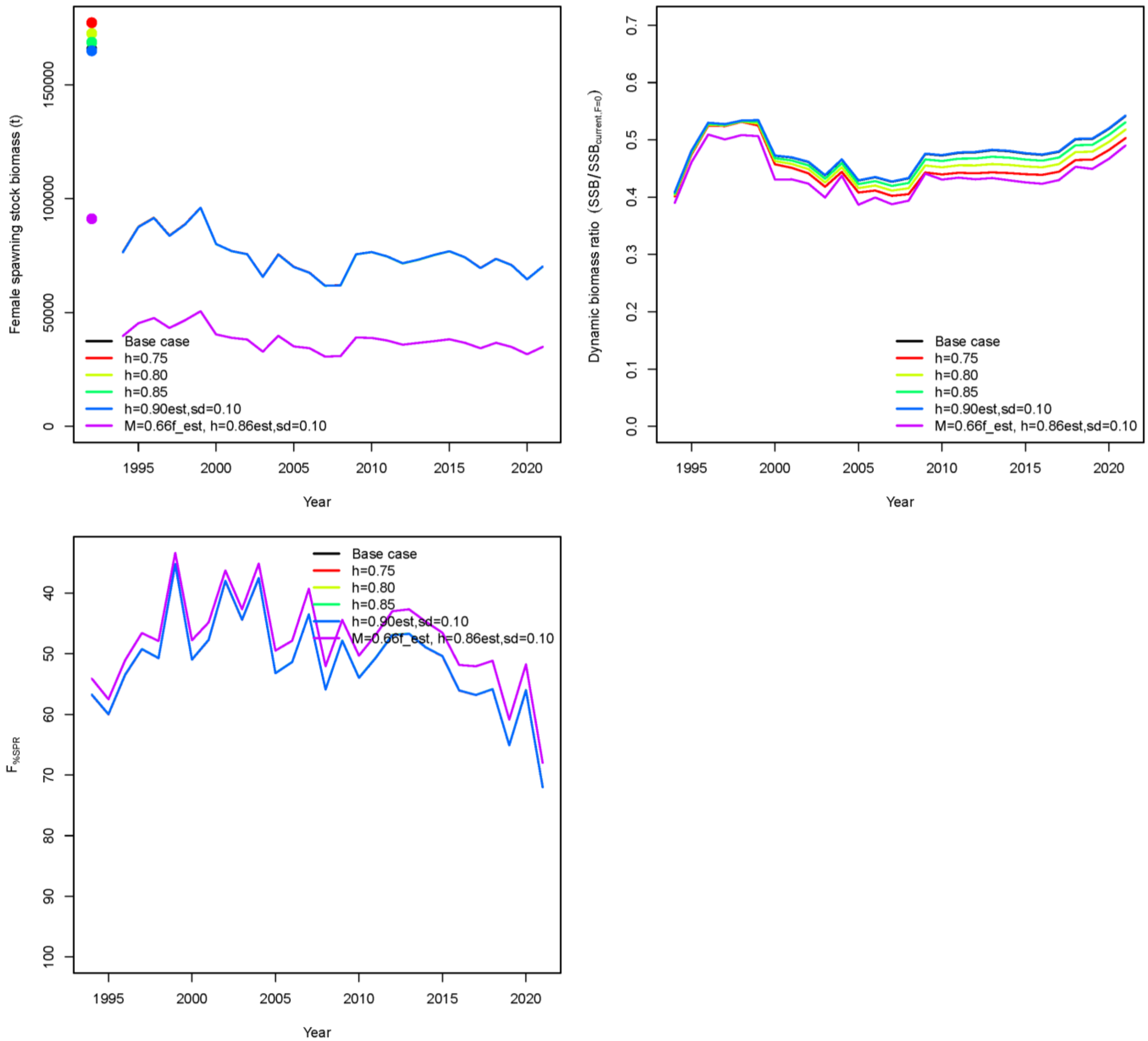

Figure 5.18. Estimated female spawning biomass (upper left), dynamic spawning biomass depletion (upper right), and fishing intensity ($F_{\%SPR}$) (lower left) for the 2023 base case model (black), and five sensitivity runs with different stock-recruitment steepness parameterization and values [fixed h=0.75 (red); 0.80 (green); 0.85 (cyan); an estimated h using a prior of $h \sim N[0.9, (0.1)^2]$. See Table 4.6 and Section 5.6.2 for details on sensitivity runs.

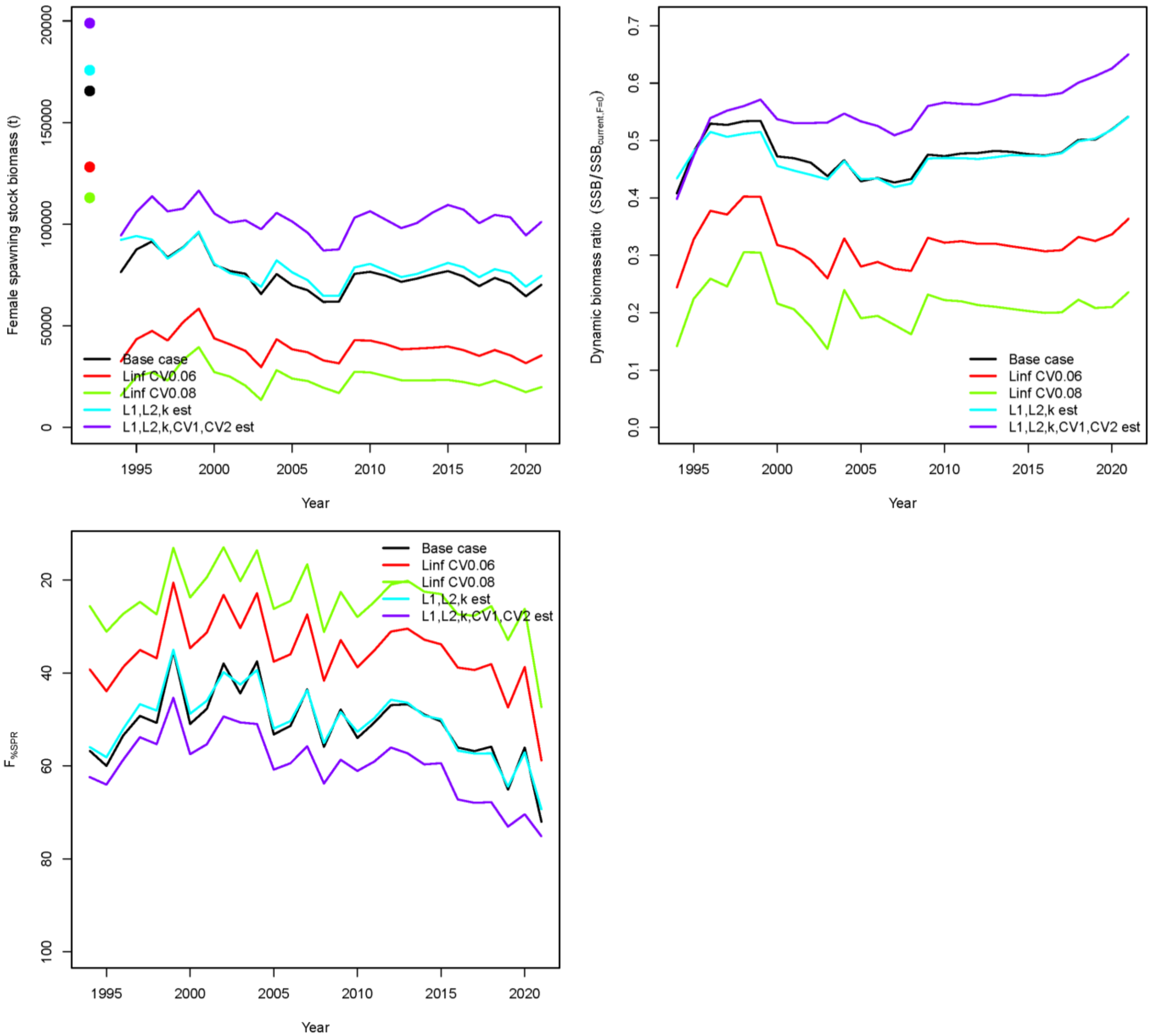

Figure 5.19. Estimated female spawning biomass (upper left), dynamic spawning biomass depletion (upper right), and fishing intensity ($F_{\%SPR}$) (lower left) for the 2023 base case model (black), and four sensitivity runs using different CV values of the L_{inf} parameter and estimating growth parameters. See Table 4.6 and Section 5.6.3 for details on sensitivity runs.

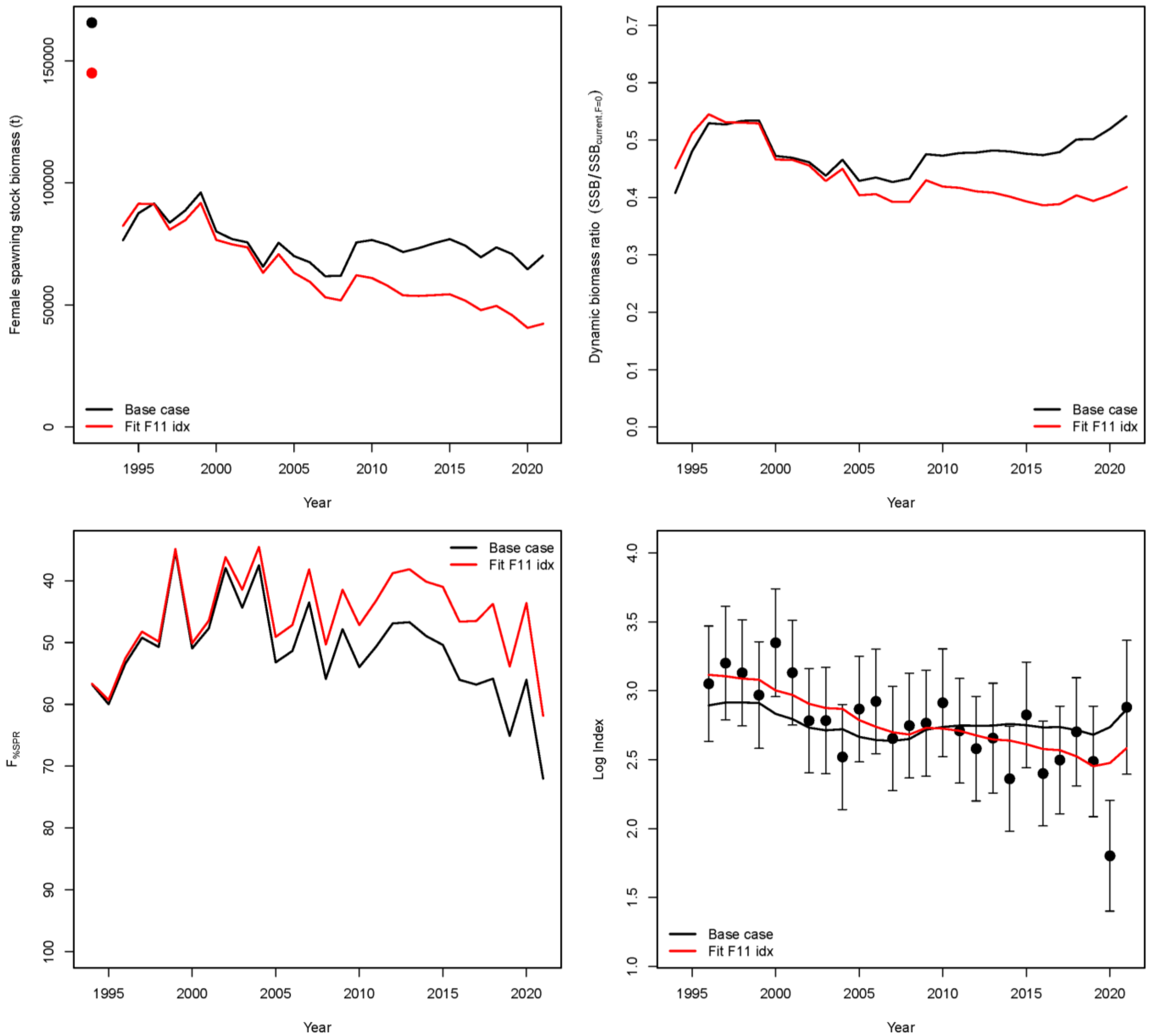

Figure 5.20. Estimated female spawning biomass (upper left), dynamic spawning biomass depletion (upper right), fishing intensity ($F_{\%SPR}$) (lower left), and fit to the F11 index (lower right) for the 2023 base case model (black), and a sensitivity run that fit to the F11 index instead of the F12 index. See Table 4.6 and Section 5.6.4 for details on sensitivity runs.

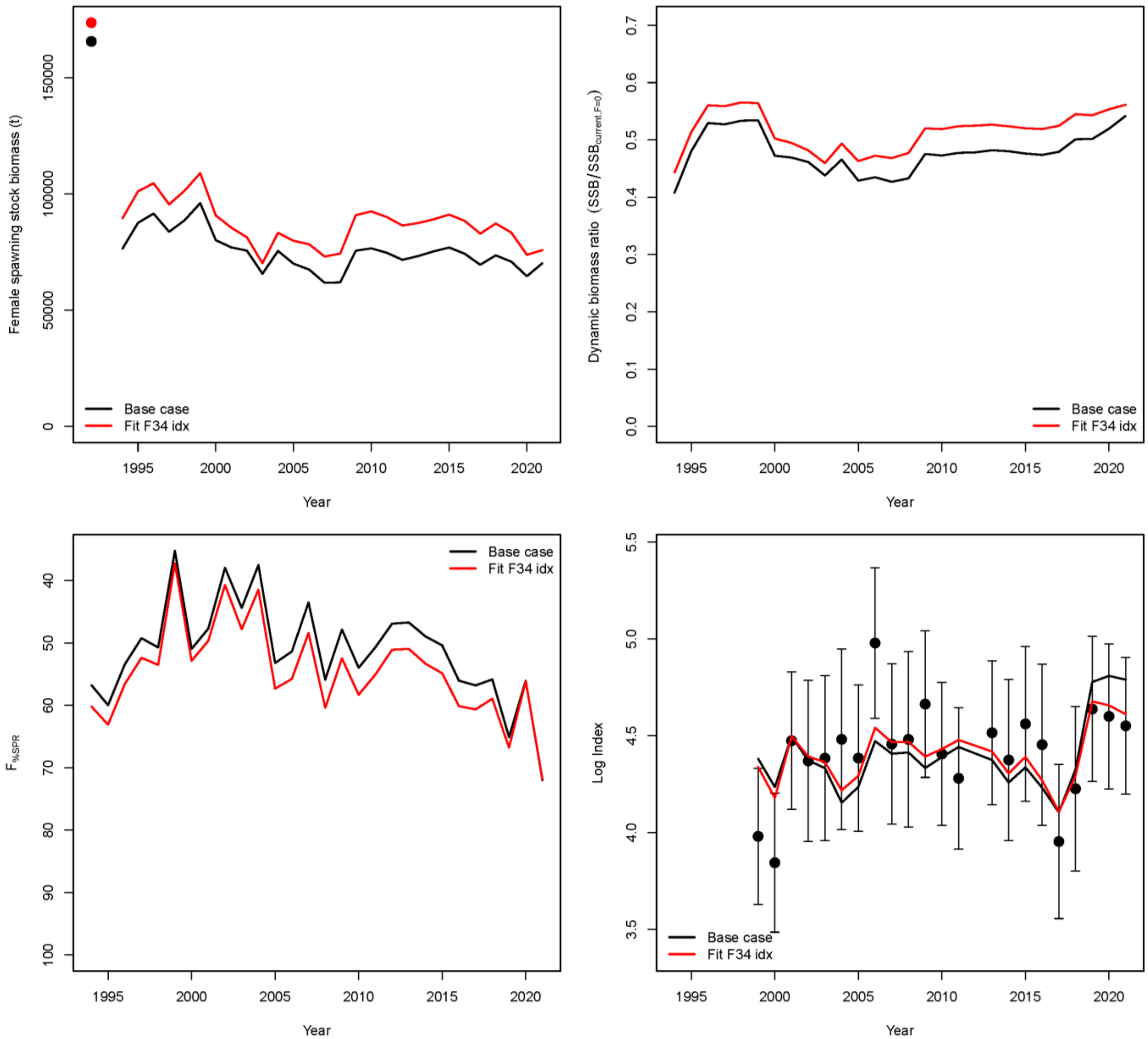

Figure 5.21. Estimated female spawning biomass (upper left), dynamic spawning biomass depletion (upper right), fishing intensity ($F_{\%SPR}$) (lower left), and fit to the F34 index (lower right) for the 2023 base case model (black), and a sensitivity run that fit to the F34 index in addition to the F12 index. See Table 4.6 and Section 5.6.5 for details on sensitivity runs.

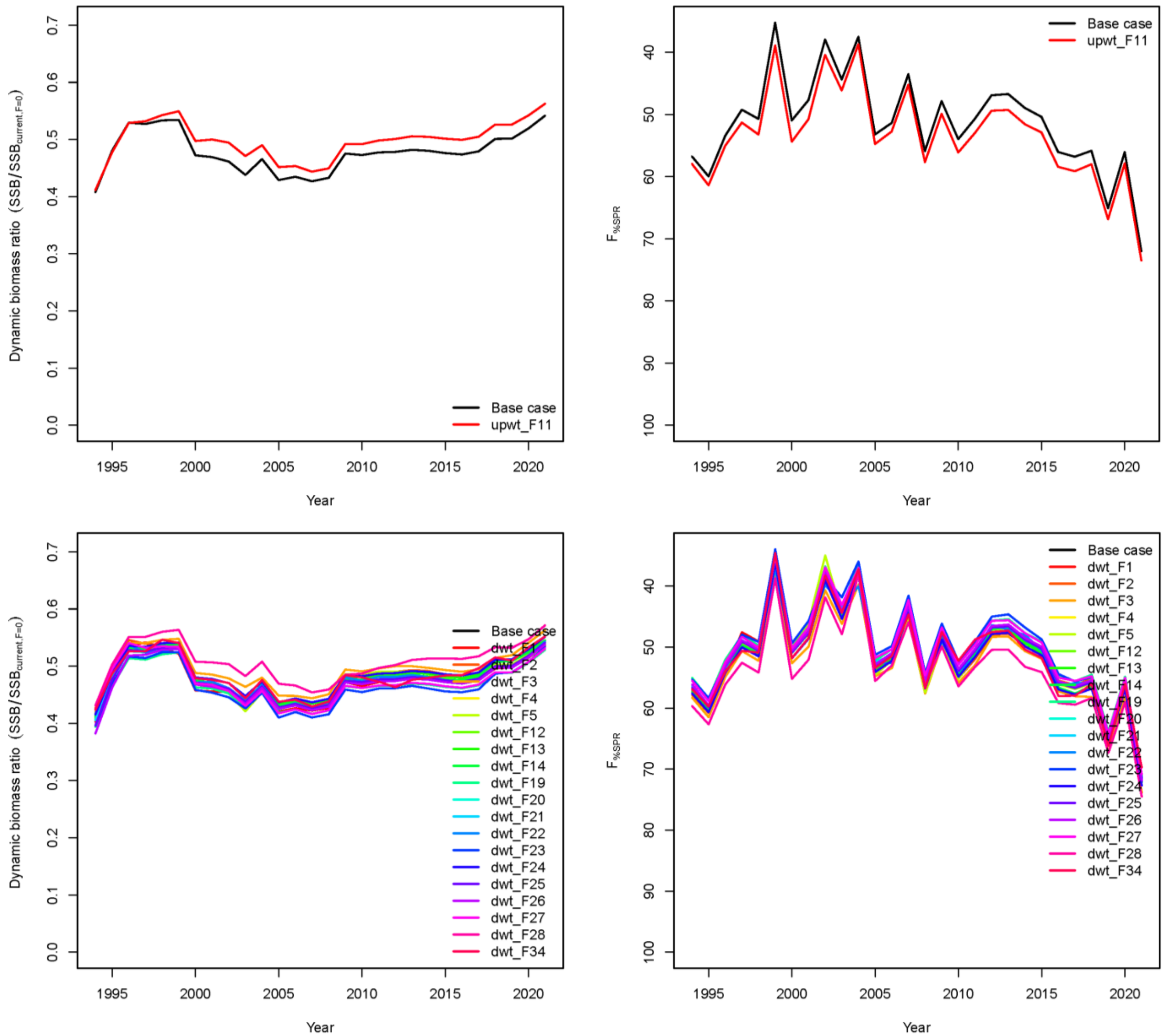

Figure 5.22. Estimated dynamic spawning biomass depletion (upper and lower left) and fishing intensity ($F_{\%SPR}$) (upper and lower right) for the 2023 base case model (black), and a series of sensitivity runs where the size composition data from each fishery were either fully weighted (F11: 1.0x; upper) or down-weighted (lower). See Table 4.6 and Section 5.6.6 for details on sensitivity runs.

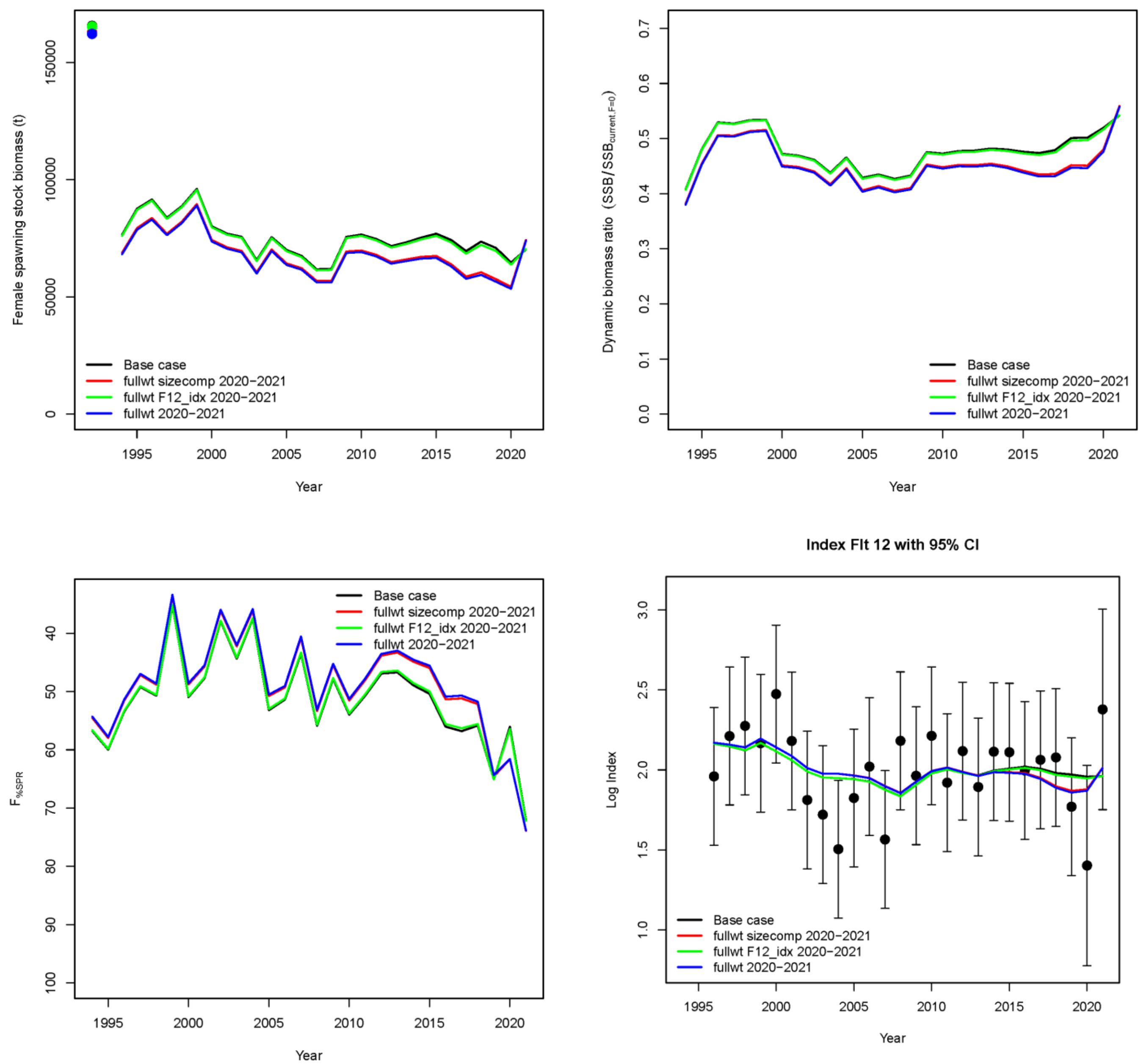

Figure 5.23. Estimated female spawning biomass (upper left), dynamic spawning biomass depletion (upper right), fishing intensity ($F_{\%SPR}$) (lower left), and fit to the F12 index (lower right) for the 2023 base case model (black), and three sensitivity runs that had fully weighted size compositions (red), F12 index (green), and both size compositions and index (blue). See Table 4.6 and Section 5.6.7 for details on sensitivity runs.

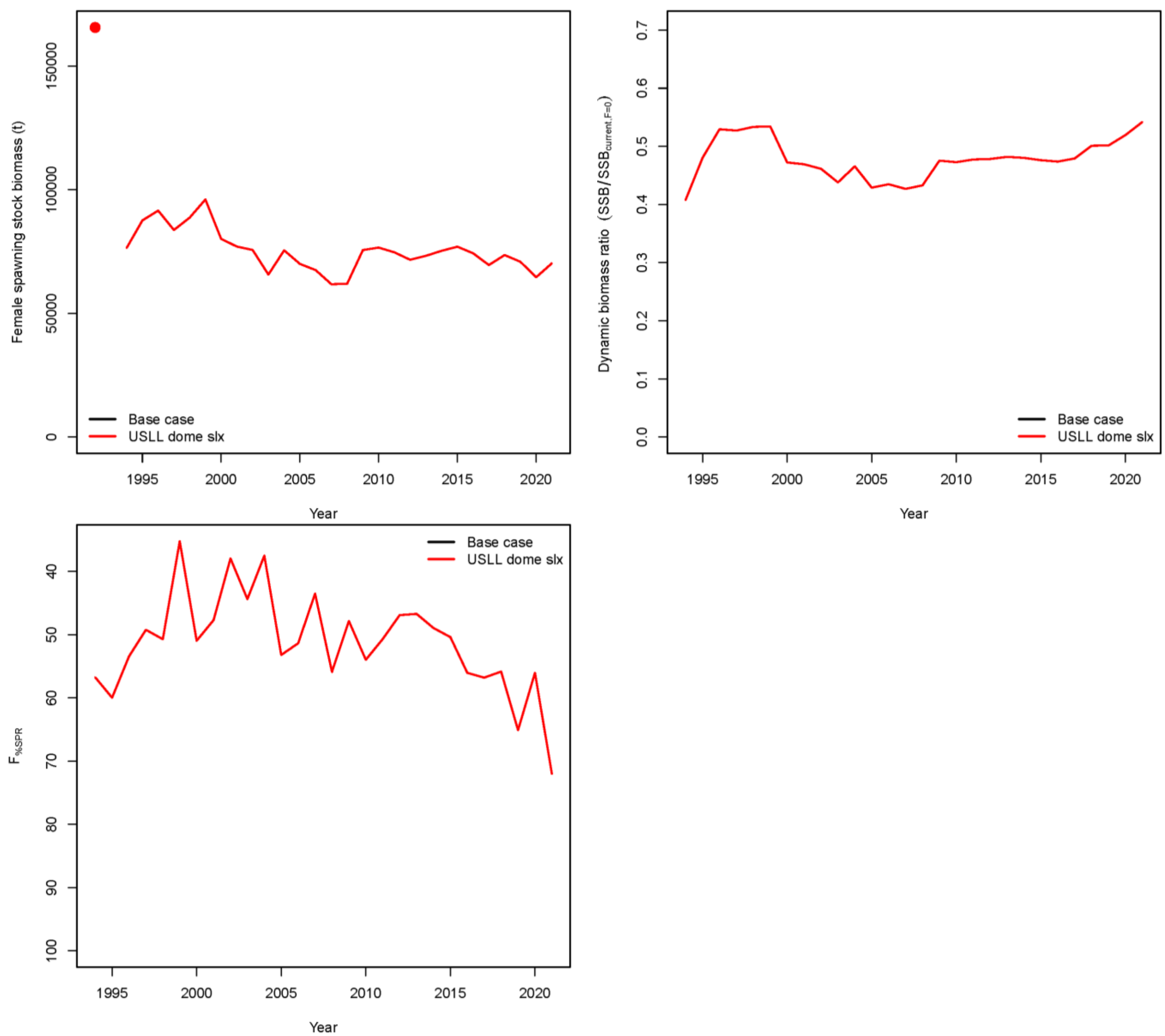

Figure 5.24. Estimated female spawning biomass (upper left), dynamic spawning biomass depletion (upper right), fishing intensity ($F_{\%SPR}$) (lower left) for the 2023 base case model (black), and a sensitivity run where the F27 US longline fleet was allowed to have a dome-shaped selectivity (red). See Table 4.6 and Section 5.6.8 for details on sensitivity runs.

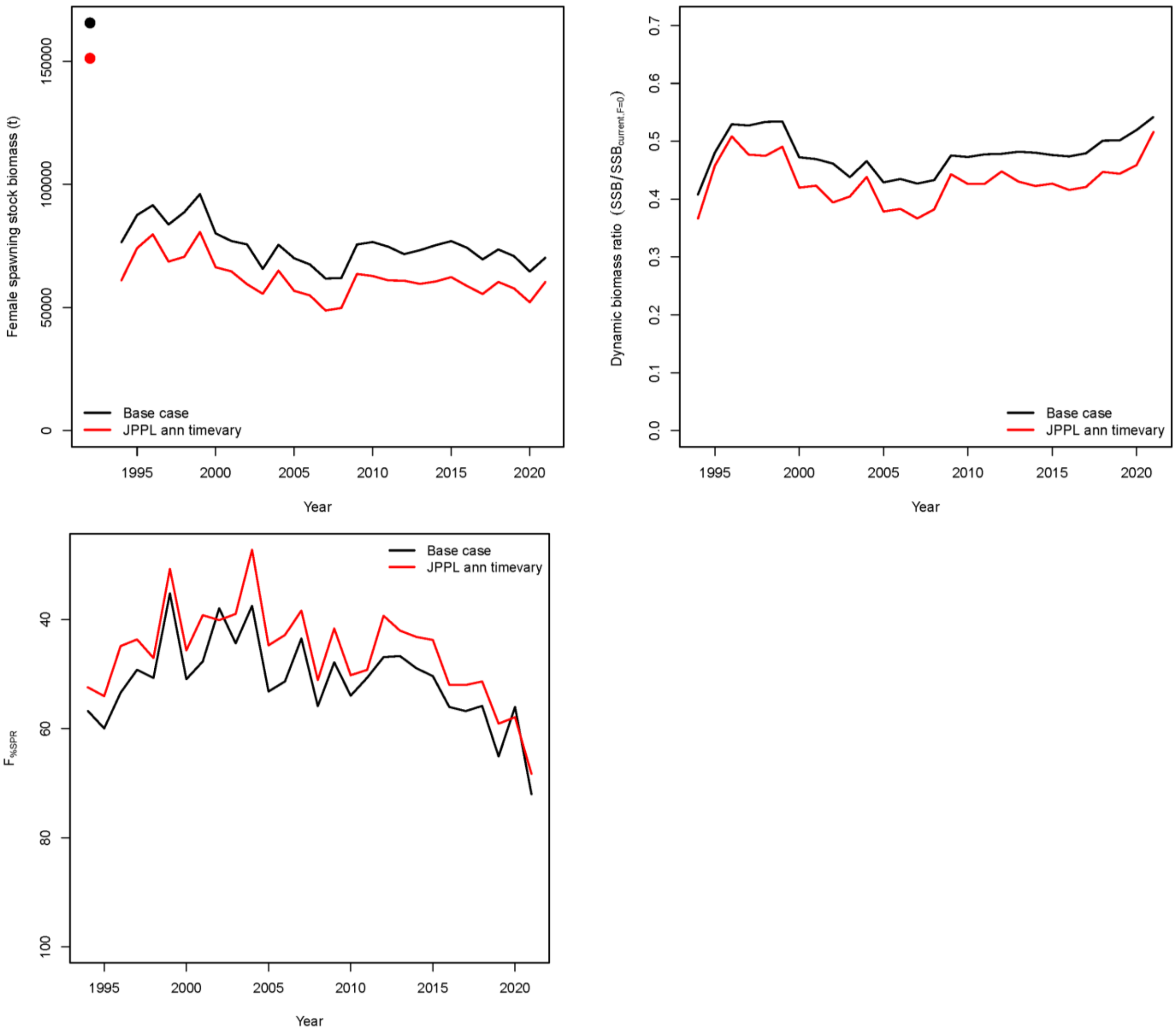

Figure 5.25. Estimated female spawning biomass (upper left), dynamic spawning biomass depletion (upper right), fishing intensity ($F_{\%SPR}$) (lower left) for the 2023 base case model (black), and a sensitivity run where the F22 and F23 Japan pole-and-line fleets had annually varying selectivities (red). See Table 4.6 and Section 5.6.9 for details on sensitivity runs.

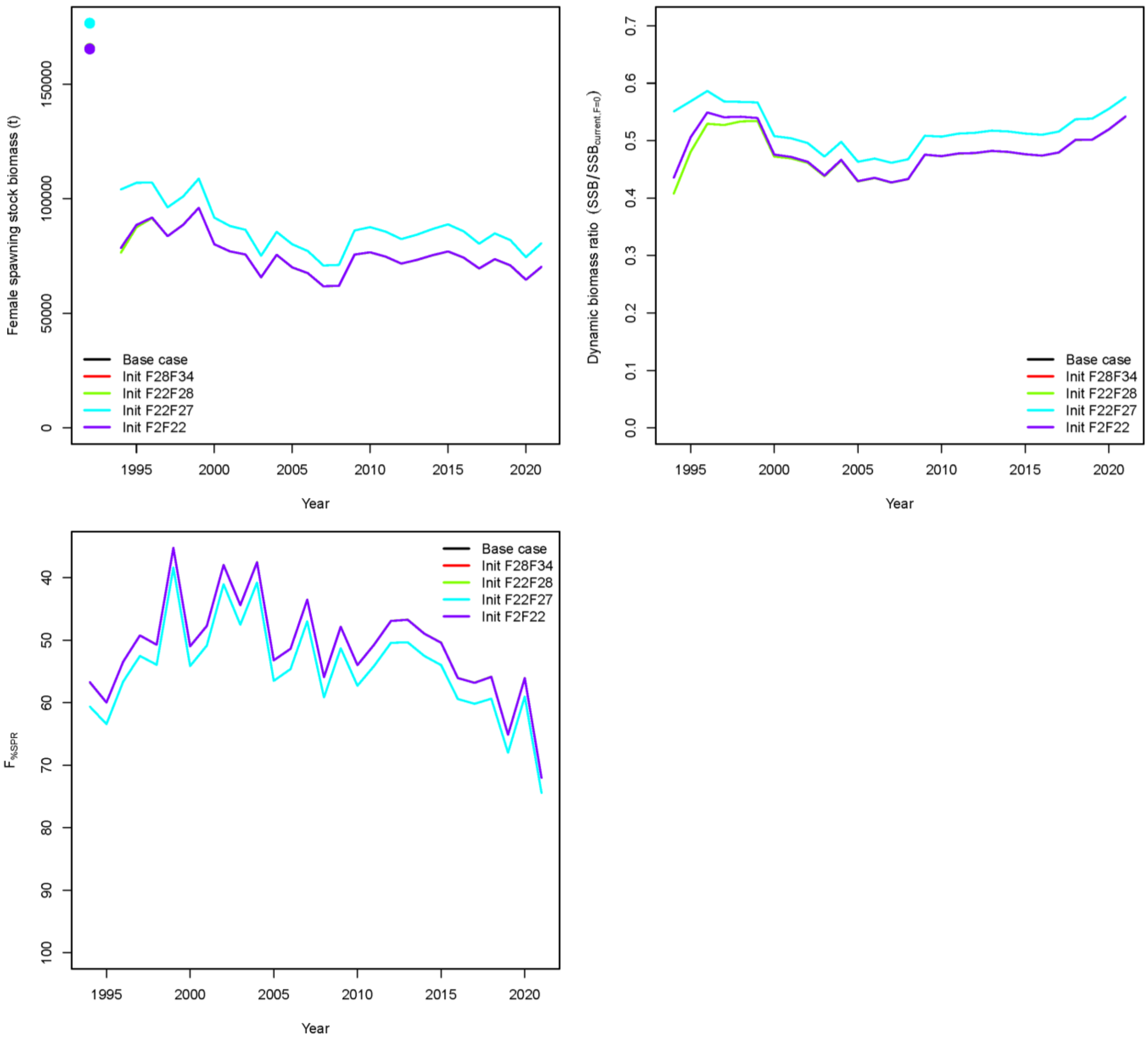

Figure 5.26. Estimated female spawning biomass (upper left), dynamic spawning biomass depletion (upper right), fishing intensity ($F_{\%SPR}$) (lower left) for the 2023 base case model (black), and four sensitivity runs with alternative initial equilibrium fleets. See Table 4.6 and Section 5.6.10 for details on sensitivity runs.

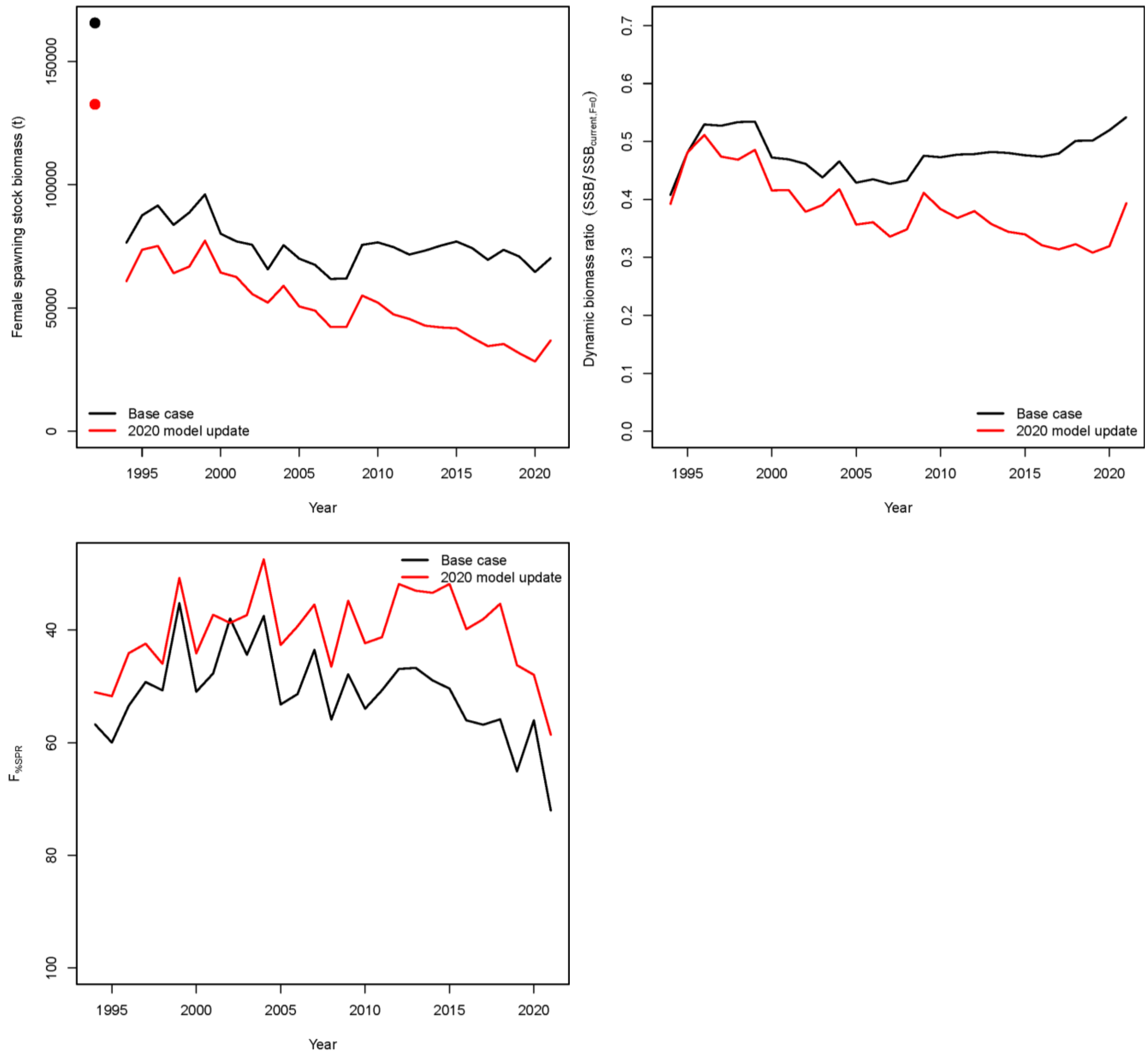

Figure 5.27. Estimated female spawning biomass (upper left), dynamic spawning biomass depletion (upper right), fishing intensity ($F_{\%SPR}$) (lower left) for the 2023 base case model (black), and a sensitivity run that followed the model structure of the 2020 base case model. See Table 4.6 and Section 5.6.11 for details on sensitivity runs.

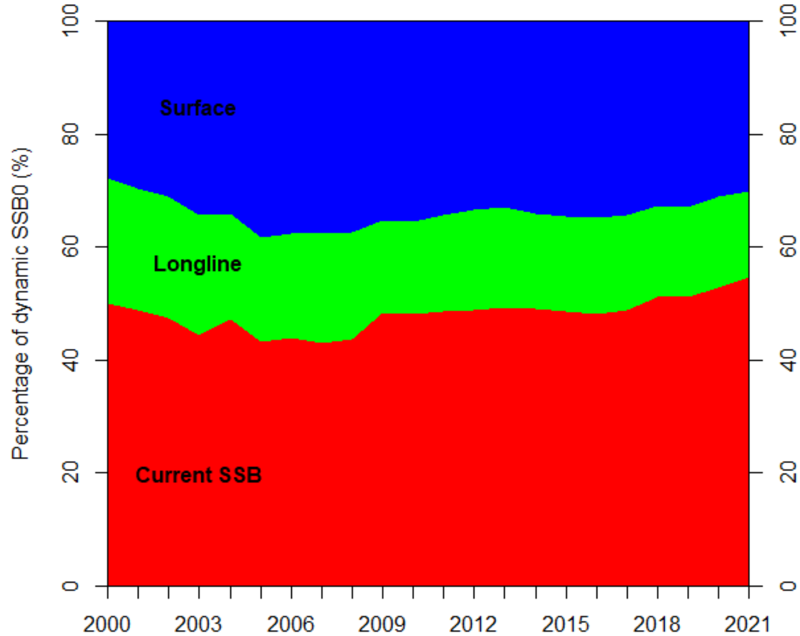

Figure 5.28. Fishery impact analysis on north Pacific albacore (*Thunnus alalunga*) showing female spawning biomass (SSB) (red) estimated by the 2023 base case model as a percentage of dynamic unfished female SSB (SSB_0). Colored areas show the relative proportion of fishing impact attributed to longline (green) and surface (blue) fisheries (primarily troll and pole-and-line gear, but including all other gears except longline).

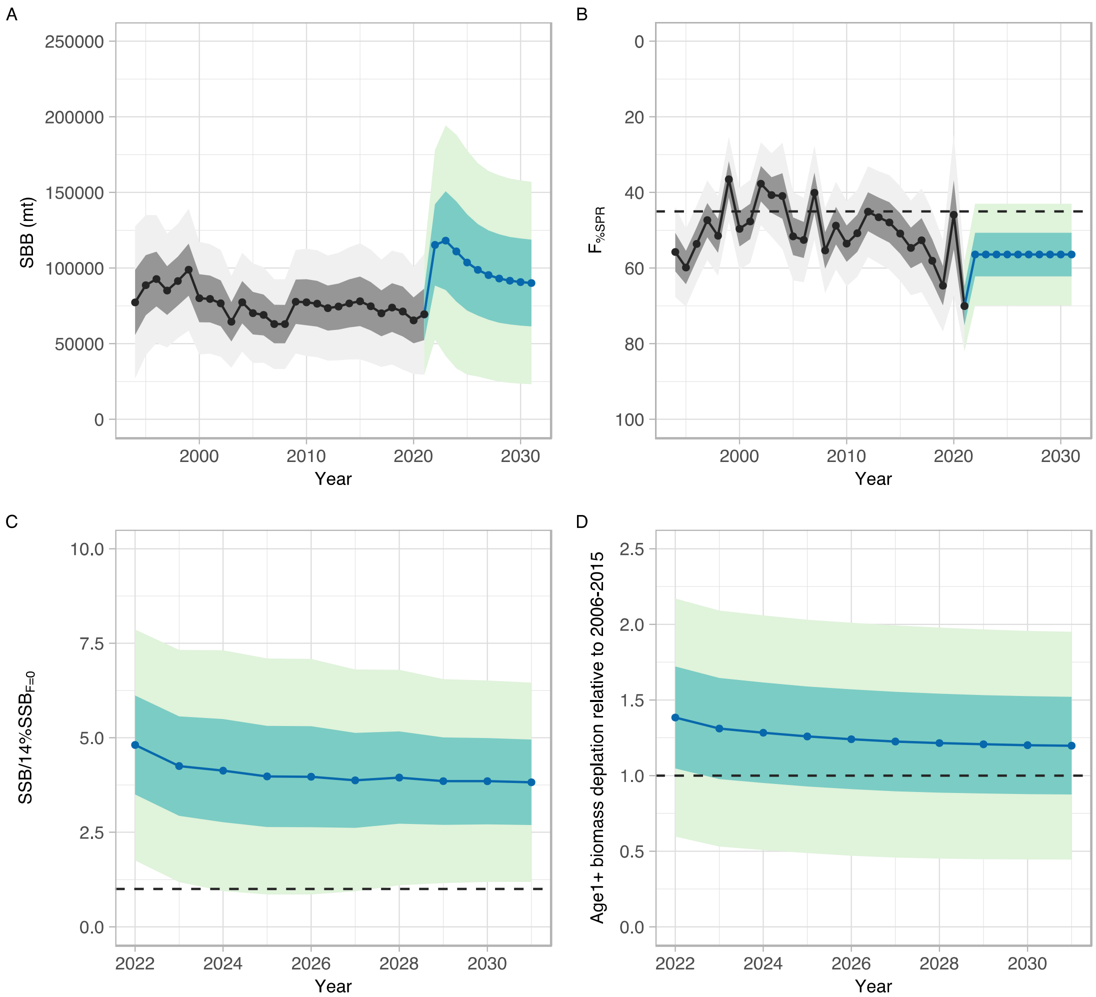

Figure 5.29. Future projection results under a constant fishing intensity ($F_{2018\text{-}2020}$) harvest scenario. Solid lines indicate mean values, uncertainty ranges indicate 60% and 95% confidence intervals, and the dashed line is the reference point, respectively. (A) Annual changes in spawning biomass; (B) Interannual changes in fishing mortality ($F_{\%SPR}$); (C) Projected ratios to the limit reference point thresholds; and (D) Projected ratios to management targets for the total biomass.

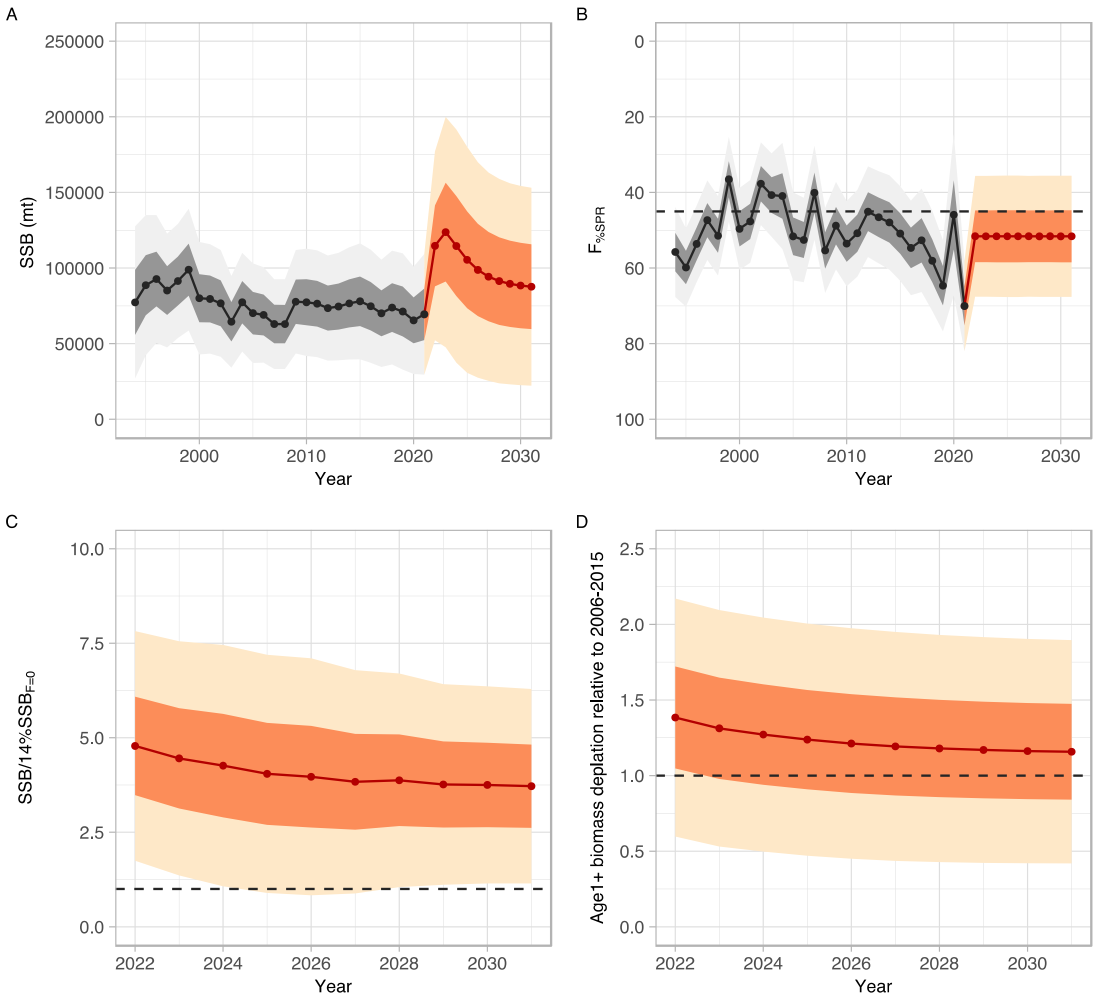

Figure 5.30. Future projection results under a randomly resampled F (2005-2019) scenario. Solid lines indicate mean values, and uncertainty ranges indicate 60% and 95% confidence intervals, and the dashed line is the reference point, respectively. (A) Annual changes in spawning biomass; (B) Interannual changes in fishing mortality ($F_{\%SPR}$); (C) Projected ratios to the limit reference point thresholds; and (D) Projected ratios to management targets for the total biomass.

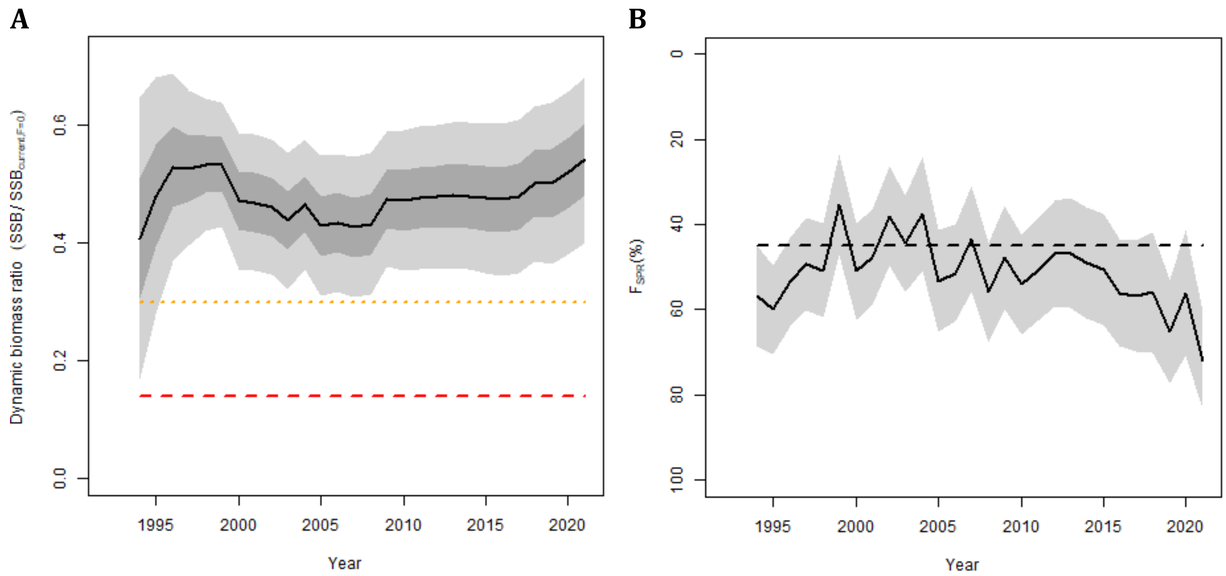

Figure 5.31. (**A**) Estimated dynamic biomass ratio ($SSB/SSB_{current,\ F=0}$) of north Pacific albacore relative to biomass-based threshold ($30\%SSB_{current,\ F=0}$) (orange dotted line) and limit ($14\%SSB_{current,\ F=0}$) reference points (red dashed line) over the modeling period (1994 – 2021); and **(B)** estimated fishing intensity relative to the fishing intensity-based target reference point ($F45_{\%SPR}$) over the modeling period (1994 – 2021). Light and dark gray areas indicate 95% and 60% confidence intervals respectively. The limit reference point is considered to be breached if the lower bound of the 60% confidence intervals overlaps the limit reference point,